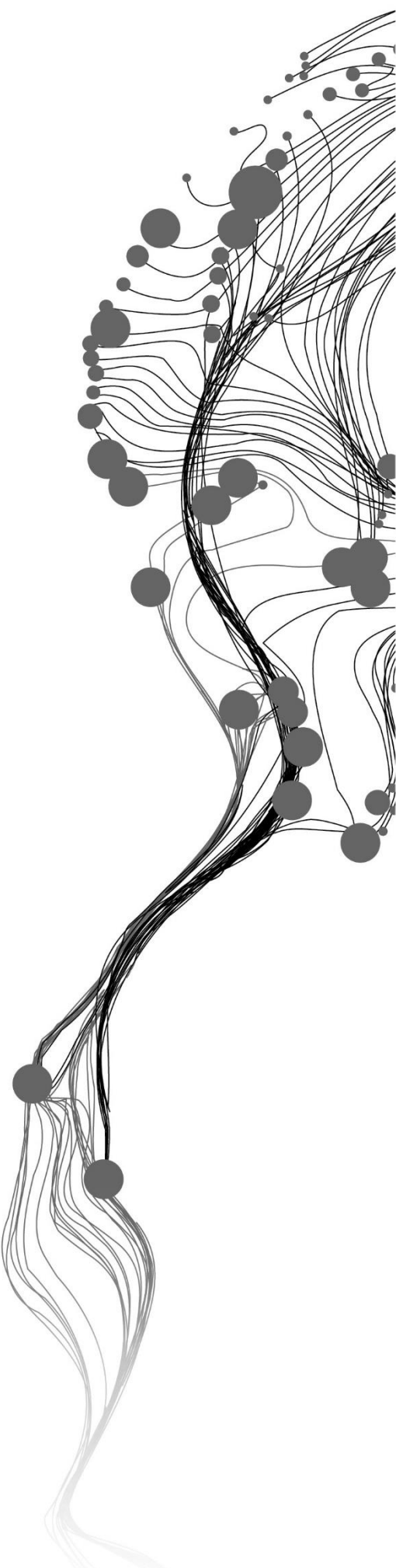


**INTEGRATING TERRESTRIAL  
LASER SCANNER AND  
UNMANNED AERIAL VEHICLE  
DATA TO ESTIMATE ABOVE  
GROUND BIOMASS/CARBON IN  
KEBUN RAYA UNMUL SAMARINDA  
TROPICAL RAIN FOREST, EAST  
KALIMANTAN, INDONESIA**

WELDAY BERHE TEFAY  
FEBRUARY 2019

SUPERVISORS:  
Dr. Y. A. Hussin  
Ir.L.M. van Leeuwen - de Leeuw

ADVISOR:  
Dr. Y. Budi Sulistioadi



# **INTEGRATING TERRESTRIAL LASER SCANNER AND UNMANNED ARIAL VEHICLE DATA TO ESTIMATE ABOVE GROUND BIOMASS/ CARBON IN KEBUN RAYA UNMUL SAMARINDA TROPICAL RAIN FOREST, EAST KALIMANTAN, INDONESIA**

**WELDAY BERHE TEFAY**

Enschede, The Netherlands, February 2019

Thesis submitted to the Faculty of Geo-Information Science and Earth Observation of the University of Twente in partial fulfillment of the requirements for the degree of Master of Science in Geo-information Science and Earth Observation.

Specialization: Natural Resource Management

**SUPERVISORS:**

Dr. Y. A. Hussin

Ir.L.M. van Leeuwen - de Leeuw

**ADVISOR:**

Dr. Y. Budi Sulistioadi (University of Mulawarman, Samarinda, Indonesia)

**THESIS ASSESSMENT BOARD**

Dr. Ir.C.A.J.M. De Bie (Chair)

Dr. Tuomo Kauranne (External Examiner, Lappeenranta University of Technology, Finland).

Dr. Y. A. Hussin (1<sup>st</sup> Supervisor)

Ir.L.M. van Leeuwen - de Leeuw (2<sup>nd</sup> Supervisor)

#### DISCLAIMER

This document describes work undertaken as part of a programme of study at the Faculty of Geo-Information Science, and Earth Observation of the University of Twente. All views and opinions expressed therein remain the sole responsibility of the author and do not necessarily represent those of the Faculty.

## ABSTRACT

About half of the terrestrial above-ground biomass carbon stored in vegetation is found in the tropical rain forests which have been influenced by anthropogenic activities. When forests are deforested the carbon stored in their biomass is released to the environment as a form of CO<sub>2</sub>, and it affects the concentration of GHG. As a result, REDD+ has been initiated under UNFCCC; it intends to monitor carbon emission and sustainable forest monitoring through its MRV mechanism.

Remote sensing method is suggested by UNFCCC to be used for its REDD+ MRV mechanism for accurate assessment of AGB. However, estimation of AGB in a multi-layered tropical forest using one single remote sensing method, either aerial imagery or ground-based, is challenging and it can lead to underestimation. Because, both the aerial and ground-based remote sensing are associated with limitations to extract both the upper and lower canopy tree parameters (DBH, height) due to occlusion. However, by integrating the aerial and ground-based remote sensing methods, the accuracy of AGB estimation can be improved. In tropical forest tree height measurement using Airborne laser scanner is more accurate. However, it is costly, and it is not always available, compared with another remote sensing such as UAV. Hence, UAV technology can be used to acquire the upper canopy tree parameters at a reasonable cost and accuracy. In other cases TLS which is a ground-based remote sensing method it can provide the height of lower canopy trees, and DBH of all canopy trees accurately. However, there are a limited number of studies on the integration of UAV and TLS derived data to estimate AGB in the tropical forests. Therefore, this study aims to test the potential of integrating UAV and TLS data to improve the accuracy of plot based AGB estimation of the multi-layered tropical rain forests.

Further, two methods of height threshold definitions were used to integrate the upper and lower canopy tree parameters which were derived from the UAV 3D image-based modeling and TLS point clouds. The lower canopies tree height measured using Leica DISTO D510 was compared with the corresponding reference TLS derived height, and the result showed R<sup>2</sup> of 0.80 and RMSE of 1m (8.37%). Hence, the Leica DISTO D510 was underestimated by 0.48m on average, and statistically, it has a significant difference (P<0.05). While the TLS derived DBH of the upper and lower canopy trees have no significant difference with the field measured reference DBH with R<sup>2</sup> of 0.99 and RMSE of 1.59m (5.54%). The UAV-CHM derived tree height was compared with the reference Leica DISTO D510 height of the upper canopy trees. Thus, the result showed R<sup>2</sup> of 0.76 and RMSE of 2.53m (13.06%). Therefore, statistically, it has a significant difference (P>0.05). The remote sensing method AGB (UAV and TLS) was also calculated based on the two techniques i.e. 1) the UAV derived height threshold and 2) the TLS derived height thresholds to integrate the upper and lower canopy tree parameters. So, the AGB integrated using the UAV derived threshold was compared with the AGB integrated using the TLS derived threshold. Hence, the result showed there is no significant difference with R<sup>2</sup> of 0.99 and RMSE of 0.24Mg (1.55%).

Furthermore, the accuracy of the remote sensing method estimated AGB was assessed using the reference field-based estimated AGB in a plot based. Thus, the result reveals that R<sup>2</sup> of 0.95 and the RMSE was 1.07Mg (6.81%). Also, the t-test showed there is no significant difference (P>0.05) between the remote sensing method and field-based estimated AGB. Thus, the overall result indicates that the integration of the UAV and TLS remote sensing can be used to extract the upper and lower canopy tree parameters and to estimate the subsequent AGB of the tropical forests in a reasonable accuracy and coast.

**Keywords:** UAV, TLS, AGB, CHM, Upper canopy, Lower canopy, Tropical rain forest, Threshold.

## ACKNOWLEDGMENTS

First of all, I would like to gratitude thank for the almighty God for everything that he provides in my life and through the journey of the M.Sc. thesis Glory to Him. I am expressing my thankfulness appreciation to the Faculty of Geo-information Science and Earth Observation (ITC), University of Twente and Netherland Fellowship Program (NFP) who granted me a scholarship to pursue MSc., in Natural Resource Management.

I would like to express my most thankful, and grateful appreciation to my first supervisor Dr. Yousif Ali Hussin for his supervision, encouragement, fieldwork support, constructive comments, and continuous support from the starting of the proposal till the end of this thesis work. Without his guidance and support, this thesis would be challenging to finish.

I would like to grateful and deepest tank to Ir. Louise van Leeuwen my second supervisor for her constructive comments, encouragements, and continuous support in all phases of my thesis work starting from the proposal until the end of my study. It is a real opportunity to do the M.Sc. thesis under her supervision.

I would like, to extend my grateful thanks to Dr. Ir.C.A.J.M. De Bie for his valuable and critical comments on the proposal presentation and mid-term presentation. I am also heartfelt thanks for Drs. Raymond Nijmeijer, NRM Course Director, for his follow up and support from the beginning of the course until the end of the study.

I am very thankful to acknowledge the University of Mulawarman, Faculty of Forestry, for their collaboration and hospitality in the field work. I am also grateful thanks to Dr. Y. Budi Sulistioadi (University of Mulawarman) for his facilitating entrance to Indonesia, providing data and organizing the field works at Indonesia. I am also grateful thanks to Ministry of Science and Technology and Higher Education of Indonesia for offering a research permit to conduct my research and fieldwork in Indonesia. I also want to say thank for the team of Mulawarman University, Faculty of Forestry students; Mr. Rafii Fauzan, Ms. Audina Rahmandana, Mr. Lutfi Hamdani, for their help in data collection and cooperation during the fieldwork in Samarinda. I would like to say thanks to my fellow students for their support in data collection and other facilities in the field.

Finally, I would like to thank all my parents for their support and encouragements. Last but not list, most profound appreciation goes to Mr. Tsegay G/Tekle (Enderta district OARD) and all my friends who encourage me and wish my success.

Welday Berhe Tesfay  
Enschede, The Netherlands  
February 2019

# TABLE OF CONTENT

---

List of figures .....	v
List of tables .....	vi
List of equations .....	vii
List of appendices .....	viii
List of acronyms .....	ix
1. INTRODUCTION.....	1
1.1. Background.....	1
1.2. Research Problem.....	2
1.3. Objectives .....	4
1.3.1. General objectives .....	4
1.3.2. Specific objectives.....	4
1.4. Research questions .....	5
1.5. Hypothesis .....	5
2. LITERATURE REVIEW.....	6
2.1. Tropical rain forest.....	6
2.1.1. Allometric Equation .....	7
2.1.2. Application of UAV in forestry.....	7
2.1.3. Application of TLS in forestry.....	8
2.1.4. Integration of TLS and UAV.....	9
2.1.5. Handheld laser instrument (tree height measurement).....	9
3. METHODS AND MATERIALS .....	10
3.1. Study area.....	10
3.1.1. Climate and topography.....	10
3.1.2. Vegetation .....	10
3.2. Materials .....	12
3.2.1. Field equipment and instruments.....	12
3.2.2. Tools and software .....	12
3.3. Method .....	12
3.3.1. Pre-fieldwork .....	14
3.3.2. Plot size .....	14
3.3.3. Sampling design.....	14
3.4. Field data collection .....	14
3.4.1. Biometric field data measurement and collection.....	14
3.4.2. Field level individual upper canopy tree identification .....	15
3.4.3. UAV data acquisition .....	16
3.4.4. TLS data collection.....	17
3.5. Data processing.....	20
3.5.1. Biometric data processing .....	20
3.5.2. TLS data processing .....	20
3.5.3. UAV image processing .....	21
3.5.4. Manual tree crown delineation (digitization).....	22
3.5.5. Tree matching and individual tree height extraction.....	23
3.5.6. Modelling of DBH from the crown projection area.....	23
3.5.7. Integration of upper and lower canopy trees using height threshold.....	23
3.5.8. Above ground biomass/ Carbon estimation.....	24

3.5.9. Data analysis .....	25
4. RESULTS .....	26
4.1. Field level upper tree crown identification .....	26
4.2. Field biometric data .....	26
4.3. TLS data and Individual tree extraction .....	26
4.4. UAV-CHM and orthomosaic image generating .....	27
4.4.1. Tree crown delineation and individual tree height extraction .....	28
4.4.2. Modelling of DBH from the crown projection area.....	29
4.5. Lower canopy tree height measurement and accuracy assessment .....	30
4.6. DBH measurement of TLS and accuracy assessment .....	31
4.7. The accuracy of upper canopy tree height assessment .....	33
4.8. Above ground biomass estimation.....	35
4.8.1. Remote sensing based AGB estimation (using UAV and TLS) .....	35
4.8.2. The relationship between AGB integrated using UAV, and TLS derived height thresholds	
35	
4.8.3. The relationship between field-based and remote sensing method estimated AGB.....	38
4.9. Above ground carbon estimation .....	41
5. DISCUSSION .....	42
5.1. Field level upper crown tree identification .....	42
5.2. Descriptive analysis of the tree parameter data.....	42
5.3. Tree extraction from TLS point cloud .....	43
5.4. Accuracy assessment of lower canopy tree height.....	44
5.5. Comparison of TLS driven DBH and field measured DBH.....	45
5.6. The accuracy of the upper canopy tree height measurements .....	46
5.7. Comparison of remote sensing method AGB integrated by separate height thresholds .....	47
5.8. The accuracy of AGB estimated by remote sensing method .....	49
5.9. Limitation of the study .....	50
6. CONCLUSIONS AND RECOMMENDATIONS.....	51
6.1. Conclusions .....	51
6.2. Recommendation .....	52
List of references .....	53
List of Appendix.....	60

## LIST OF FIGURES

---

Figure 1: Illustration of tropical rainforest canopy strata. Source; (Layers of a Rainforest, n.d.).....	3
Figure 2: Conceptual diagram of the study.....	4
Figure 3: Structure of tropical rainforest (A) and parts of AGB and BGB/ Carbon stock (B).....	6
Figure 4: Illustration of structure from motion image acquiring (a) and types of UAV - b, c.....	7
Figure 5: Operating system of TLS - left side and RIEGL VZ 400 TLS -right.....	8
Figure 6: Single and multiple scanning positions.....	9
Figure 7: Study area of KRUS tropical forest location. ....	11
Figure 8: Shows flow chart of the research method. ....	13
Figure 9: Illustration of plot based biometric data collection. Source; (Asmare, 2013) modified .....	15
Figure 10: Illustration of individual upper canopy trees identification by Avenza Map (Plot 22). ....	16
Figure 11: Phantom 4 DJI UAV-left, and GCP 60x60cm marker-right.....	16
Figure 12: TLS multi-scanning position.....	18
Figure 13: Circular-left and cylindrical- right retroreflectors. Source:(UNAVOC, n.d.). ....	18
Figure 14: Illustration of circular and cylindrical retro-reflectors (a) and mounted tree tags (b). ....	19
Figure 15: Manual identification and extraction of individual trees in RiSCAN Pro (Plot-15). ....	20
Figure 16: Illustration of tree height and DBH measurements (Plot 6). ....	21
Figure 17: Shows manually delineated tree crowns (Plot 11). ....	22
Figure 18: Identification of fully detected and not fully detected trees on TLS point cloud. ....	24
Figure 19: Part of the CHM generated by subtracting DTM from DSM. ....	28
Figure 20: Tree crown delineation -right and tree height extraction-left.....	29
Figure 21: Developed model and model validation of CPA. ....	29
Figure 22: The relationship between field measured and TLS derived lower canopy height.....	30
Figure 23: The relationship between field and TLS measured DBH of the upper and lower canopy trees.....	32
Figure 24: The relationship between field measured and UAV-CHM derived upper canopy trees. ....	34
Figure 25: AGB estimated by using TLS and UAV derived thresholds to integrate the upper and lower canopies.....	37
Figure 26: Plot-based estimated AGB using remote sensing method and field-based. ....	39
Figure 27: Relationship between field-based and remote sense method estimated AGB. ....	40
Figure 28: Remote sensing method and field-based estimated above-ground biomass carbon (Mg). ....	41
Figure 29: Distribution of field measured, and TLS derived DBH (cm) on a histogram.....	43
Figure 30: Effect of vegetation stacked on tree stem for DBH measurement.....	45
Figure 31: Illustration of stem condition and its effect in TLS- DBH measurements.....	46
Figure 32: Illustration of tropical rain forest tree parameter acquisitions and its effects.....	49



## LIST OF TABLES

---

Table 1: List of field instruments and equipment used in the research.....	12
Table 2: List of software packages and tools used for the study.....	12
Table 3: RIEGL YZ 400 TLS specification source: (RIEGL RIEGL VZ-400 VZ-400, 2017).....	17
Table 4: Proportion of upper canopy tree identified at field level and manually digitized tree crowns result. .....	26
Table 5: Number of missed trees per plot.....	26
Table 6. Descriptive statistics of tree extracted from TLS point cloud per plots.....	27
Table 7. Results of Pix4D UAV-Image processing.....	27
Table 8: Proportion of tree height extracted from UAV-CHM per plot.....	28
Table 9: Descriptive statistics of TLS and field measured lower canopy heights.....	30
Table 10: Relationship between field measured and TLS derived lower canopy tree heights.....	31
Table 11. F-test for the lower canopy tree height measured using Leica DISTO, and TLS derived height.....	31
Table 12. A t-test for field measured, and TLS derived lower canopy heights.....	31
Table 13: Descriptive statistics of TLS and field measured DBH.....	32
Table 14: Relationship between field and TLS measured DBH of the lower and upper canopy trees.....	32
Table 15: F-test for TLS and field measured DBH for a variance.....	33
Table 16: The t-test assuming equal variance for the field measured and TLS derived DBH of the lower and upper canopy trees.....	33
Table 17: Descriptive statistics of field measured and extracted from UAV-CHM of the upper canopy tree heights.....	33
Table 18: Relationship between field measured and UAV-CHM derived upper canopy tree heights.....	34
Table 19. F-test for equal or un equal variance.....	34
Table 20. The t-test between field measured and UAV-CHM derived upper canopy tree height.....	35
Table 21. The input tree parameters used for upper and lower canopies AGB estimation.....	35
Table 22: TLS derived defined height thresholds to integrate the upper and lower canopy trees per plot.....	36
Table 23: Determined UAV minimum height threshold.....	36
Table 24: Descriptive statistics of TLS derived threshold upper and lower canopies.....	36
Table 25: Lower canopy trees miss-categorized as part of upper canopies and their AGB.....	37
Table 26: The relationship of AGB estimated using TLS and UAV derived height threshold to integrate the upper and lower canopy trees.....	37
Table 27: The t-test assuming equal variance.....	38
Table 28: Relationship between field-based and remote sensing method (TLS threshold) estimated AGB. .....	38
Table 29. Descriptive statistics of plot based estimated AGB using field-based and remote sensing method.....	39
Table 30: Relationship between field-based and remote sensing method estimated AGB per plot.....	40
Table 31: F-test equal variance or un equal variance.....	40
Table 32: The t-test for a significant difference between field-based and remote sensing method estimated AGB.....	41
Table 33: Descriptive statistics of carbon stock.....	41

## LIST OF EQUATIONS

---

Equation 1: Allometric equation (AGB).....	24
Equation 2: Above-ground biomass carbon.....	24
Equation 3: Root Mean Square Error.....	25
Equation 4: Root Mean Square Error percent.....	25
Equation 5: Bias equation.....	25

## LIST OF APPENDICES

---

Appendix 1: Slope correction table.....	60
Appendix 2: Field data collection sheet.....	61
Appendix 3: Illustration of the UAV flight plan.....	61
Appendix 4: Distribution of tree parameters.....	62
Appendix 5: Summary of field recorded biometric data.....	63
Appendix 6: Relationship between field measured, and TLS derived height of the lower canopy trees.....	64
Appendix 7: Relationship between field measured and TLS derived DBH of the lower and upper canopies. .....	64
Appendix 8: Relationship between field measured and UAV derived upper canopy tree heights. ....	65
Appendix 9: Relationship between the AGB estimated using UAV derived, and TLS derived height threshold to integrate the upper and lower canopy trees.....	65
Appendix 10: Descriptive statistics of field-based and remote sensing estimated AGB.....	66
Appendix 11: Scatter plot between field-based and remote sensing method estimated AGB. ....	66
Appendix 12: The t-test for field-based and remote sensing method estimated AGB.....	66
Appendix 13: Relationship between field-based and remote sensing method estimated AGB. ....	67
Appendix 14: Relationship between field-based and remote sensing method estimated AGB. ....	67
Appendix 15: Summary of field-based and remote sensing method upper canopies tree parameters.....	68
Appendix 16. Summary of field-based and remote sensing method lower canopies tree parameters. ....	69
Appendix 17: Summary of remote sensing method estimated AGB/carbon of the lower and upper canopies.....	70
Appendix 18: Orthomosaic image of 2017 and 2018 KRUS tropical rain forest.....	71

## LIST OF ACRONYMS

---

AGB	Above Ground Biomass
AGBC	Above ground Biomass Carbon
ALS	Airborne LiDAR Scanner
CF	Conversion Factor
CHM	Canopy Height Model
CPA	Canopy projection Area
D	Diameter
DBH	Diameter at Breast Height
DGPS	Differential Global Positioning System
DSM	Digital Surface Model
DTM	Digital Terrain Model
FAO	Food and Agricultural Organization, of the United States
GCP	Ground Control Points
GPS	Global Positioning System
H	Height
Kg	Kilogram
KRUS	Kebun Raya Unmul Samarinda
LiDAR	Light Detection and Ranging
Mg	Megagram
MRV	Monitoring Reporting and Verification
REDD+	Reducing Emission from Deforestation, and Forest Degradation
RMSE	Root Mean Square Error
TLS	Terrestrial Laser Scanner
UAV	Unmanned Arial Vehicle
UNFCCC	United Nations Conventions on Climate Change
$\rho$	Density



# 1. INTRODUCTION

## 1.1. Background

Forests have a vital role in global climate change mitigation through their nature of carbon sequestration (Pan et al., 2011). According to Gibbs et al. (2007), forests have the highest carbon-storing capacity in the terrestrial ecosystem. From the total carbon stock in the terrestrial ecosystem, about 80% of the carbon is storing in the aboveground forest biomass (The World Bank, 2015). Thus, tropical rain forests are one of the largest terrestrial forest ecosystems which are storing a large amount of carbon stock. According to Hunter et al. (2013) about half of the Above Ground Biomass Carbon (AGBC) stored in the vegetation was found in tropical rain forests.

Even though forest plays a crucial role in climate control, deforestation and forest degradation have been a serious problem in many developing countries as a result of human-induced activities (Mohren et al., 2012). When forests are cut down (removed) the carbon stored in their biomass is released to the environment in the form of CO<sub>2</sub>, and it influences the concentration of Green House Gases (GHG) (Gibbs et al., 2007). According to FFPRI. (2012), developing countries account for about 20% of the anthropogenic carbon dioxide emission from deforestation and forest degradation. Nowadays, the increment of carbon dioxide emission to the environment as a result of deforestation and forest degradation has been the major concern of the world (UNFCCC, 2011). As a result, many countries signed an agreement regarding the climate change conventions focusing on the causes, mitigation mechanisms and consequently reducing the emission of carbon to the atmosphere.

Reducing Emission from Deforestation, and forest Degradation,(REDD+) is initiated under the UNFCCC which is focusing on Monitoring, Reporting, and Verification (MRV) mechanism of AGB/carbon stock, and for sustainable protection of the forest ecosystem (UNFCCC, 2011). Besides, the international agreement on climate change offers financial support to developing countries as compensation for countries practicing afforestation and forest conservation (Gibbs et al., 2007). The UNFCCC needs an annual report from each participating country regarding the amount of sequestered carbon on forests through the MRV mechanism (United Nations, 2018). Thus, to minimize uncertainties and doubts on the amount of carbon sequestered the UNFCCC requires an accurate and transparent way of estimating aboveground biomass/carbon stock for its management purpose (Peltoniemi et al., 2006). However, estimation of AGB in tropical rain forests many challenges due to the complexity of the vertical canopy structure of the forests (Hunter et al., 2013). Tropical rain forests are found in countries near to the equator such as Indonesia.

Indonesia has broad coverage of coastal and tropical rainforests including the East Kalimantan forests. However, it is one of the countries which has a significant effect on the increment of national Green House Gases (GHG) resulting from deforestation and forest degradation (The World Bank., 2015). Accordingly, in the national and international agreement for climate change, Indonesia is one of the countries which was committed or agreed to reduce carbon emission from deforestation and forest degradation through the Ministry of Forestry and Environment (Indrarto et al., 2012). Thus, the REDD+ program is being implemented under the Ministry of Forest and Environment to improve the governance and management of the forests. REDD+ program provides financial support for developing countries to reduce carbon emission from deforestation (Gibbs et al., 2007). However, to get the incentive, developing

countries have to measure and report the amount of forest biomass conserved to UNFCCC through REDD+ Measuring, Reporting, and Verification system (MRV) (United Nations, 2018). Therefore, an accurate, efficient and reliable estimation of biomass using cost-effective method was demanded by developing countries and REDD+ program (Peltoniemi et al., 2006; FFPRI, 2012). For this reason, different methods and approaches have been developed to estimate forest biomass.

There are different techniques and methods used to estimate the above-ground forest biomass/carbon stock. The destructive method is the most accurate technique which contains cutting, drying and weighing of the biomass. However, it is time-consuming, unsustainable, labor intensive and it covers a small area (Chave et al., 2014). The other method is the non-destructive method which uses tree parameters as an input to estimate AGB using the allometric equation (Basuki et al., 2009). Forest parameters can be measured manually at field level and remotely by using remote sensing. Thus, the estimation of AGB by using remote sensing technology is recommended by UNFCCC for the MRV of carbon stock (FFPRI, 2012).

Remote sensing technology has a decisive role in monitoring and mapping of AGB/carbon stock through a non-destructive method by using different techniques. Many studies are carried out using various remote sensing techniques to estimate and map forest AGB/carbon stock for the last few decades (Brovkina et al., 2017). The Light Detection and Ranging (LiDAR), very high-resolution optical sensors, and Synthetic Aperture Radar (SAR) are among the commonly used remote sensing techniques (FFPRI, 2012). These remote sensing techniques can be used for large scale forest monitoring and estimation including tropical rain forests. While this is true, in dense tropical forests using low to medium resolution optical remote sensing techniques, has some drawbacks in assessing forest parameters (Hyde et al., 2006). Generally, tropical rainforests are composed of broad-leaved trees, and it has dense canopies (Smith, 2015). Hence, the complexity in vertical structure and the density of the forest makes it difficult to measure forest parameters using optical remote sensing (Larjavaara & Muller-Landau, 2013). While this is true, by integrating Aerial-based and ground-based remote sensing method such as UAV and TLS, the upper and lower canopy tree parameters can be extracted accurately to improve the AGB estimation (Aicardi et al., 2017).

## 1.2. Research Problem

Estimation of carbon stock in the multi-layered tropical rain forest (Figure 1) remains with uncertainties due to the density of the forest and other problems (Hunter et al., 2013). In tropical forest data acquisition by aerial imagery can cover a vast and inaccessible area. However, it is not always effective because the lower canopy tree cannot be retrieved or assessed due to foliage and occlusion (Aicardi et al., 2017). Nowadays, various type of research has been done to improve the uncertainties in forest biomass estimation by integrating different remote sensing techniques, for instance; combining TLS and ALS for tree height measurement of the lower and upper canopy respectively (Fritz et al., 2011). Thus, air-borne Lidar has a better accuracy measuring tree height of the upper tropical forests. Although, this can pose a financial constraint and not always available (Aicardi et al., 2017). Comparatively, using UAV and TLS have the potential to assess the upper and lower canopy tree parameters for the tropical rain forest with a reasonable cost and accuracy.

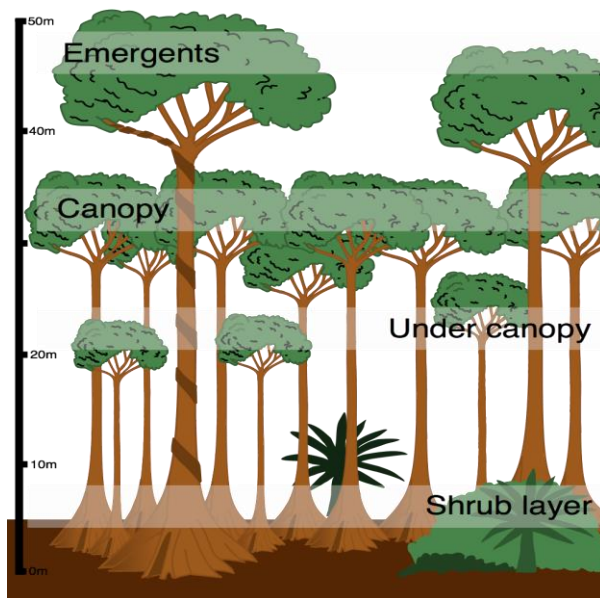


Figure 1: Illustration of tropical rainforest canopy strata. Source; (Layers of a Rainforest, n.d.)

Unmanned Aerial Vehicle (UAV) is a lightweight and cost-effective technology which has the potential to acquire high spatial and temporal resolution images. Besides, the structure from motion (SfM) of UAV allows constructing 3D objects from 2D overlapping images using image-based modeling (Micheletti et al., 2015). The important forest parameter, Canopy Projection Area (CPA) is the area clutch by the outer edge of the tree crown on the flat terrain (Gschwantner et al., 2009). Previous studies show that the CPA has a relationship with DBH (Hirata et al., 2009; Song et al., 2010). From UAV image-based modeling, the derivatives of tree parameters such as Canopy Projection Area (CPA), height, and DBH can be extracted accurately and enables to estimate AGB (Næsset et al., 2004). Furthermore, the quality and accuracy of UAV derived CHM (height) depends on the number and distribution (configuration) of ground control points (GCP) used for mosaicking the UAV images (Nex & Remondino, 2014). However, in the closed canopy and multi-layered structure of tropical forests, UAV has a limitation to assess the lower-canopy trees, unlike the upper canopy the point cloud of the UAV can be blocked by the upper tree crowns (canopies), and it cannot penetrate the closed upper tree crowns to detect the lower canopy trees (Aicardi et al., 2017).

Terrestrial Laser Scanner (TLS) technology is a ground-based active remote sensor which can retrieve the vertical and horizontal tree parameters accurately through its dense point clouds (Jung et al., 2011). TLS data acquisition can generate a high level of 3D point clouds which enables extraction of tree parameters accurately (Calders et al., 2015). Thus, TLS data can substitute for the conventional measurement of tree parameters (Kaasalainen et al., 2014). Ramirez et al. (2014) mentioned that TLS could retrieve tree parameters such as; height, DBH, tree number, position, and tree volume accurately. However, in dense and multi-layered canopy forests, it cannot assess the actual peak of the upper canopy trees due to occlusion. Therefore, assessment of tropical rain forest AGB using UAV or TLS a stand-alone can lead to underestimation. Thus, plot-based integration of UAV and TLS derived tree parameters can complement each other to overcome the limitations encountered on each to estimate AGB in a reasonable cost and accuracy (Aicardi et al., 2017). However, there are a limited number of studies on the integration of UAV, and TLS remote sensing method to estimate plot based AGB in tropical rain forests.

Therefore, this study aims to integrate UAV and TLS derived forest parameters of the KRUS tropical forest to improve a plot based AGB estimation, by using the UAV derived height threshold, and TLS



derived height thresholds to integrate the upper and lower tree canopies, at East Kalimantan, Indonesia. The conceptual diagram of the study is showing in Figure 2.

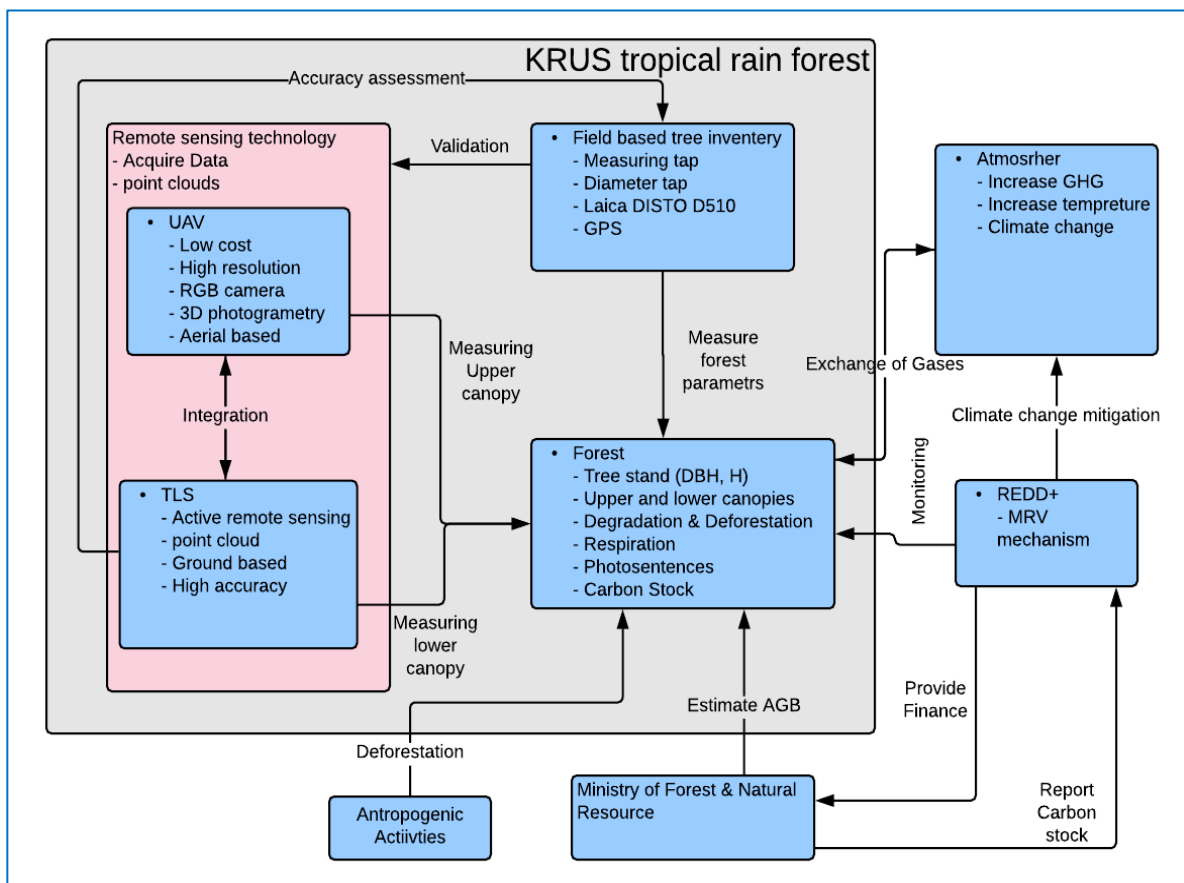


Figure 2: Conceptual diagram of the study.

### 1.3. Objectives

#### 1.3.1. General objectives

The main objective of this research is to test the potential of integrating Terrestrial Laser Scanner (TLS), and Unmanned Aerial Vehicle (UAV) data to improve the accuracy of plot based AGB/carbon stock estimation in KRUS tropical rainforest, East Kalimantan, Indonesia.

#### 1.3.2. Specific objectives

1. To assess the accuracy of field measured height as compared to TLS derived height of the lower canopies.
2. To assess the accuracy of TLS derived DBH as compared to field measured DBH of lower and upper canopies.
3. To assess upper canopy tree height using CHM derived from UAV point cloud and assess its accuracy.
4. To compare the remote sensing method estimated AGB (UAV+TLS) integrated by using the UAV derived, and TLS derived height thresholds for integrating the upper and lower canopy trees.
5. To estimate AGB/carbon stock using the integration of UAV and TLS and compare its accuracy with field measured AGB/carbon stock on a plot base.

#### 1.4. Research questions

1. What is the accuracy of field-measured tree height as compared to TLS derived tree height of the lower canopies?
2. How accurate is the TLS derived DBH, as compared to field measured DBH of the lower and upper canopy trees?
3. How accurate is the upper canopies tree height derived from UAV-CHM as compared to field measured heights?
4. What is the amount of AGB estimated from the integration of UAV and TLS integrated using the UAV derived height and the TLS derived height as a threshold to combine the upper and lower canopy trees?
5. What is the estimated AGB using the integration of UAV and TLS data as compared to field measured AGB on a plot base?

#### 1.5. Hypothesis

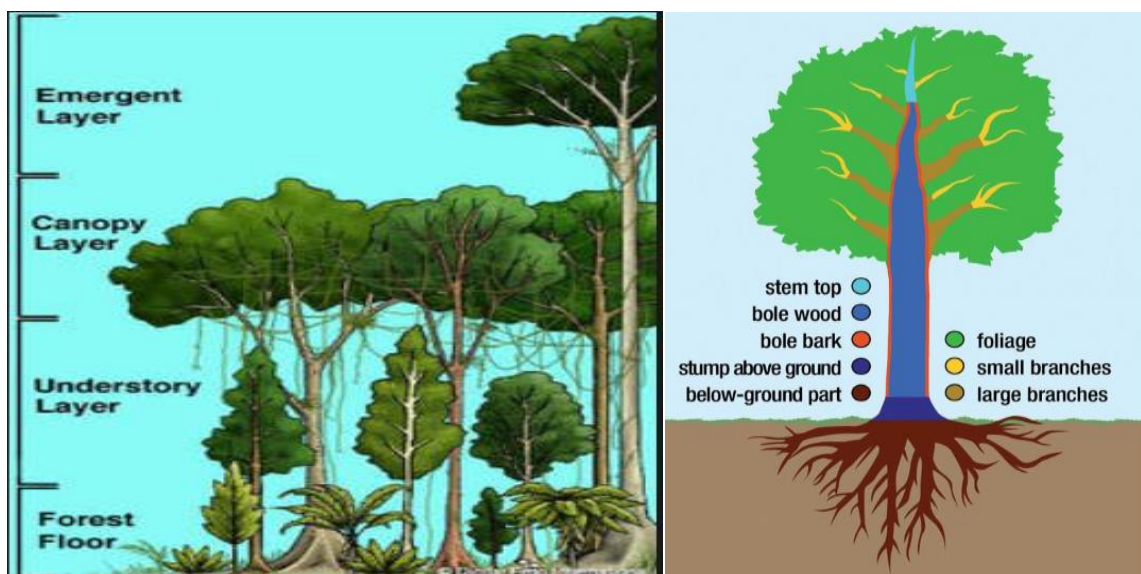
1. Ho: There is no significant difference between the field measured tree height as compared to TLS, derived height of the lower canopy.  
Ha: There is a significant difference between the field, measured tree height as compared to TLS, derived height of the lower canopy.
2. Ho: There is no significant difference between the TLS derived DBH of lower and upper canopies as compared to field measured DBH.  
Ha: There is a significant difference between the TLS derived DBH of lower and upper canopies as compared to field measured DBH.
3. Ho: There is no significant difference between the height derived from UAV-CHM and field measured height.  
Ha: There is a significant difference between the height derived from UAV-CHM and field measured height.
4. Ho: There is no significant difference, between the remote sensing method AGB, integrated using the UAV, derived height, and the TLS derived height as a threshold to integrate the upper and lower canopies.  
Ha: There is a significant difference between the remote sensing method AGB integrated using the UAV derived height, and the TLS derived height as a threshold to integrate the upper and lower canopies.
5. Ho: Plot-based estimated AGB using integrating TLS and UAV has no significant difference as compared to the field estimated AGB of the tropical rain forests.  
Ha: Plot-based estimated AGB using integrating TLS and UAV has a significant difference as compared to the field estimated AGB of the tropical rain forests.

## 2. LITERATURE REVIEW

### 2.1. Tropical rain forest

Tropical rainforests are composed of broad-leaved, evergreen trees found in the hot and moist region of the tropics (Smith, 2015). It has complex and dense vertical canopy structure namely the emergent canopy, continuous canopy and understory canopy (Figure 3) from top to lower respectively (Mohd Zaki & Abd Latif, 2017). The tropical rainforests have many advantages to a human being such as environmental goods and services. Among this, climate regulation is a typical role as a result of sequestering a large amount of carbon in its biomass (Stas, 2011). Tree biomass is defined as the total mass (volume) of the above and below-ground dry weight of the tree per unit area. Thus, the stem, leaf, and branches are considered as aboveground biomass (Gschwantner et al., 2009). On the other hand, below ground biomass refers to the total life root biomass found below the surface (Ravindranath et al., 2008).

In the tropical forest carbon is stored in different parts such as; soil organic matter, dead woods, understory vegetations and in the stand forests (Vashum, 2012). In this study, forest biomass is considered as the aboveground live biomass of the tropical forest trees in which its carbon content is half of its biomass (Basuki et al., 2009) (Figure 3). Truly, 80% of the terrestrial carbon is stored in the forest ecosystem and out of this 50 % is found in tropical forest (The World Bank, 2015). Thus, tropical forests have an important role in carbon sequestering, and it needs an accurate and cost-effective estimation of AGB/carbon stock to support the global aim of REDD+ (Gibbs et al., 2007; FAO, 2010). According to Gibbs et al. (2007), there is no methodology yet which measures carbon stock directly across the terrestrial forest ecosystem. However, there are techniques and models which were developed from a destructive sampling method by using different equations and relations such as allometric equation using measured tree DBH and height.



A. Source ("Layers of a Rainforest," n.d.)

B. Source (Gschwantner et al., 2009)

Figure 3: Structure of tropical rainforest (A) and parts of AGB and BGB/ Carbon stock (B).

### 2.1.1. Allometric Equation

The allometric equation is an approach which is developed by the relationship of forest parameters (i.e., DBH and height) with the total tree body mass destructively to estimate AGB (Beets et al., 2012). Based on the accuracy of input tree parameters the developed allometric equation is the most reliable non-destructive method of forest biomass estimation (Wang, 2006). Depending on such criteria there are different allometric equations which are developed by various researchers using destructive data. Based on the study area and forest type selection of site-specific and a species-specific allometric equation is essential for precise AGB estimation (Basuki et al., 2009). In the same way, consideration of climatic condition and forest structure have a role in the accurate estimation of forest biomass (Yuen et al., 2016). The tropical rainforest has a diverse, mixed type of species, for this reason, the generic allometric equation developed by Chave et al. (2014) was appropriate (Hunter et al., 2013).

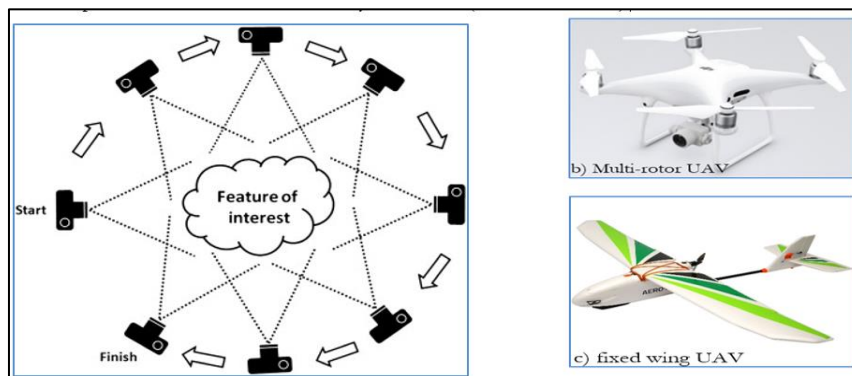
Allometric equation

$$AGB_{est} = 0.0673 \times (\rho D^2 H)^{0.976}$$

Where;  $AGB_{est}$  is Above Ground Biomass estimated (KG),  $\rho$  is wood density ( $g/cm^3$ ),  $D$  is diameter at breast height (cm), and  $H$ , is tree height (m). Source (Chave et al., 2014).

### 2.1.2. Application of UAV in forestry

Unmanned Aerial Vehicle (UAV) or Unmanned aircraft was developed in 1961 by Lawrence and Elmer Sperry in America (Nonami., 2007). Initially UAV is designed for the military purpose, but later on, due to the applicability and availability, its demand increases by civilians application (Zhang et al., 2016). There are two types of UAV categories namely; fixed wings and multi-rotors (copters) (Figure 4). These technologies have some differences in terms of flight time, area coverage and payloads. For the photogrammetric application, the fixed-wing aircraft which needs a larger area to take-off is preferable for a wider coverage data acquisition whereas the multi-rotors needs a small space to take-off, and it is preferable for small areas data acquisition (Turner et al., 2012). Photogrammetry is a science which uses a sequence of 2D images using structure from motion (SfM) technique to construct 3D objects and enables to perform measurements on the object without having any physical measurement (Ordonez et al., 2010). Nowadays, UAV photogrammetry uses for surveillance, topographic applications, video, forest monitoring and for 3D Image-Based Modelling (IBM). The UAV image-based modeling uses for biomass estimation by generating 3D dense point clouds and extracting forest parameters (Kachamba et al., 2016). A recent study by Mtui (2017) shows that image-based modeling of UAV derived point cloud can be used to extract tree height and crown dimension in the tropical rain forests. In forest monitoring, application of UAV is a promising technology due to the availability in low cost and spatial resolution, and the data do not need of atmospheric correction since the UAV fly low altitude (Getzin et al., 2012).

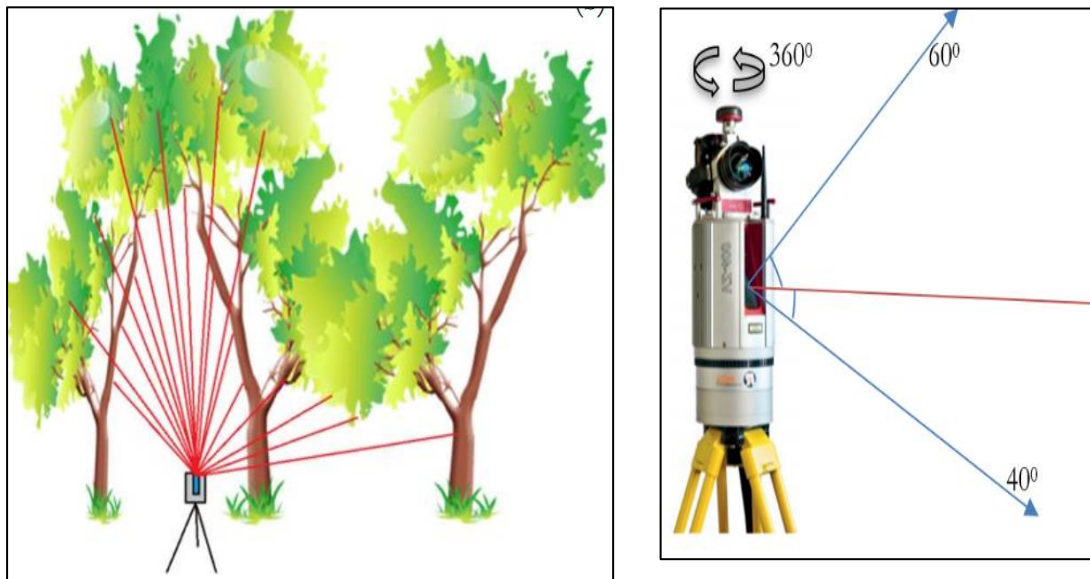


A. Image acquisition using structure from motion (SfM) source: (Westoby et al., 2012).

Figure 4: Illustration of structure from motion image acquiring (a) and types of UAV - b, c.

### 2.1.3. Application of TLS in forestry

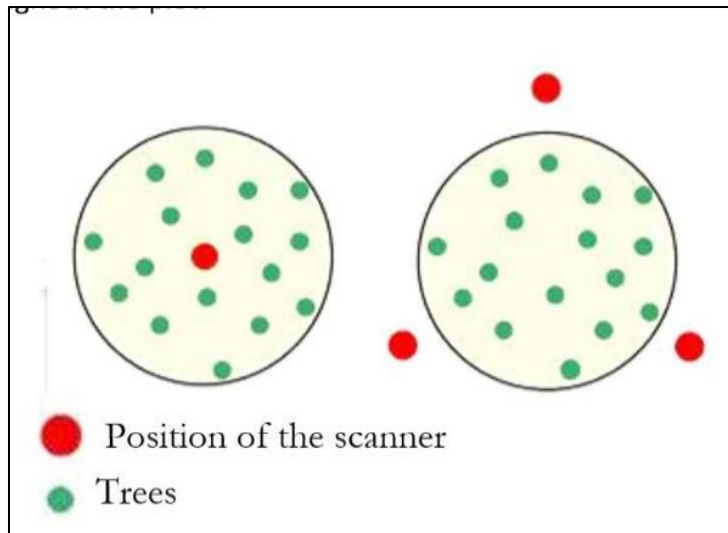
Terrestrial Laser scanner also called terrestrial LiDAR is a ground-based technology which enables to acquire 3D point cloud data from the surrounding object by emitting laser beams. LiDAR is one of the active remote sensors which sends a pulse in the non-visible wavelength range and records the coordinate of the object by measuring the distance between the sensor, and the targets object using the point cloud travel time and the speed (Dassot et al., 2011). The instrument is fixed on a tripod (Figure 5) and the complete horizontal rotation with the vertical angular view of the mirror allows to acquire a hemispherical scanning (Dassot et al., 2011). Forest parameters like DBH, height, number, and position of tree and tree crown can be retrieved from the scanned point cloud which can be used for estimation of AGB (Bienert et al., 2006). RIEGL VZ-400 TLS was used in this research. It has an attached Digital Single Lens Reflex camera (DSLR) which can enable to acquire the colored RGB imagery of all scanned objects with the corresponding scan of the 3D point clouds. The RIEGL VZ-400 Terrestrial Laser Scanner is a ground-based remote sensor which can acquire an accurate forest structure through its dense point cloud (Newnham et al., 2015).



Source: (AWK-WIKI, 2016, cited in Bazezew, 2017), Source: (RIEGL RIEGL VZ-400 VZ-400, 2017).

Figure 5: Operating system of TLS - left side and RIEGL VZ 400 TLS -right.

There are two types of scanning techniques in terms of the scanning position namely; the single scanning position and multiple scanning positions (Bienert et al., 2006). In the multi-scanning method, the scanning process is taken from four different positions of the sampling plot to construct a 3D structure of the objects. While in the single scanning position method the location of the scanner is placed only in one position (e.g., inside of the plot) of the object and only one side of the object is detected by the TLS technology. The multi-scan method provides a complete 3D structure of the objects depending on the number of scanning positions, and it also needs more time for each scan (Dassot et al., 2011). As shown in Figure 6 in forestry application the single scan is placed at the center of the sample plot while in the multiple scans the scanning positions are placed inside (i.e., the center of the plot) and outside of the sample plots (Bienert et al., 2006). Studies show that TLS derived DBH and height are very accurate when it compares with field-measured tree parameters (Calders et al., 2015).



Source:(Bienert et al., 2006).

Figure 6: Single and multiple scanning positions.

#### 2.1.4. Integration of TLS and UAV

The emerging Unmanned Aerial Vehicle (UAV), which has a high spatial resolution can be used for different applications including forest monitoring. Through UAV 3D image-based modeling CHM (tree height) and orthomosaic images of forest structure can be generated from the structure from motion (SfM) images (Kachamba et al., 2016). In the forestry application, the aerial acquisition of tree parameters in dense canopy forests has associated with a limitation to detect the lower canopy tree (Aicardi et al., 2017). In the other case, TLS is a ground-based remote sensing technology in which basic forest parameters like DBH, height, crown and tree position can acquire accurately (Bienert et al., 2006). However, in dense and multi-layered canopies TLS cannot assess the most upper tree canopies due to occlusion. Based on this, previous studies show that in forests which have a multi-layered canopy structure integration of aerial acquisition and ground-based acquisition using remote sensing methods enables to extract all the upper and lower canopy tree parameters. Therefore the combination of TLS and UAV derived tree parameters have a significant advantage to improve the accuracy of AGB estimation (Aicardi et al., 2017).

#### 2.1.5. Handheld laser instrument (tree height measurement)

The accuracy of biomass estimation in tropical forests depends on the accuracy of individual tree height measurements and the subsequent plot based biomass (Hunter et al., 2013). Likewise, the accuracy of tree height measurement depends on the type of materials used, the experience of the observer and forest structure. In tropical forests using traditional field-based height, measurement has been influencing by the understory vegetation and the layered canopies which limits the line of view (Larjavaara & Muller-Landau, 2013). There are different types of handheld instruments which can be used for the tree height measurements. A study by Williams et al. (1994) have tested five hand-held devices for reliable tree height measurements, and the laser height finder like Leica DISTO D510 has produced fair result comparatively with the others hand-held instruments. Besides, in tropical rainforest, TLS can measure an accurate height of the under-canopy trees rather than Leica DISTO D510 laser instrument.

## 3. METHODS AND MATERIALS

### 3.1. Study area

Kebun Raya Unmul Samarinda (KRUS) educational forest also known as Unmul Samarinda Botanical Garden is one of the tropical rain forests found in Eastern Kalimantan province, Indonesia. It is located approximately 10 kilometers to the north side of Samarinda city and covers an area of 300 hectares (Trimurti, 2018). The forest is used for different educational research purposes as a conservation forest by the Mulawarman University of Indonesia, and in 2010 some part of the area (62 ha) is decided to be used as a recreational area. In the past, the KRUS tropical forest was one of the areas affected by fire in East Kalimantan, and later the forest develops as secondary forests (Diana et al., 2002). The geographical location of the KRUS tropical rain forest is between 0°25'10" N and 117°14'14" E in the East Kalimantan province as shown in Figure 7.

#### 3.1.1. Climate and topography

The KRUS conservation forest is characterized by an average annual temperature of 29.9 °C maximum and 21.4 °C minimum. The rain-fall ranges are between 2000 and 2500 mm/year, and the rainfall type is slightly seasonal in which the intensity of the rainfall is somewhat lower from June to October. The soil type of the study area is Ultisols (Ohta & Effendi, 1992). The forest area has partially undulating terrain surface.

#### 3.1.2. Vegetation

The vegetation category of the forest was a Dipterocarpace type of primary natural forest. Later as a result of fire disaster in 1983 the vegetation type replaced by a fast-growing species and has developed as a secondary forest (Trimurti, 2018). The forest is dominated by the species like *Homalanthus*, *Trema*, *Mollotus*, and *Macarange* which are emerging by fast-growing and succession after the forest was burned (Diana et al., 2002). Nowadays, the forest is categorized as conservation forest which includes secondary forest reserve and collection zone (natural and artificial forest) (Trimurti, 2018). In general, it has multi-layered canopy strata and has a high level of species diversity. The existence of multi-layered canopy structure and density of the forest compliance with the overall objective of this study to test the potential of the remote sensing methods to extract accurate tree parameters of the upper and lower canopies.

The location of KRUS tropical forest.

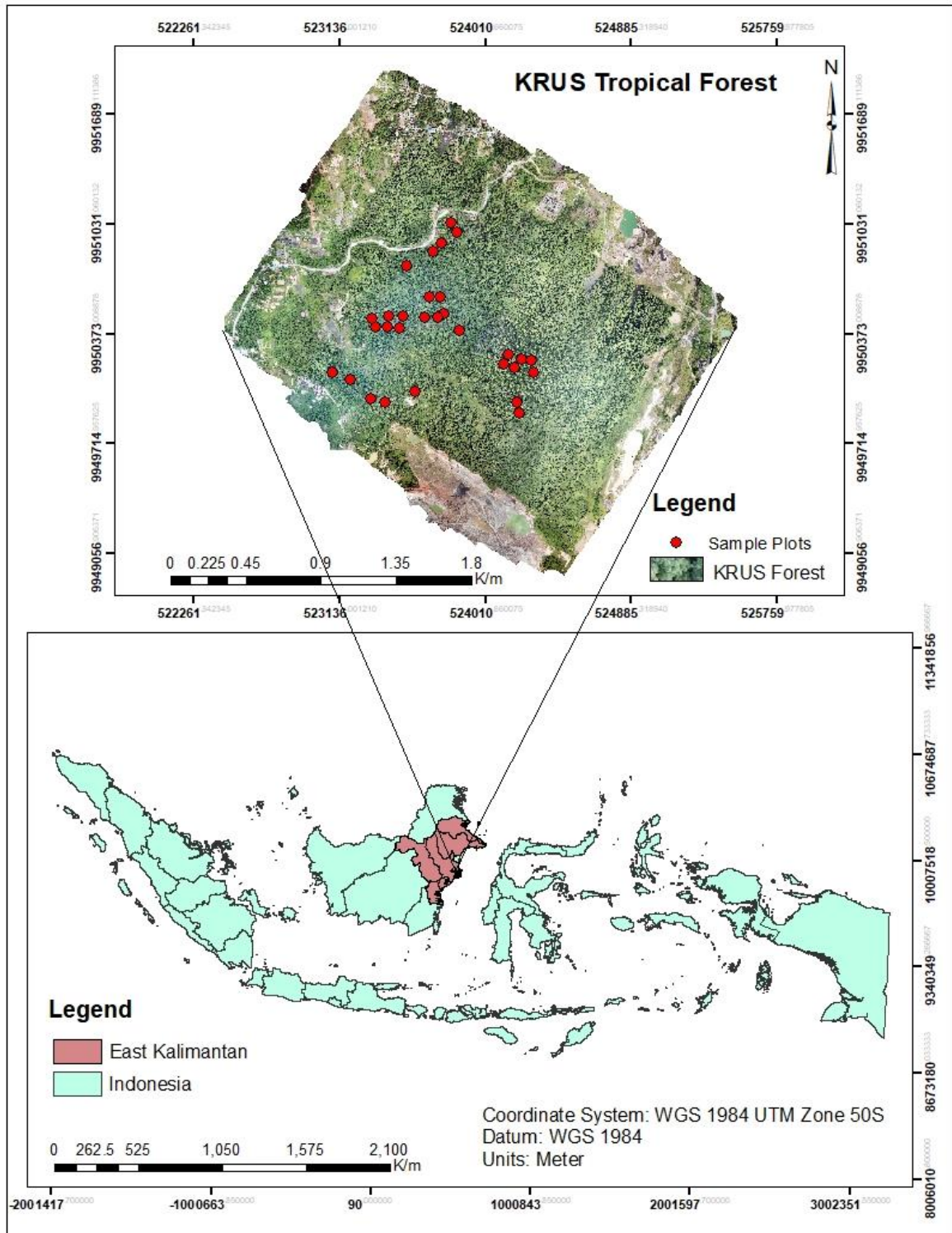


Figure 7: Study area of KRUS tropical forest location.



## 3.2. Materials

### 3.2.1. Field equipment and instruments

To collect the data different materials and equipment were used in the field. The details of the field instruments used are shown in Table 1.

Table 1: List of field instruments and equipment used in the research.

S/N	Instruments /equipment	Purpose /Specific function
1	UAV Phantom 4 DJI	Acquiring 2D sequence images
2	RIEGL VZ-400 - TLS	Tree acquisition (scanning)
3	Orthomosaic image of 2017	Sample plot designing and upper tree crown identification
4	GPS (Garmin)	Positioning and navigation
5	Tablet/Mobile	Navigation and tree crown identification
6	Measuring tap (30m)	Plot layout and setting
7	Diameter tape (5m)	Tree DPH measurement
8	Leica DISTO D510	Tree height measurement
9	Suunto clinometer	Slope measurement
10	Tree tag	Tagging tree number
11	Datasheets	Recording data
12	Binder	Binding the data sheets

### 3.2.2. Tools and software

The collected remote sensing data were acquired using various tools, and for processing and analyzing different application packages were used. Detail of the tools and software are listed in Table 2.

Table 2: List of software packages and tools used for the study.

S/N	Software	Purpose
1	RiSCAN PRO	TLS data processing
2	Pix4D	UAV data processing
3	ArcGIS 10.6	Data processing, extraction
4	CloudCompare	Analyzing point clouds
5	ERDAS IMAGINE	Image processing
6	Mendeley Desktop	Citation and referencing
7	Lucid chart	Flowchart preparation
8	Microsoft Excel	Data analysis
9	Microsoft Word	Proposal and Thesis writing
10	Microsoft power point	Presentation of proposal and results
11	SPSS	Statistical analysis

## 3.3. Method

The method has four main parts as shown in the flow chart in Figure 8.

- 1) Field biometric measurement and estimation of AGB  
Tree parameters which include DBH, height, and coordinates were collected for all sample plots. Besides, field derived DBH were used to assess the accuracy of TLS derived DBH.
- 2) UAV data acquisition and processing (upper canopy data extraction)  
From the UAV 3D image-based modeling, the ortho-mosaic image and CHM (DSM–DTM) was generated. These data were used for the delineation of CPA and extraction of tree height.

- 3) TLS scanning data and tree extraction (lower canopy data measurement)  
The multi-scanned TLS data were registered and used to extract tree height for the lower canopy and DBH for both upper and lower canopies. Each tree derived from TLS was matched with its corresponding field recorded tree number. The accuracy of TLS derived DBH (upper and lower canopy) were assessed using the field measured DBH.
- 4) Integration of upper and lower canopies and estimation of AGB from the integrating UAV and TLS derived tree parameters using two techniques. Then, the AGB estimated using the two thresholds was compared. Finally, the remote sensing method estimated AGB was validated and assessed its accuracy using the field based estimated AGB.

**Flow chart of the study.**

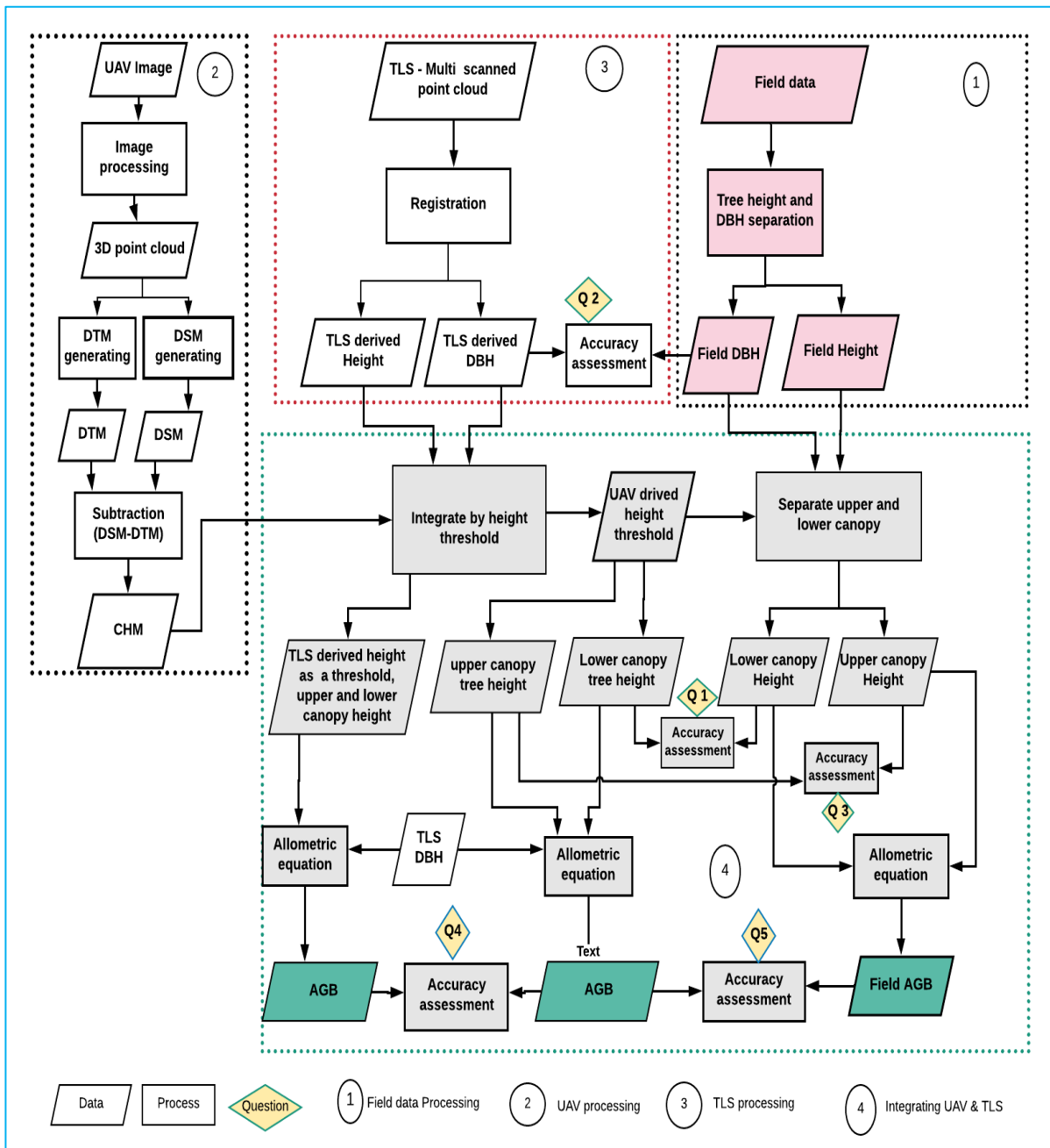


Figure 8: Shows flow chart of the research method.

### **3.3.1. Pre-fieldwork**

Pre-fieldwork preparation was essential for data collection. Thus, equipment's such as GPS, Leica DISTO D510, Tablet, and TLS are tested at nearby forest (Park) areas in Enschede before going to the field. Besides, field data collection sheets (Appendix 2) and the orthomosaic image of 2017 were prepared. UAV flight plan and UAV components such as the battery, memory card, and cables were organized.

### **3.3.2. Plot size**

The sampling plots were designed as circular in shape with a size of 500m<sup>2</sup> and radius of 12.62m. Besides, at the sloping area, the radius of the plot was corrected based on the slope correction table attached in appendix 1 (Abegg et al., 2017). The circular plots were suitable for TLS scanning positions, and the number of trees stands on the edge are less as compared to the square plots. As mentioned by Maniatis & Mollicone. (2010) Circular plots are preferable than rectangular sample plots because the method minimizes trees found (standing) on the corner edge. In addition, wider sample plot which is more than 500 – 600 m<sup>2</sup> increases the time and cost of data collection whereas its result has no significant effect on the accuracy of the data (Ruiz et al., 2014).

### **3.3.3. Sampling design**

In this study, a purposive sampling method was adopted by considering the undergrowth vegetation, terrain type, time availability, and accessibility to the road. Thus, the selected sample plots were covered/represent the genuine characteristics of all the variation of the forest structure in the study area. It is a non-probability sampling method in which plots were selected by the accessibility of the forest area. Moreover, the difficulty of holding and transporting of the TLS instrument with a very heavy weight of 28 KG was another reason why the purposive sampling was preferred. Based on this, data were collected from 30 circular plots, and the center of the plots was recorded by GPS on the data collection sheet.

## **3.4. Field data collection**

### **3.4.1. Biometric field data measurement and collection**

The biometric field data collection was done within October 2018, and it has included measurements of tree height and DBH. Diameter tape and Leica DISTO D510 were used to measure DBH and height respectively. From each sample plot (500m<sup>2</sup>) the following data; Plot (Plot number, radius, slope, coordinate), and Individual tree parameters (Tree number, DBH, Height, coordinate) (Figure 9) were recorded. Trees with DBH < 10cm were not considered because these trees have insignificance contribution to biomass (Brown, 2002). Tree DBH was measured at 1.3m sub-height of the stem from the base of the tree, while buttress trees were measured from the highest side of the ground base. In case of fork tree, if the fork height was below 1.3m, it was considered as more than one trees, and if the fork height was above 1.3m from the base of the tree, it was considered and measured as one tree.



Figure 9: Illustration of plot based biometric data collection. Source; (Asmare, 2013) modified

### 3.4.2. Field level individual upper canopy tree identification

In multi-layered forests such as KRUS tropical forest, identification of the upper canopy from the lower canopy and matching of the upper canopy (CPA) with its respective DBH was a challenging task. Thus, during the biometric data collection, the individual upper canopy tree crowns were identified using Avanza Map, Locus Map, and manual inspections. The orthomosaic image of 2017 KURUS forest was prepared as a Map by clipped into different large-scale Maps and uploaded on the Tablet and Mobile. Both Maps have a navigation GPS pointer and a button which can be used to make a placemark on the visible upper tree crowns on the orthomosaic image. Thus, using the navigating GPS on screen, and by physical observation on the actual trees, a placemark was pinned on the upper tree crowns, and the tree number was given as the same number with its corresponding DBH it founds in the tree tag mounted in the stem.

Furthermore, the Avenza Map enable to measure the radius of the plot and plotting the layout of the plot circle (500m<sup>2</sup>) on the Map simultaneously with the biometric data recording time. Hence, the generated plot circle helped as a reference to move and to identify the trees within the sample plot because the GPS of the Avenza Map shows whether the location (track) movement was inside the sample plot or outside the circle (Figure 10).

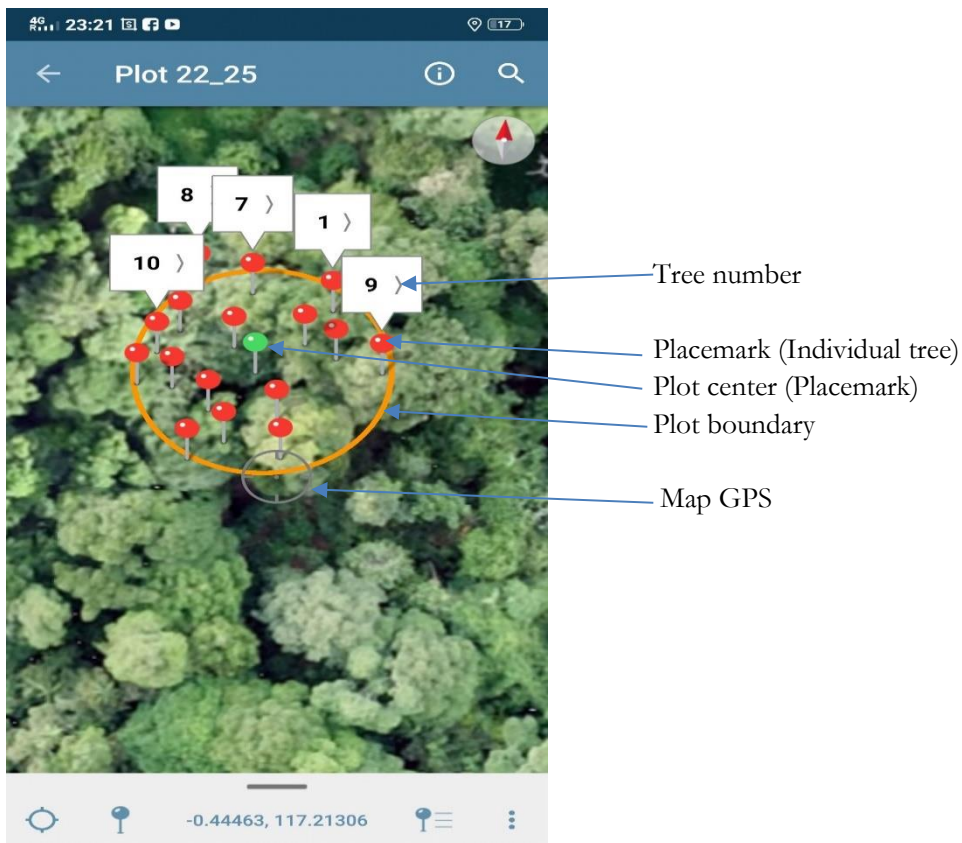


Figure 10: Illustration of individual upper canopy trees identification by Avenza Map (Plot 22).

### 3.4.3. UAV data acquisition

The Phantom 4 DJI multi-rotary UAV (Figure 11) was used to acquire a sequence of 2D over-lapping images because in tropical forests vertical flight is required to take-off and landing of the UAV inside the forest within the existing open area (Aicardi et al., 2017).



Figure 11: Phantom 4 DJI UAV-left, and GCP 60x60cm marker-right.

### Ground control point

UAV image acquisition was considering the number and configuration of GCP. Based on the availability of existing open space of the forest, evenly distributed ground control points were used to ensure the quality of image matching and geo-referencing (Nex & Remondino, 2014). The pre-identified open places were pre-marked using the GCP marked board, (Figure 11) and in each center of the marked board, the coordinates (X, Y, Z) were recorded as GCP using Differential GPS (DGPS). Hence, these GCPs were used for the spatial referencing (geo-referencing) of the 3D image-based modeling of the UAV data.

### Flight planning

PIX 4D capture application was used for the mission planning, and the technical parameters settings such as overlapping, flight height and speed were defined in the setting button (Appendix 3). The flight height (altitude) were defined based on the height of the trees and the terrain elevation level. The highest terrain elevation points and height of the tree were taken as a reference to decide the flight height in each flight mission to reduce the risk of collision among the emergent tree and UAV. Take-off and landing point were selected at places which have a little bit higher altitude and have more open space to avoid the connection loss between the UAV and the remote-control device.

#### 3.4.4. TLS data collection

For the TLS data acquisition, RIEGL VZ-400 TLS (Table 3) which can emit and record a pulse up to 600m with a wavelength of near infrared 1550 nm was used (Bienert et al., 2006). The scanning approach can be single or multiple scans. So, to increase the density of the 3D point clouds, multiple scans with one central and three outer scans were applied for each sample plot (Maas et al., 2008). The digital camera attached with the device was used to acquire an RGB image with each corresponding scan positions.

Table 3: RIEGL YZ 400 TLS specification source: (RIEGL RIEGL VZ-400 VZ-400, 2017).

S/N	Specification	Level
1	Scan angle vertically and horizontal (Degree)	100, 360
2	Precision (mm)	3
3	Accuracy (mm)	5
4	Minimum range (m)	1.5
5	Maximum range (m)	600
6	Laser wavelength – Near-infrared (nm)	1550
7	Weight (kg)	9.6



#### The setting of the scan positions

From the center of the sample plots more than 12.62m radius were cleared from the foliage and undergrowth vegetations to reduce occlusion. Then, the center scan position of the plot was located carefully in a place where the TLS can view the trees in such a way that to minimize occlusions created by tree trunks. The plot center was used for the center scanning position, (Figure 12) and the other three scan points were located outside of the circular plot positioned around 120° by undermining the tree trunk blocking effect. According to Liang et al. (2012), trees stem near to TLS can influence the scanning process of the point cloud by blocking the point cloud and creating a shadow behind it.

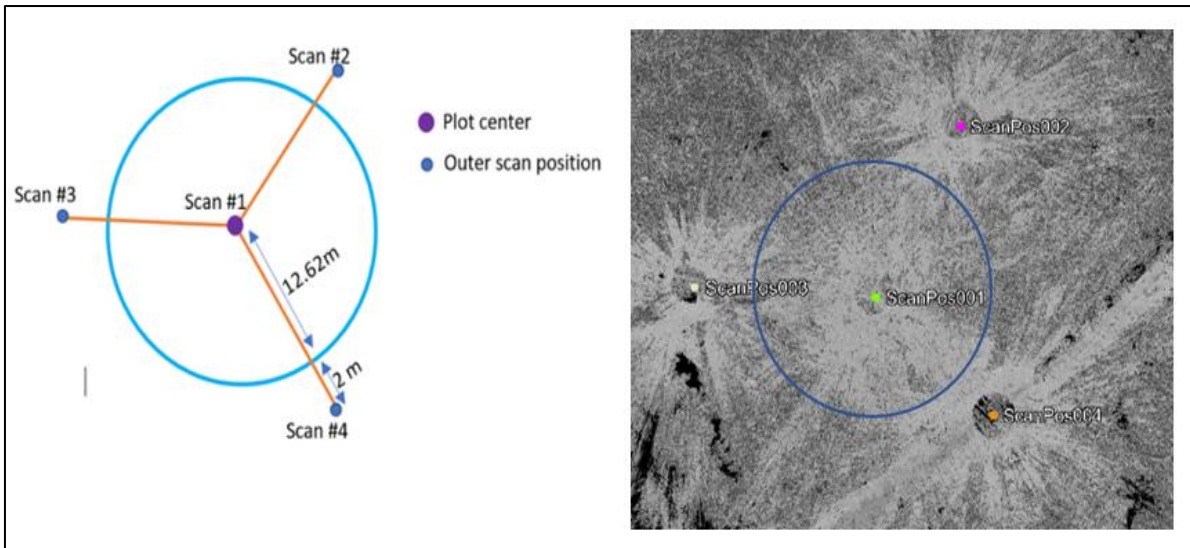


Figure 12: TLS multi-scanning position.

### The setting of the reflectors and tree tags

After the plot preparation and locating positions of scanning, all trees found inside the circular plot which have  $\geq 10$  cm DBH (Figure 14b) were tagged on each tree stem by visible marked tree tags for tree identification purpose. Along with, more than ten (10) circular and twelve (12) cylindrical retro-reflectors (Figure 13) were used at different height and orientation. The circular retro-reflectors are mounted on the tree stem on the view to the central scan position in which at least one reflector was visible to the three outer scans. The cylindrical retro-reflectors are pointed on top of sticks and located in different height orientations, and positions within the circular plot in such a way that the reflectors were visible to all the scan positions (Figure 14a).

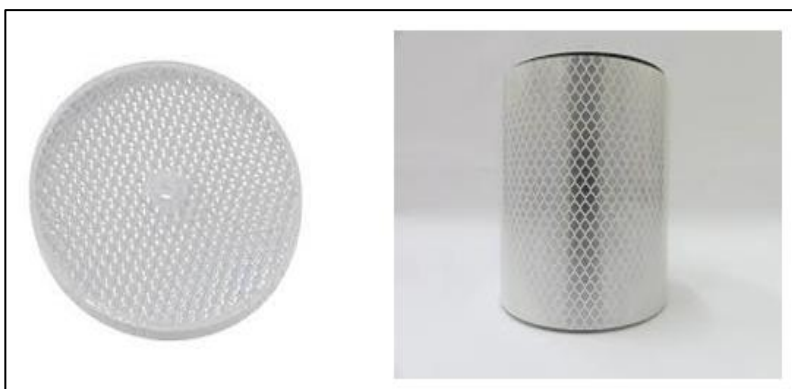
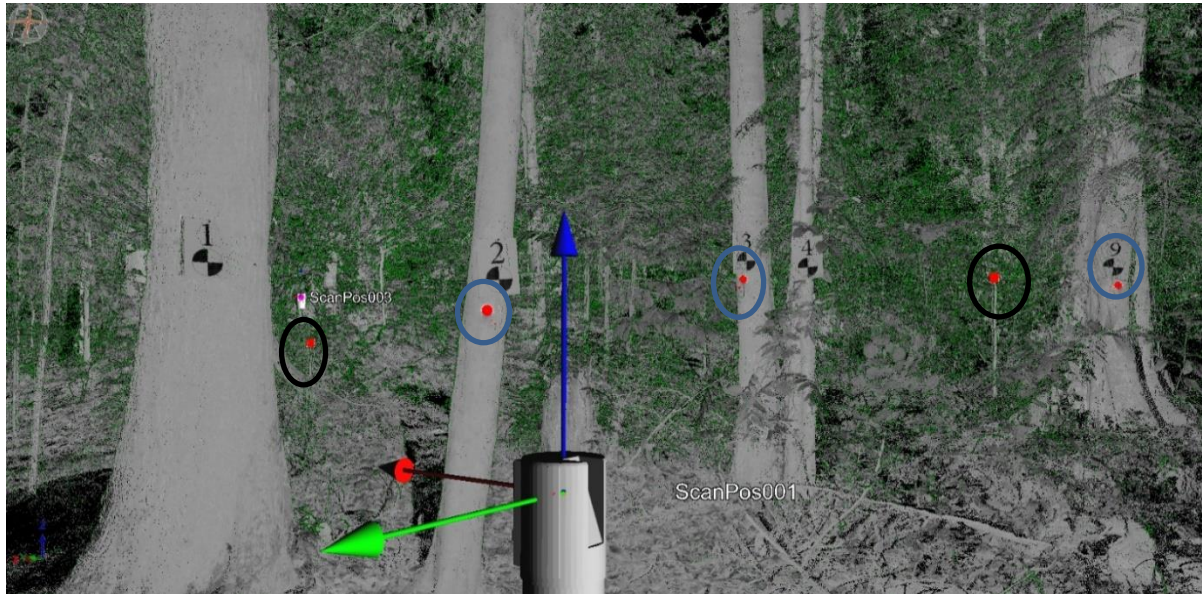


Figure 13: Circular-left and cylindrical- right retroreflectors. Source:(UNAVOC, n.d.).

The cylindrical and circular retroreflectors were used for georeferencing the outer position scan, with the center position scanned point clouds (Bienert et al., 2006). Therefore, for the registration purpose, there must be a minimum one circular and four cylindrical retro-reflectors visible in the tie point. Therefore, to reduce the error of registration twelve (12) cylindrical and greater than ten (10) circular retro-reflectors were used in each plot.



a. Circular and cylindrical retro-reflectors (Plot 6).



b. Marked tree tags (Plot-6).

Figure 14: Illustration of circular and cylindrical retro-reflectors (a) and mounted tree tags (b).

### Setup of the TLS and data acquisition

Setup of the TLS starts from fixing of the optical head with the tripod and mounting the camera with the TLS head properly. Then, the tripod legs were leveled manually to adjust the position setup. According to (UNAVOC, 2013) the leveling of the TLS stand by the triploid could be close to one degree, and the point should be at the center with the decimal number  $\leq 0.4$ . Along with, the different functions and setups were defined including plot number, date, the density of point clouds (Panorama 40). After each plot was scanned, the data was transferred to a hard disk device.



### 3.5. Data processing

The field data and remote sensing method data were processed using different applications.

#### 3.5.1. Biometric data processing

The collected field data were transferred to an Excel file from the data recording sheet for further analysis. The data collection includes tree height, DBH, center plot location and individual tree coordinates (X, Y). From 30 circular sample plots, 699 individual trees were recorded. Descriptive statistics of the forest parameters were carried out in Microsoft Excel, and the subsequent individual tree Above Ground Biomass (AGB) was calculated using the allometric equation developed by Chave et al. (2014) which is more appropriate for tropical rain forests (Chave et al., 2014).

#### 3.5.2. TLS data processing

##### Registration of scan positions

The three outer scanned locations were registered to the central scan position based on the tie points of the cylindrical and circular retroreflectors in RiSCAN PRO v2.1 software automatically. Registration is the process of transforming the multi-scanned positions of the TLS point clouds from the local system into a common reference system (Bienert et al., 2006). As pointed by Holopainen et al. (2014) the artificial circular and cylindrical retro-reflectors are used to transfer the local system of the three outer scan positions into the common reference system with the center scan position. To reduce registration error more than seven (>7) Tie points were used to be selected automatically by the RiSCAN Pro for registration of multi-scans.

##### Extraction of plots and individual trees

After the registration was conducted, the four scanned point clouds were displayed in one view as a single scanned point cloud. The point cloud of each scan was applied the “color from image” which enables to view the point cloud as a true color resulting from the image captured by the RGB camera mounted on the top of the device. Then based on the radius of the plot (500m<sup>2</sup>) filtering were applied using the range tool and manual selection to exclude the point clouds found outside the boundary of the sample plot.

Individual tree extraction was done from the extracted plot by identifying the individual tree and saved it as a new point cloud. Individual trees were identified by the tree tag mounted on their stem by displayed in different color schemes. The extracted individual tree was cleaned, all the undergrowth trees and other branches which comes from other tree using the selecting tool on the RiSCAN PRO software (Figure 15).

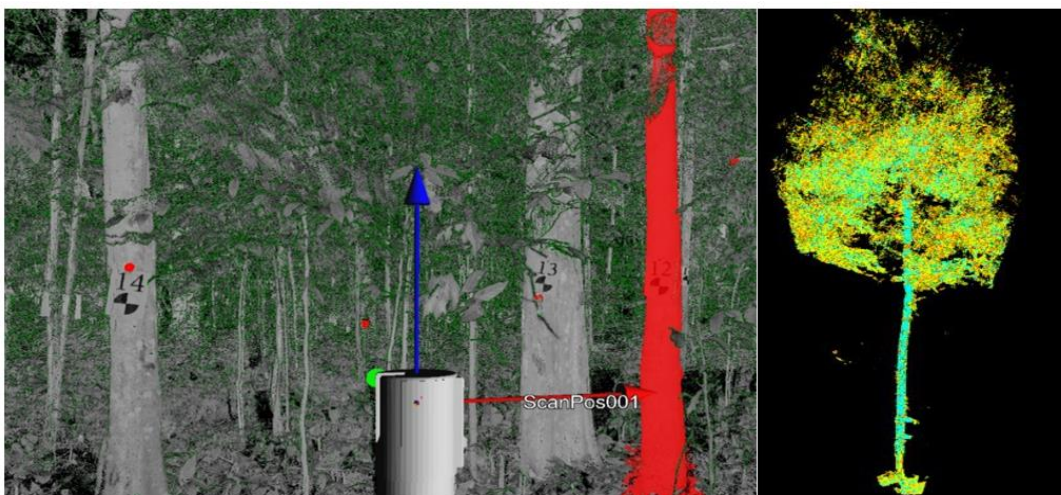


Figure 15: Manual identification and extraction of individual trees in RiSCAN Pro (Plot-15).

### Tree height and DBH measurements

The tree parameters DBH and height of the extracted individual trees were measured manually using the distance measurement tool (point to point) in the RiSCAN PRO software. Tree height was measured from the base of the ground to the highest top canopy of the tree vertically (Figure 16), and the measured height was recorded in an Excel sheet. Tree DBH was measured horizontally at 1.3m sub height of the stem from the base of the tree. (Figure 16).

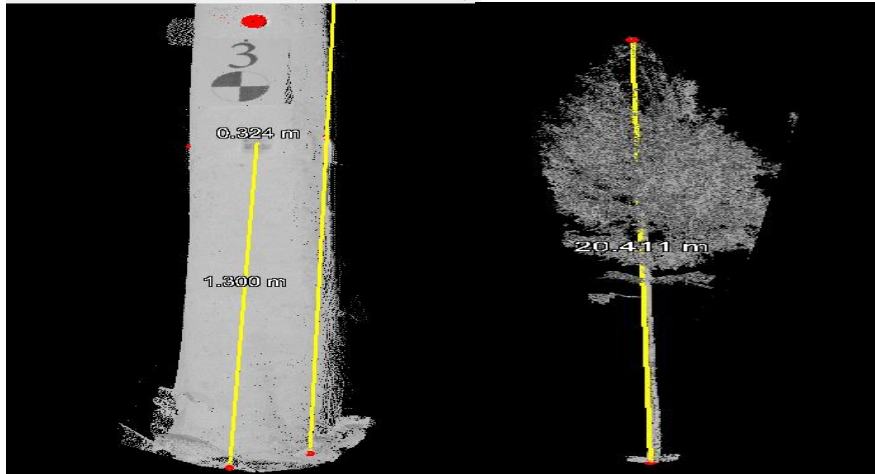


Figure 16: Illustration of tree height and DBH measurements (Plot 6).

#### 3.5.3. UAV image processing

The 2D images acquired by UAV were processed using Pix4D Photogrammetric software to generate the Digital Terrain Model (DTM) Digital Surface Model (DSM) and orthomosaic images. The overlapping images processing on the Pix4D consists of the following three steps.

##### Initial processing

This stage includes uploading of the 2D-images to the Pix4D software. The camera position and image alignments of the flight missions were identified by the software automatically. The GCP which are collected by DGPS were imported for georeferencing of the images based on the Tie points. Based on the imported GCP, the images were sorted to the nearest GCP coordinate, and this was followed by manual placement of pointers in each image which have GCP marker with its corresponding GCPs coordinate. After marker placements were completed checkpoints were selected to assess the accuracy of image georeferencing. Then the key points (tie points) of the adjacent images found at the same location were matched, and the images calibration and optimization were carried out. As pointed at Pix4D (2018) the initial processing involves camera calibration and image matchings. Thus, the quality report of all the initial processing was produced as an output.

##### Point cloud and mesh processing

This stage has two sections namely; point cloud densification and point cloud classification. To increase the density of 3D point cloud and the 3D image modeling the full-size image scale and optimal point density was used in the point cloud densification setting parameters. This step increases significantly the density of point cloud generated from the initial processing (Pix4D, 2018).

### Orthomosaic image, Digital Surface Model and Digital Terrain Model processing

Pix4D software allows generating DSM, DTM and orthomosaic images automatically from the output of the second process (Pix4D, 2018). So, all the essential parameters needed to produce the DSM, DTM and orthomosaic images were selected and processed.

### Canopy Height Model (CHM) generating

The generated DSM and DTM were imported to ArcGIS to produce the CHM. In the arc toolbox, DTM was subtracted from DSM using the Raster calculator function. Then the resulted CHM (DSM-DTM) was used to extract individual tree heights.

#### 3.5.4. Manual tree crown delineation (digitization)

The orthomosaic image generated from the Pix4D processing were used further for segmentation of CPA of individual trees. Image delineation is the process of image classification based on criteria in which the image was subdivided into non-overlapping objects (Fan et al., 2004). In this study, a manual digitizing method was applied because this study was conducted in a plot based and the number of the sample plots and trees was manageable. The delineation was performed only on trees which were found inside the sample plot. Evidently, the UAV resulted orthomosaic image has a high spatial resolution, and individual tree crowns are visible on the orthomosaic image. Previous studies show that manual delineation of tree crowns was used as a reference to validate for the automated segmentation from such algorithms (Benz et al., 2004). Therefore, the manual delineation can be used to delineate tree crowns in a plot based.

The coordinates of trees and individual tree number was matched with its corresponding tree crowns. Then, each tree crown was digitized based on the shape and color of their crown by looking and manual interpretation of the image (Figure 17). Thus, the segmented tree crowns were used further for maximum tree height extraction from CHM and to predict DBH.

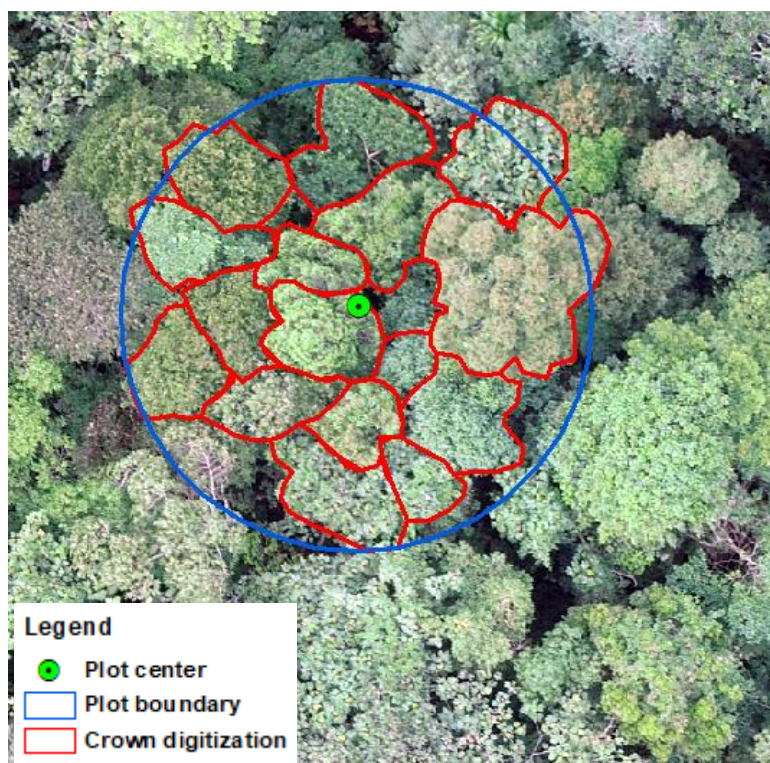


Figure 17: Shows manually delineated tree crowns (Plot 11).

### **3.5.5. Tree matching and individual tree height extraction**

For extraction of the tree heights, first tree location matching with the corresponding field recorded data were conducted. On the 2018 orthomosaic UAV image those trees recognized by Avenza and Lucas Map were matched by manual inspection on each segmented crown. Afterward, few tree crowns which were not identified at field level were matched by looking their position on the point cloud of TLS, tree information (height, DBH) and using the GPS coordinate recorded in the field. After tree matching was conducted, the local maximum height of each crown was extracted from the CHM using zonal statistics in ArcGIS software.

### **3.5.6. Modeling of DBH from the crown projection area**

A model was developed using a relationship between the calculated crown area (CPA) from the digitized crowns, and field measured DBH for only selected trees. Then the developed model was validated using a linear regression model.

### **3.5.7. Integration of upper and lower canopy trees using height threshold**

In this study, forest parameters were acquired using Aerial-based UAV, and the ground-based TLS remote sensing techniques and the extracted tree parameters were integrated. Thus, to reduce error during the integration of UAV and TLS derived tree parameters in which trees were not counted twice or missing, the height threshold was defined to separate the individual tree as upper canopies or lower canopies. The thresholds are 1) UAV derived minimum height and 2) the TLS derived height (fully detected).

#### **UAV derived minimum height**

The visible crowns on the orthomosaic image were digitized, and all the tree heights were extracted from the CHM for all the sample plots. Thus, the minimum tree height extracted from the CHM was determined in each sample plot. Afterward, the minimum height found in each plot was considered as a threshold for each plot, and individual trees height greater than or equal to the defined threshold was considered as part of the upper trees and the rest trees derived from TLS their height is less than the defined threshold was considered as part of lower canopies. The tree height extracted from the CHM is the estimation of the vertical distance of the tree from the top of the tree crown to the base of the tree.

#### **TLS derived height**

The extracted trees from the TLS point cloud were displayed, and their shape was observed manually on RiSCAN PRO screen. Then if the top of the canopy has a conical shape, it considered as fully detected (Figure 18A). However, if the top of the canopy has a flat shape, it was identified as a not fully detected tree. Besides, the trees which were found side by side was observed; if the point cloud of the TLS precedes the shorter tree and detects the tallest tree, then the shorter tree was considered as fully detected trees (Figure 18B). Thus, for trees which are fully detected by the point cloud of the TLS, their height was determined, and the measured height was considered as a threshold to separate the upper and lower canopies (Figure 18C).

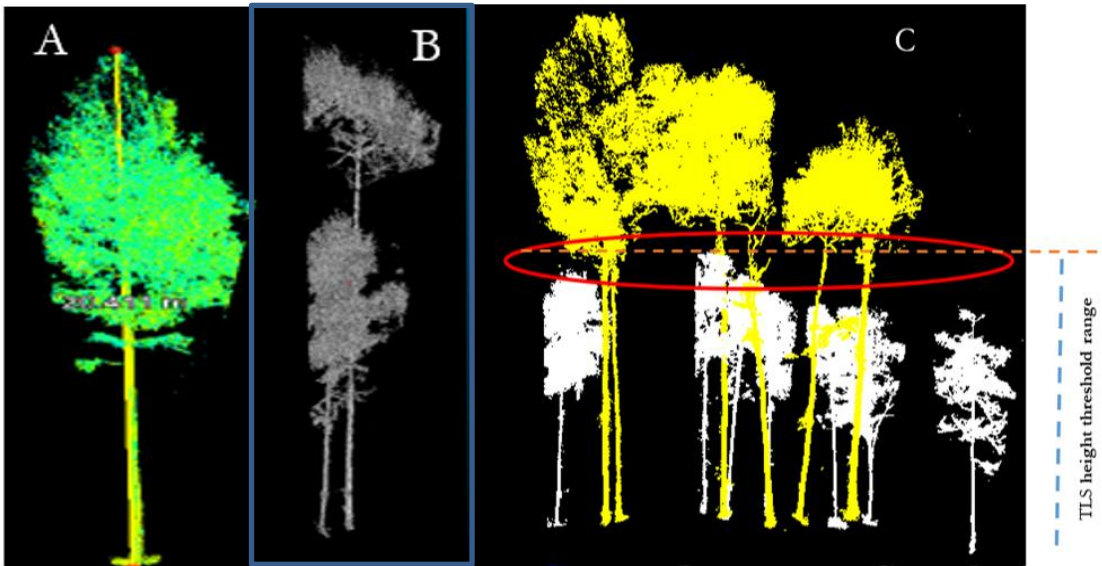


Figure 18: Identification of fully detected and not fully detected trees on TLS point cloud.

### 3.5.8. Above ground biomass/ Carbon estimation

Above ground biomass estimation were calculated based on the collected forest parameters namely; DBH, wood density, and height. The allometric equation which is a non-destructive method was applied to estimate the AGB. The allometric equation was a widely used method which is developed by the relationship of tree parameters such as height, DBH, species with the corresponding dry biomass. The study area has a diverse mixed species; thus the generic allometric equation developed by Chave et al. (2014) is more appropriate for tropical rain forests (Chave et al., 2014). In this study, the recommended average wood density  $0.57\text{g/cm}^3$  was used for all species in the allometric equation calculation. Therefore, field-based AGB and remote sensing based AGB was estimated for all individual trees found within the sample plot.

Equation 1: Allometric equation (AGB).

$$\text{AGB} = 0.0673 * (\rho D^2 H)^{0.976} \text{----- Equation 1}$$

Where;

$\rho$ = wood density ( $\text{g/cm}^3$ ).    D = DBH (cm).    H= height in (m).

Carbon stock was calculated from the output estimated AGB. According to IPCC, (2006) carbon was 0.47 of the above-ground biomass. Thus, the conversion factor from AGB to carbon is 0.47.

Equation 2: Above-ground biomass carbon.

$$\text{C} = \text{AGB} \times \text{CF} \text{----- Equation 2.}$$

Where;

C = carbon in (Mg).

CF = conversion factor (0.47).

### 3.5.9. Data analysis

Different statistical analysis was conducted to assess the relationship between the tree parameters. In forestry studies, regression analysis is mostly used to assess the quantitative relationship between two or more forest variances. Thus, to determine the relationship between the tree parameters (i.e., DBH, and height) which are measured using field-based and remote sensing method, the scatter plot and regression analysis was used. Also, the field based AGB was compared with the remote sensing method estimated AGB. Afterward, to assess the correlation and accuracy, the Pearson correlation ( $r$ ) and the coefficient of determination ( $R^2$ ) were used. To determine whether the two variables, have an equal variance or not F-test was used. The output of F-test was used to determine the type of t-test which includes the t-test equal variance or t-test unequal variance.

Furthermore, to calculate the error between the two variables the Root Mean Square Error (RMSE), Bias and The RMSE (%) were used (Equation 3, 4, 5)

Equation 3: Root Mean Square Error.

$$RMSE = \sqrt{\frac{\sum_{i=1}^n (y_i - \hat{y})^2}{n}} \text{----- Equation 3.}$$

Equation 4: Root Mean Square Error percent.

$$RMSE (\%) = \frac{RMSE}{\left(\frac{\sum_{i=1}^n (y_i)}{n}\right)} \times 100 \text{----- Equation 4.}$$

Equation 5: Bias equation.

$$Bias = \frac{\sum_{i=1}^n (y - \hat{Y})}{n} \text{----- Equation 5.}$$

Where;

$n$ :	Number of samples
RMSE:	Root Mean Square Error
RMSE (%):	Root Mean Square Error present
$y$ :	Variables
$\hat{Y}$ :	Estimated Variable

## 4. RESULTS

### 4.1. Field level upper tree crown identification

To reduce error in the tree matching process, the upper canopy tree crowns which are visible on the orthomosaic image of 2017 were identified using Avenza and Lucas Maps as described in see section 3.4.2. Of the 699-field recorded trees, 388 (55.5%) upper canopy trees were recognized from the 2017 orthomosaic images in the field. The minimum, average, and maximum identified trees crowns per plot were 6, 13, and 19 respectively.

On the orthomosaic image of 2018 generated from UAV images, 436 upper tree crowns which were found inside the sample plot was digitized manually. Hence, the proportion of field level identified tree crown was 88.99 % of the manually digitized crowns. The minimum, average and maximum number of tree crown digitized from the orthomosaic images was 7, 15, and 24 respectively and the detail is listed in Table 4.

Table 4: Proportion of upper canopy tree identified at field level and manually digitized tree crowns result.

Plot No.	1	2	3	4	5	6	7	8	9	10
Field identified crowns	15	10	6	14	15	17	11	13	10	13
Delineation result	18	12	7	14	17	20	11	16	10	15
Plot No.	11	12	13	14	15	16	17	18	19	20
Field identified crowns	14	14	12	13	10	13	11	14	17	19
Delineation result	16	16	12	13	11	15	12	17	22	24
Plot No.	21	22	23	24	25	26	27	28	29	30
Field identified crowns	11	13	14	15	14	11	12	11	14	12
Delineation result	12	13	14	16	14	14	15	12	14	14

### 4.2. Field biometric data

Biometric data of 699 individual trees were collected from the 30 circular sample plots. The average tree height and DBH were 16.46m and 28.39cm respectively. Further, the field recorded data were matched with the corresponding tree parameters extracted from TLS as well as UAV for comparison and accuracy assessment. The details and descriptive statistics are described in Appendix 5.

### 4.3. TLS data and Individual tree extraction

From the total 699 fields recorded 619 (88.6%) trees were extracted from TLS point cloud, and 80 (11.4%) individual tree was missed as shown in Table 5. These 80 trees were not visible the tree tag mounted in their stem.

Table 5: Number of missed trees per plot.

Plot No.	1	2	3	4	5	6	7	8	9	10	11	12	13	14	15
No. tree	27	22	18	20	27	29	17	24	17	24	25	33	23	26	29
Missed tree	7	7	1	2	3	1	0	4	4	3	1	6	1	3	2
Plot No.	16	17	18	19	20	21	22	23	24	25	26	27	28	29	30
No. tree	37	21	26	31	27	19	17	21	20	17	23	21	19	20	19
Missed tree	5	2	3	4	3	0	6	1	0	3	2	1	3	1	1

The result shows that the number of extracted/missed trees were varying from sample plot to sample plot which depends on the density of the undergrowth vegetation. Of the 80 missed trees 41 trees are lower canopies, and 39 trees are upper canopies because the 39 trees were identified their crowns in the field using the Avenza Maps. The descriptive statistics are shown in Table 6.

Table 6. Descriptive statistics of tree extracted from TLS point cloud per plots.

	No of trees/plot	Missed tree/ Plot	Extracted Trees/ Plot
Minimum	17.0	0.0	11.0
Mean	23.3	2.7	20.6
Maximum	37.0	7.0	32.0
Sum	699	80	619

#### 4.4. UAV-CHM and orthomosaic image generating

From the UAV image based-modeling the Digital Surface Model (DSM), Digital Terrain Model (DTM) and orthomosaic images were generated using the Pix4D software. The generated orthomosaic image was used to digitize tree crown delineation and for tree matching process between the field recorded and the UAV derived upper canopy trees. The orthomosaic image has an average ground sampling distance of 4.9 cm, and a total of 147ha was covered. Detail of the Pix4D processing results is listed in table 7.

Table 7. Results of Pix4D UAV-Image processing.

Summary	Quantity in unit
Average ground sampling distance	4.9cm
Area coverage	147.8 ha
Geo-referencing RMSE (GCP)	0.2cm
Camera model name	FC220_4.7_4000x3000 (RGB)

The CHM was generated by subtracting DTM from DSM using the raster calculator on ArcGIS, and the maximum height of the CHM was found 50m as shown in Figure 19.



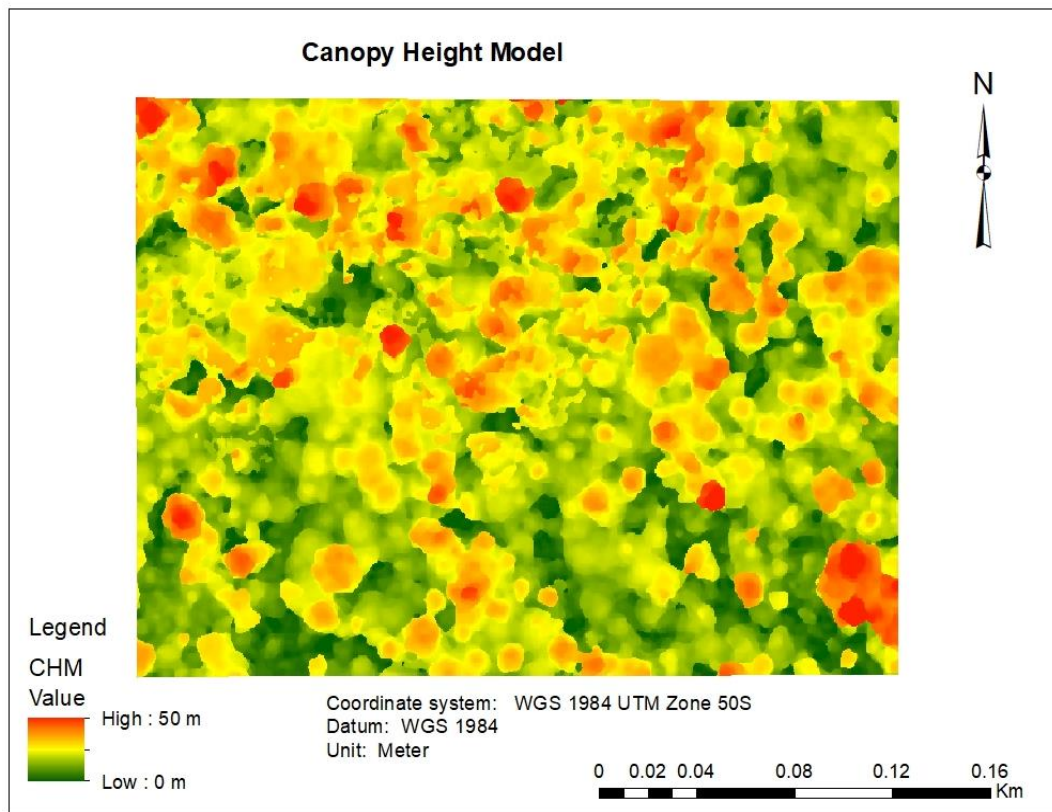


Figure 19: Part of the CHM generated by subtracting DTM from DSM.

#### 4.4.1. Tree crown delineation and individual tree height extraction

From the entire 30 sample plots, 436 upper canopy trees crowns were digitized manually (Figure 20). The digitized tree crowns were matched with the corresponding field recorded biometric data as mentioned in (section 3.5.5). Then, the extraction of value to point from the local maxima CHM was conducted. This step enables us to attribute the highest value of the segmented crown to the corresponding tree number as shown in Figure 20. By doing this 436-tree height was extracted of the 699 trees recorded in the field. The minimum, average and maximum number of trees extracted per plot were 7, 14.5 and 24 respectively (table 8).

Table 8: Proportion of tree height extracted from UAV-CHM per plot.

Plot. No	1	2	3	4	5	6	7	8	9	10	11	12	13	14	15
Total tree	27	22	18	20	27	29	17	24	17	24	25	33	23	26	29
Extracted tree	18	12	7	14	17	20	11	16	10	15	16	16	12	13	11
Plot. No	16	17	18	19	20	21	22	23	24	25	26	27	28	29	30
Total Tree	37	21	26	31	27	19	17	21	20	17	23	21	19	20	19
Extracted tree	15	12	17	22	24	12	13	14	16	14	14	15	12	14	14

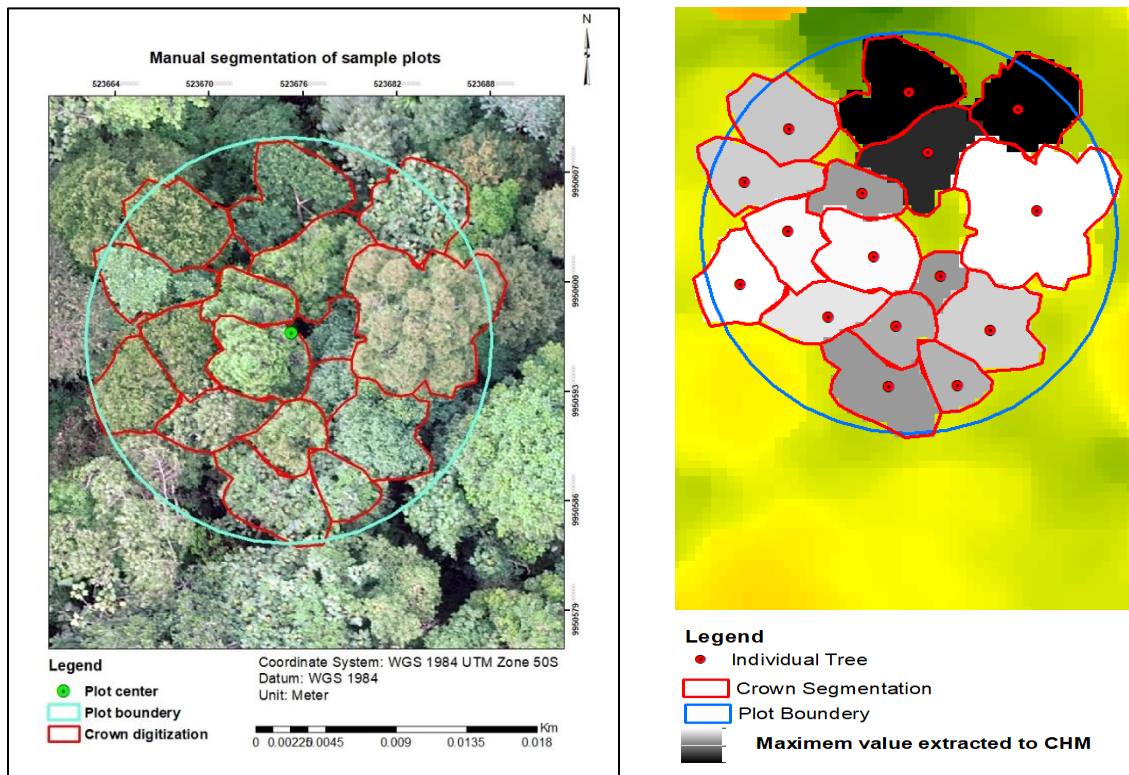


Figure 20: Tree crown delineation -right and tree height extraction-left.

#### 4.4.2. Modeling of DBH from the crown projection area

The modeling of DBH is carried out only for 39 upper tree crowns which were missed from the TLS point cloud tree extraction. Because their DBH is needed for the AGB estimation. While for the other trees the TLS derived DBH was used. Previous studies show that tree Crown Projection Area (CPA) has a relationship with the diameter at breast height (Song et al., 2010). Thus, of the 39 upper canopy data set 24 (60%) of the tree was used randomly for the model development, and 15 (40 %) of the trees were used for validation of the model. As a result, the DBH of the missing trees (39) were predicted, and the result of the model is illustrated in Figure 21.

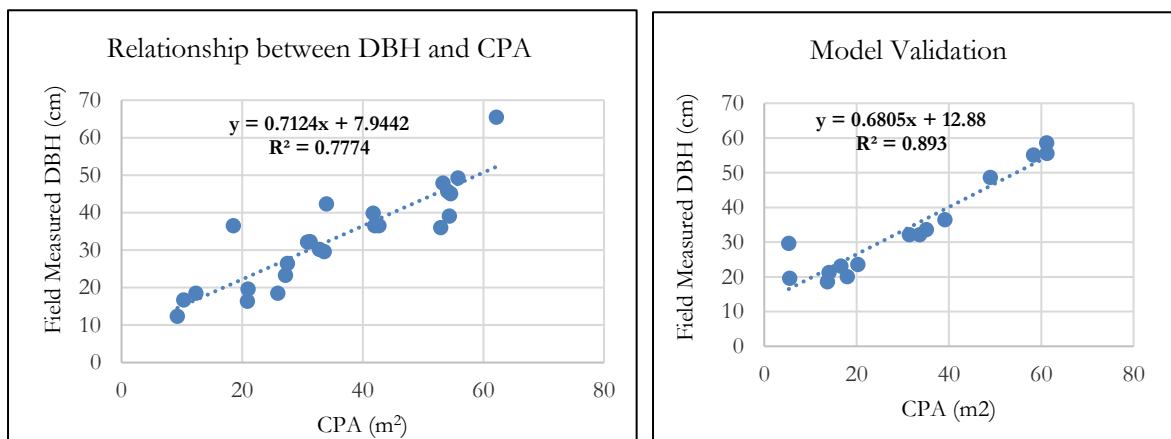


Figure 21: Developed model and model validation of CPA.

The linear regression result shows a coefficient of determination ( $R^2$ ) of 0.77, 0.89 for the model development and model validation respectively. Thus, the observed DBH and the manually delineated crowns have a relationship. Then, the DBH of 39 upper canopy trees were predicted based on the developed DBH and used as an input to calculate the subsequent AGB.

#### 4.5. Lower canopy tree height measurement and accuracy assessment

Of the 699 field recorded trees, 222 (33.7 %) trees extracted from TLS were categorized as a lower canopy and used to validate for the corresponding tree height measured by hand-held Leica DISTO D510. The descriptive statistics of the lower canopy tree heights are shown in Table 9, and its further details are in Appendix 16.

Table 9: Descriptive statistics of TLS and field measured lower canopy heights.

Descriptive statistics	Field measure Height (m)	TLS derived Height (m)
Minimum	6.70	6.08
Mean	11.50	11.98
Maximum	15.90	16.50
Standard Deviation	1.93	1.95
Count	222.0	222.0

The accuracy of field measured lower canopy tree height was assessed using the linear regression considering the TLS derived height as a reference. Thus, the linear regression result shows a coefficient of determination ( $R^2$ ) of 0.8 as shown in Figure 22, and the RMSE was 1.0 m (8.37 %).

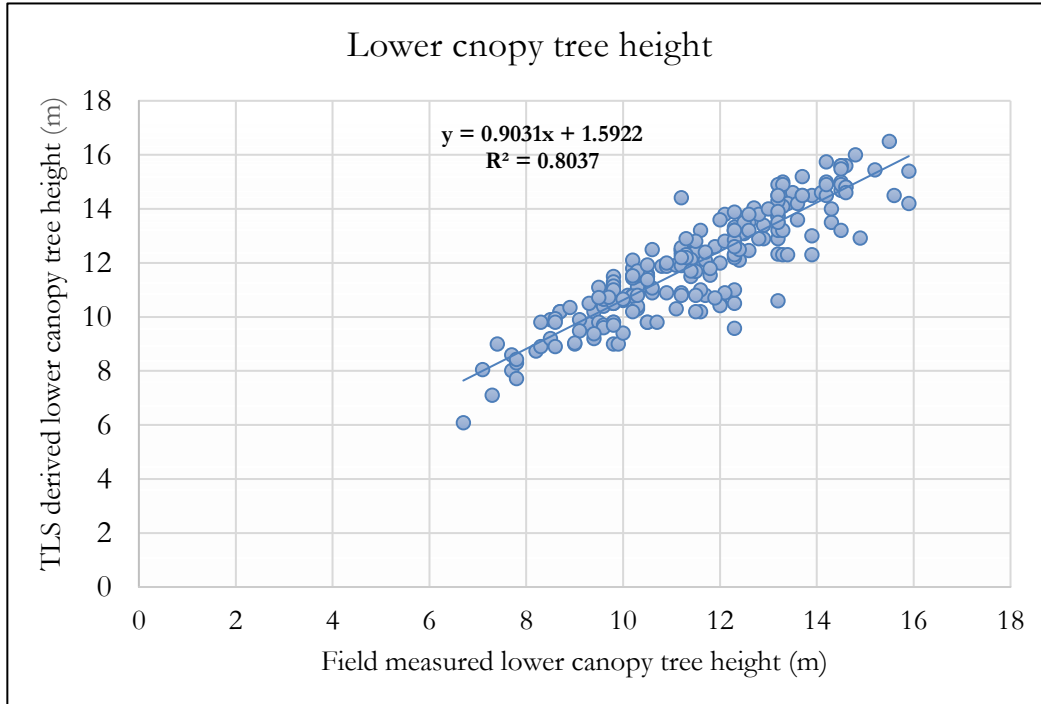


Figure 22: The relationship between field measured and TLS derived lower canopy height.

The result shows field measurement height using Leica DISTO D510 was underestimated for the lower canopy tree height by the mean of 0.47m as shown in Table 10. The details of the linear regression are listed in Appendix 6.

Table 10: Relationship between field measured and TLS derived lower canopy tree heights.

Field against TLS	Regression				RMSE	
	Observation	R <sup>2</sup>	r	Bias (m)	(m)	(%)
Lower canopy height (m)	222	0.803	0.896	0.48	1.0	8.37

#### F-test for variance

F-test was conducted for the lower canopy tree height derived from TLS and field measured using Leica DISTO D510. The details of the F-test are shown in Table 11.

Table 11. F-test for the lower canopy tree height measured using Leica DISTO, and TLS derived height.

	TLS derived height (m)	Field measured height (m)
Mean	11.97513511	11.49729731
Variance	3.797890542	3.742979037
Observations	222	222
df	221	221
F	1.014670535	
P(F<=f) one-tail	0.456945661	
F Critical one-tail	1.248279823	

The F-test result shows, F-statistics < F-critical ( $P > 0.05$ ): then it has equal variance. Hence, t-test equal variance was selected for the statistical analysis.

#### The t-test assuming equal variance

A t-test was applied between the lower canopy tree height derived from TLS and field measurement to assess the accuracy of field measured height whether it has a significant difference or not. The result shows that t-statistics was greater than t-critical ( $P < 0.05$ ) (Table 12). Therefore, the field measured tree height has a significant difference as compared to the TLS derived tree height of the lower canopies.

Table 12. A t-test for field measured, and TLS derived lower canopy heights.

	TLS derived height (m)	Field measured height (m)
Mean	11.97513511	11.49729731
Variance	3.797890542	3.742979037
Observations	222	222
df	442	
t Stat	2.592664254	
P(T<=t) one-tail	0.004919616	
t Critical one-tail	1.648308349	
P(T<=t) two-tail	0.009839231	
t Critical two-tail	1.965345591	

The t-statistics reveals that t-statistics was > t-critical ( $P < 0.05$ ): hence, the measurement of lower canopy tree height have a significant difference.

#### 4.6. DBH measurement of TLS and accuracy assessment

From the total 699 trees recorded at field level, 619 (88.6%) tree were extracted from the TLS point cloud, and individual tree DBH was measured using RiSCAN PRO. Afterward, the field measured DBH was

used as a reference to validate and to assess the accuracy of TLS derived DBH, and the descriptive statistics of the DBH are shown in Table 13.

Table 13: Descriptive statistics of TLS and field measured DBH.

Descriptive statistics	Field measured DBH (cm)	TLS derived DBH (cm)
Minimum	10.00	8.50
Mean	28.83	28.23
Maximum	101.50	99.90
Standard Deviation	16.69	16.36
Count	619.00	619.00

The Accuracy of DBH measured from the point cloud of TLS was assessed using the field measured DBH. Thus, the coefficient of determination ( $R^2$ ) shows 0.99 (Figure 23) in which the TLS based DBH measurement explains 94.46 % of the field based measured DBH. Also, the TLS measurement has a high correlation with the field measured DBH.

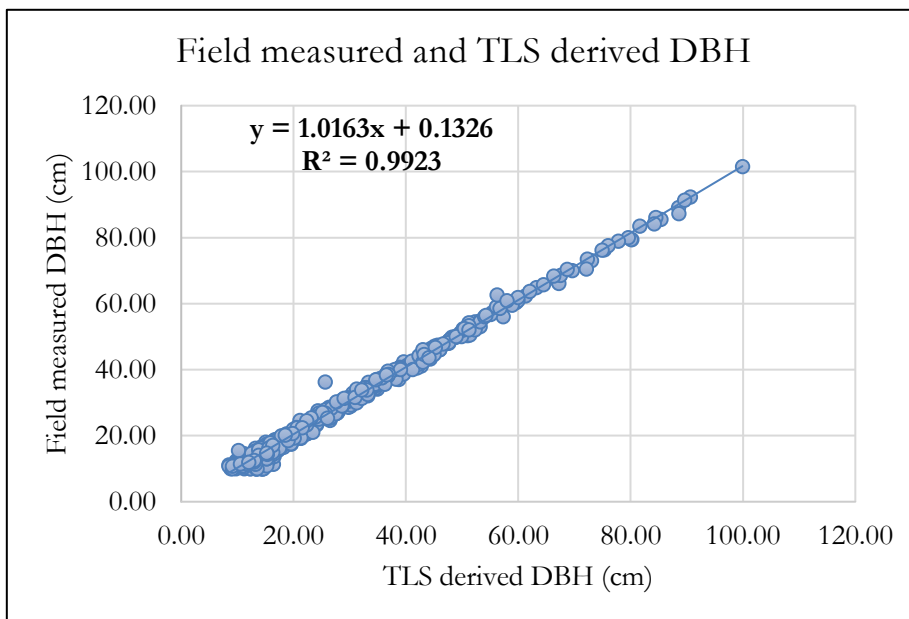


Figure 23: The relationship between field and TLS measured DBH of the upper and lower canopy trees.

The TLS measurement indicates a small underestimation of the tree DBH measurement with the 0.59cm on average, and the RMSE was 1.59 cm (5.54%) (Table 14). Appendix 7 shows the linear regression between field and TLS measured DBH.

Table 14: Relationship between field and TLS measured DBH of the lower and upper canopy trees.

TLS against Field	Regression				RMSE	
	Observation	$R^2$	r	Bias (cm)	(cm)	(%)
DBH (cm)	619	0.99	0.996	0.59	1.59	5.54

### F-test for variance

F-test was conducted to determine which type of t-test to be used to find if there is a significant difference between the field measured and TLS derived DBH measurements (Table 15).

Table 15: F-test for TLS and field measured DBH for a variance.

	Field DBH (cm)	TLS DBH (cm)
Mean	28.83	28.23
Variance	278.51	267.57
Observations	619.00	619.00
df	618.00	618.00
F	1.04	
P(F<=f) one-tail	0.31	
F Critical one-tail	1.14	

The F statistics result shows, F-statistics < F-critical (P > 0.05). Thus, it has equal variance; then t-test equal variance was applied.

#### The t-test for the field measured, and TLS derived DBH

The t-test assuming equal variance was conducted between the field measured DBH, and TLS derived DBH of the lower canopy trees (Table 16). The result shows t-statistics was less than t-critical (P > 0.05) thus, there is no significant difference among the TLS derived, and field measured DBH.

Table 16: The t-test assuming equal variance for the field measured and TLS derived DBH of the lower and upper canopy trees.

	Field measured DBH (cm)	TLS DBH (cm)
Mean	28.8276252	28.23418414
Variance	278.5126514	267.5747654
Observations	619	619
df	1236	
t Stat	0.631817761	
P(T<=t) one-tail	0.263811403	
t Critical one-tail	1.64608738	
P(T<=t) two-tail	0.527622805	
t Critical two-tail	1.961885147	

The t-test result reveals t-stat was < t-Critical (p > 0.05) thus, there is no significant difference between the measured DBH.

#### 4.7. The accuracy of upper canopy tree height assessment

In this study, the accuracy assessment of upper canopy tree height was conducted for trees extracted from UAV-CHM. Based on the defined height threshold tree heights which have more than the threshold height were considered as upper-canopies. Of the 699-field recorded trees, 436 trees were categorized as upper canopy trees and validated using the field based height measured by Leica DISTO D510. The descriptive statistics are listed in Table 17, and its detail is described in Appendix 15.

Table 17: Descriptive statistics of field measured and extracted from UAV-CHM of the upper canopy tree heights.

Descriptive statics	Field measured height (m)	Tree height extracted from UAV-CHM (m)
Minimum	10.10	10.23
Mean	19.39	20.59
Maximum	34.00	36.12
Standard Deviation	4.06	4.65
Count	436.00	436.00

The linear regression between the field measured and UAV derived upper canopy height shows a coefficient of determination ( $R^2$ ) of 0.768 (Figure 24) and a correlation ( $r$ ) of 0.87.

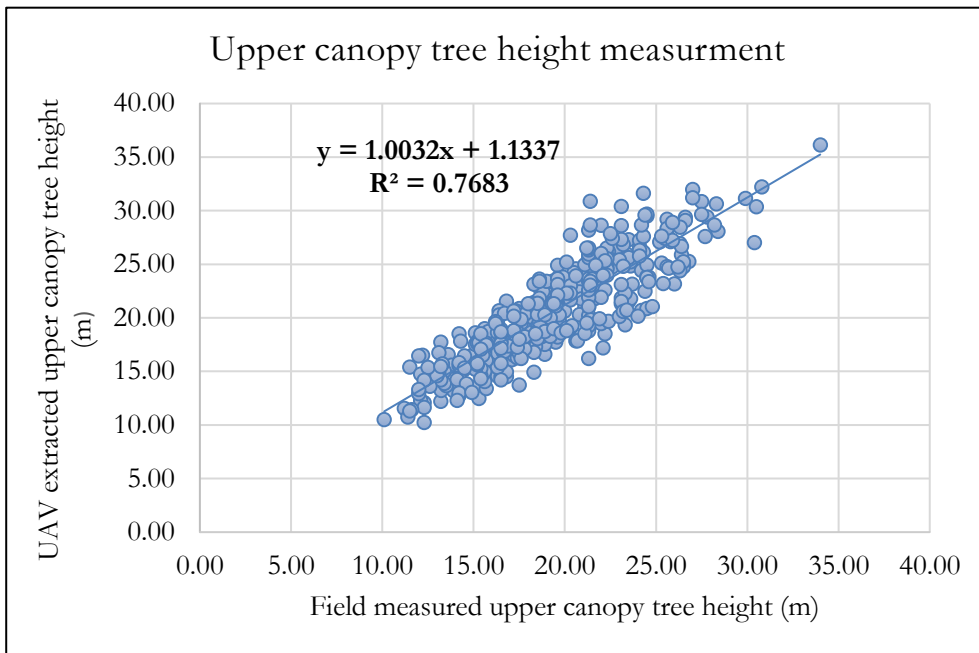


Figure 24: The relationship between field measured and UAV-CHM derived upper canopy trees.

The RMSE was found 2.53m as shown in Table 18. Thus, the UAV derived upper canopy height was overestimated as compared with the field measured height. The Leica DISTO D510 pulse measurement is influenced by the dense undergrowth vegetations and foliage to detect the most top of the upper canopy trees depending on the openness of the forest. The details of the regression result are attached in Appendix 8.

Table 18: Relationship between field measured and UAV-CHM derived upper canopy tree heights.

UAV-CHM against Field measured	Regression				RMSE	
	Observation	$R^2$	$r$	Bias (m)	(m)	(%)
Upper canopy height (m)	436	0.768	0.876	1.2	2.53	13.06

### F-test for the field measured, and UAV-CHM derived upper canopy tree height

F test was conducted to find for variance (Table 19).

Table 19. F-test for equal or un equal variance.

	UAV-CHM derived height (m)	Field measured height (m)
Mean	20.59408904	19.39827979
Variance	21.63850319	16.51991718
Observations	436	436
df	435	435
F	1.309843322	
P(F<=f) one-tail	0.002486194	
F Critical one-tail	1.171051336	

Thus,  $F\text{-statistics} > F\text{-Critical}$  ( $P > 0.05$ ) then, it has unequal variance. Thus, the t-test unequal variance was applied to find out whether it has a significant difference or not.

#### The t-test for un-equal variance of the upper canopy tree height

The result shows t-statistics was greater than t-Critical at ( $P < 0.05$ ) so, there is a significant difference between field-measured tree heights, and UAV-CHM derived upper canopy tree heights. The details are shown in Table 20.

Table 20. The t-test between field measured and UAV-CHM derived upper canopy tree height.

	UAV-CHM derived height (m)	Field measured height (m)
Mean	20.59409	19.39828
Variance	21.63850	16.51992
Observations	436.00000	436.00000
df	855.00000	
t Stat	4.04213	
t Critical one-tail	1.64664	
P(T<=t) two-tail	0.00006	
t Critical two-tail	1.96274	

The result of the t-test shows, t-statistics  $>$  t-Critical ( $P < 0.05$ ) then, there is a significant difference among the upper canopy tree height measurements.

### 4.8. Above ground biomass estimation

#### 4.8.1. Remote sensing based AGB estimation (using UAV and TLS)

The upper and lower canopy tree parameters derived from the remote sensing method was integrated using two methods, i.e., the UAV defined height threshold, and the TLS derived height thresholds as mentioned in section 3.5.7. Afterward, AGB was estimated using the same allometric equation developed by (Chave et al., 2014). The AGB of upper canopy trees was calculated using the input parameters derived from UAV (height) and TLS (DBH) including the average wood density (0.57). Besides, for 39 individual upper canopy trees in which their DBH were not found from the TLS point point cloud, the predicted DBH from CPA was used. while, for the lower canopy tree, TLS derived height and DBH with the average wood density were used. The details are shown in Table 21.

Table 21. The input tree parameters used for upper and lower canopies AGB estimation.

Canopy strata	UAV derived tree parameter		TLS derived tree parameter	
	Height (m)	DBH (cm)	Height (m)	DBH (cm)
Upper Canopy	X	X (39 trees)	-	X
Lower Canopy	-	-	X	X

#### 4.8.2. The relationship between AGB integrated using UAV, and TLS derived height thresholds

The upper and lower canopies tree parameters extracted using UAV and TLS were integrated using the TLS derived (fully detected) height, and UAV derived minimum height thresholds. Thus, the AGB is also calculated in two ways based on the method integration.

#### TLS derived height threshold

The minimum, average and maximum defined height thresholds were 12, 16.2 and 19 respectively and the details of the thresholds in each plot are shown in Table 22.



Table 22: TLS derived defined height thresholds to integrate the upper and lower canopy trees per plot.

Plot. No	1	2	3	4	5	6	7	8	9	10	11	12	13	14	15
Threshold	17	14	18	19	15	19	16	16	18	18	16	14	17	16	16
Plot. No	16	17	18	19	20	21	22	23	24	25	26	27	28	29	30
Threshold	16	18	15	12	14	17	17	17	18	15	19	17	15	16	12

Based on the threshold, of the 658 total trees extracted using the remote sensing method 274 (41.6%) were an upper canopy, and 376 (57%) were lower canopy trees. Thus, sum of the integrated number of trees was 650 because eight (8) trees are miss-categorized as part of the upper canopies.

### UAV derived height thresholds

The minimum, average and maximum height threshold recorded from the UAV-CHM extracted height were 10.2, 14.4 and 18.1 respectively and the detail of the thresholds are shown in Table 23.

Table 23: Determined UAV minimum height threshold.

Plot. No	1	2	3	4	5	6	7	8	9	10	11	12	13	14	15
Threshold	12.1	17.2	18.1	16.8	11.5	10.5	11.6	14.6	17.2	15.2	14.5	16.1	17.2	14.5	16
Plot. No	16	17	18	19	20	21	22	23	24	25	26	27	28	29	30
Threshold	15.9	13.7	12.9	15.8	10.2	14.2	14.2	13.8	16.1	11.3	16.2	13.6	15.3	12.3	13

Of the total (658) UAV, and TLS extracted trees, 436 (66.3 %) are an upper canopies, and 222 (33.7 %) trees are lower canopies. Thus, the result shows there is no missing or double counting of individual trees to integrate the tree parameters. Besides, comparing with the result of TLS derived height threshold the number of the lower canopies were decreased while the number of upper canopies was increased because the defined average height threshold of TLS was slightly higher than the height threshold of UAV. Besides, there is no missing or double counting of trees. The details of the descriptive statistics of the tree parameters are shown in Appendix 15.

Based on the above-mentioned integration method of upper and lower canopies, AGB was estimated, and the descriptive statistics are shown in Table 24.

Table 24: Descriptive statistics of TLS derived threshold upper and lower canopies.

descriptive statistics	Upper and lower canopy trees using TLS threshold			Upper and lower canopy trees using UAV threshold		
	Number of trees	AGB (Kg)	AGB (Mg/plot)	Number of trees	AGB (Kg)	AGB (Mg/plot)
Minimum	13.00	7632.32	7.63	13.00	7572.16	7.57
mean	21.67	15529.23	15.53	21.93	15596.40	15.59
Maximum	32.00	25960.53	25.96	32.00	25960.53	25.96
STDV	4.54	4756.20	4.75	4.69	4727.18	4.73
sum	650.00	465877.00	465.87	658.00	467892.04	467.89
Count	30	30	30	30	30.00	30.00

The estimated AGB using TLS derived height threshold was compared with the AGB estimated using the UAV derived height threshold on a scatter plot. The result shows  $R^2$  of 0.99 (Figure 25) and details of the regression are listed in appendix 9.

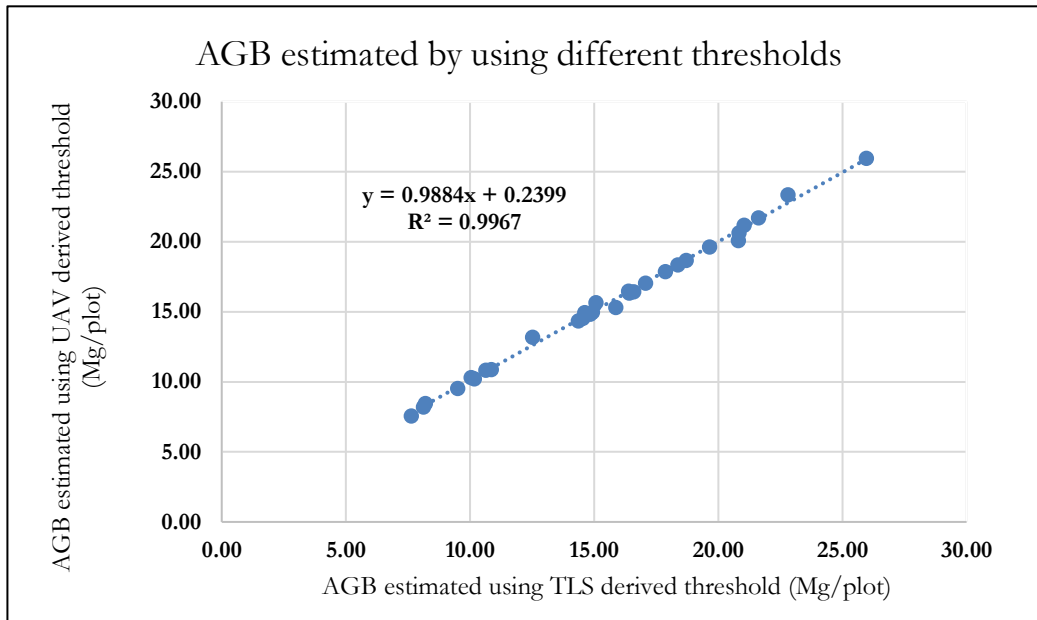


Figure 25: AGB estimated by using TLS and UAV derived thresholds to integrate the upper and lower canopies.

The AGB estimated using TLS derived height threshold has a slight variation as compared with the AGB estimated using UAV derived height threshold. Besides, the total output number of integrated upper and lower canopies trees are not equal (Table 24) because eight trees which are not detected by UAV were categorized as part of upper canopies. The details of the miss-categorized trees are in Table 25.

Table 25: Lower canopy trees miss-categorized as part of upper canopies and their AGB.

Plot No	No of tree	AGB based on TLS data (Kg)	AGB based on UAV data	Remark
2	2	162.01	-	Tree crowns are not detected by UAV imaging but categorized as part of an upper canopy
12	2	677.61	-	
19	3	184.99	-	
30	1	69.29	-	
Sum	8	1093.90 (1.093Mg)	-	

The RMSE was 0.27Mg which was 1.78 % of the plot based estimated AGB. The detail of the RMSE shown in Table 26.

Table 26: The relationship of AGB estimated using TLS and UAV derived height threshold to integrate the upper and lower canopy trees.

TLS threshold against UAV threshold	Regression			RMSE	
	Observation (Plot)	R <sup>2</sup>	r	Bias (Mg)	(Mg) (%)
Estimated AGB (Mg)	30	0.99	0.998	0.06	0.27 1.78

### The t-test assuming equal variance

The t-test was conducted to find out if there is a significant difference between the two estimated AGBs (Table 27).

Table 27: The t-test assuming equal variance.

	UAV derived threshold	TLS derived threshold
Mean	15.58872504	15.52923332
Variance	22.17200411	22.62146464
Observations	30	30
df	58	
t Stat	0.048686644	
P(T<=t) two-tail	0.961336289	
t Critical two-tail	2.001717484	

The result shows, t-statistics < t- critical ( $P > 0.05$ ); Hence, there is no significant difference between the AGB estimated using TLS derived, and UAV derived height threshold which is used to integrate the upper and lower canopy trees of the tropical forests.

Furthermore, the plot based estimated AGB using TLS derived threshold was compared with the field based AGB to establish a relation. The regression result shows that ( $R^2$ ) of 0.94. The RMSE was 1.11Mg which was 7.22 % of the total plot based estimated AGB (Table 28). Detail of the scatter plot in (Appendix 11), and the regression results are indicated in Appendix 13.

Table 28: Relationship between field-based and remote sensing method (TLS threshold) estimated AGB.

RS method against Field based	Regression				RMSE	
	Observation (Plot)	$R^2$	r	Bias (Mg)	(Mg)	(%)
Estimated AGB (Mg)	30	0.94	0.97	0.08	1.11	7.22

#### A t-test assuming equal variance

The estimated AGB has an equal variance. Thus, t-test assuming equal variance was conducted to find out if there is a significance difference (appendix 12). Thus, the result shows t-statistics < t-critical so, there is no significant difference between the field-based and remote sensing method (TLS derived threshold) estimated AGB.

#### 4.8.3. The relationship between field-based and remote sensing method estimated AGB.

Of the total 699 field recorded tree 658 trees were detected using the remote sensing method. So, 41 lower canopy trees are missed because their stem is not detected by the point cloud of TLS as well as UAV. Thus, these trees are not included to compare the field-based and remote sensing method of AGB estimations.

The result of field-based and remote sensing method estimated AGB using the same allometric equation (Equation 1) were compared in a plot based. The average plot based estimated AGB using field-based and remote sensing method was 15.44 and 15.59 Mg/plot respectively. The detail of the statistical analysis are shown in Table 29.

Table 29. Descriptive statistics of plot based estimated AGB using field-based and remote sensing method.

descriptive statistics	Field AGB (Mg)			Remote sense method AGB (Mg)		
	Lower canopy	Upper canopy	Sum	Lower canopy	Upper canopy	Sum
Minimum	0.13021	7.60564	8.20894	0.16632	6.88691	7.57216
mean	0.86710	14.60247	15.44066	0.87756	14.74809	15.59640
Maximum	3.09175	24.30564	24.72876	2.88950	25.53039	25.96053
Standard Deviation	0.65150	4.45665	4.38346	0.61959	4.78718	4.72718
sum	25.14581	438.07411	463.21992	25.44924	442.44280	467.89204
Count	30	30	30	30	30	30

The plot based estimated AGB using field-based and remote sensing method was presented using a bar graph in Figure 26.

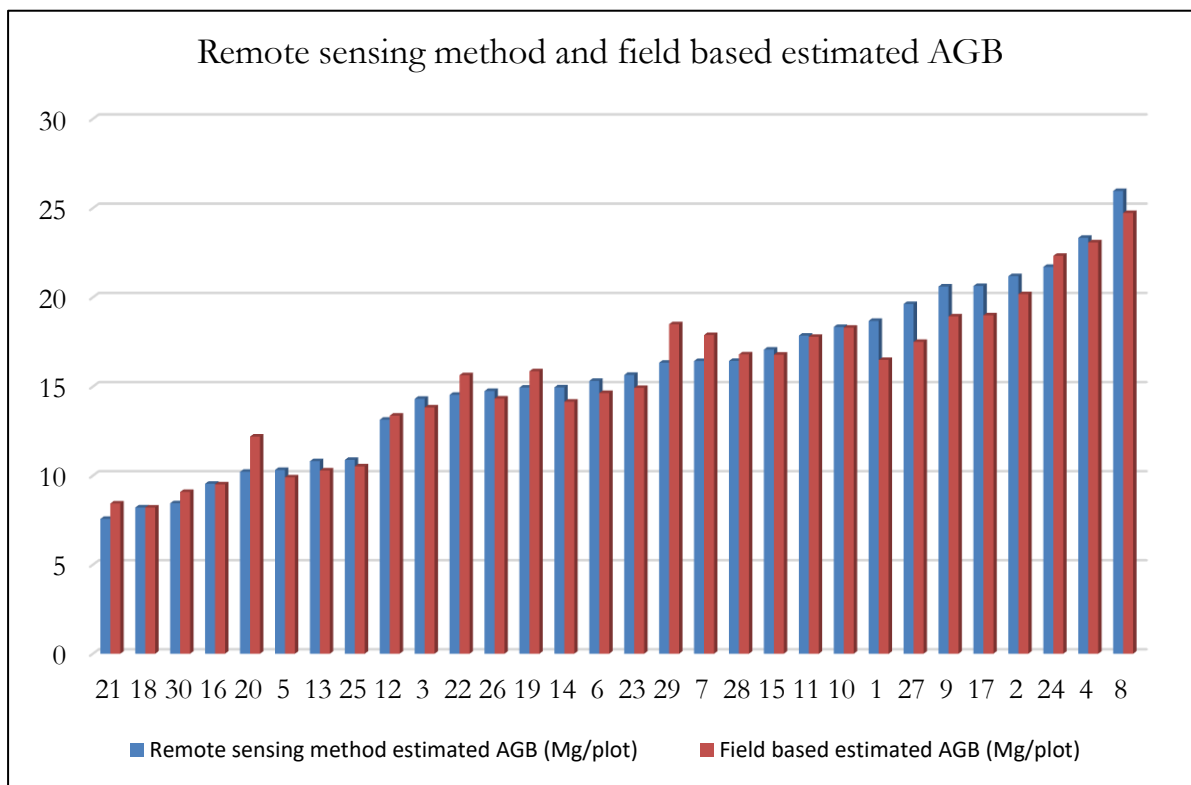


Figure 26: Plot-based estimated AGB using remote sensing method and field-based.

The relationship between the field-based and remote sensing method AGB was assessed using the linear regression analysis to determine the accuracy and to validate the remote sensing method AGB (Figure 27). The output result shows a coefficient of determination ( $R^2$ ) of 0.95 and the Pearson correlation was 0.97.

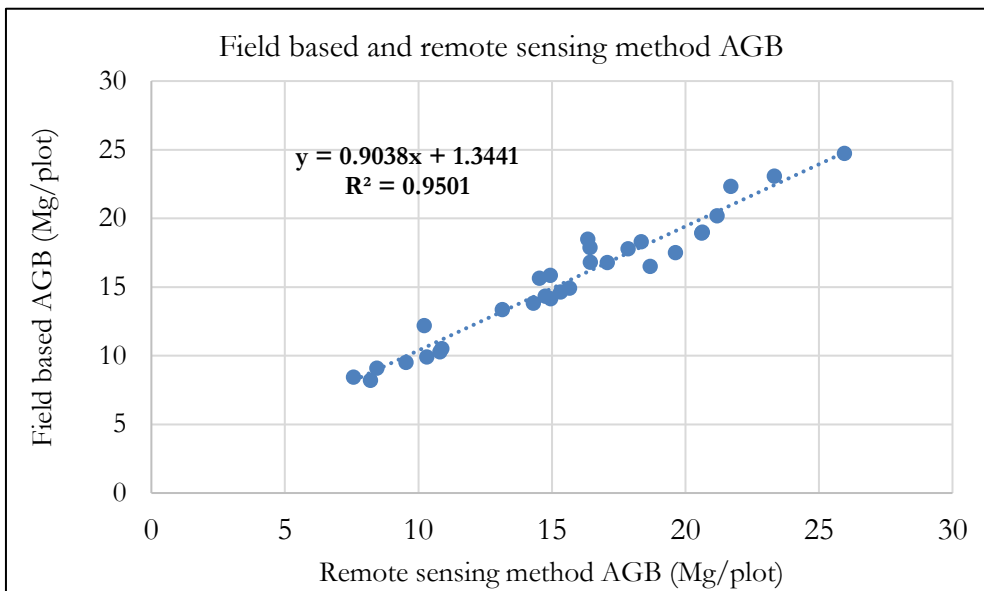


Figure 27: Relationship between field-based and remote sense method estimated AGB.

The remote sensing method was overestimated by the mean of 0.15Mg comparing with the field based estimated AGB. The RMSE was 1.07 (Table 30) which is (6.95%), and small variation in AGB was created due to the difference in height measurement of the lower and upper canopy trees. Detail of the regression analysis is shown in Appendix 9.

Table 30: Relationship between field-based and remote sensing method estimated AGB per plot.

Remote sensing against Field based	Regression			RMSE		
	Observation	R <sup>2</sup>	r	Bias (Mg)	(Mg)	(%)
Estimated AGB	30	0.95	0.97	0.15	1.07	6.95

### F-test for equal or unequal variance

F-test was conducted for the remote sensing method, and field-based estimated AGB (Table 31).

Table 31: F-test equal variance or un equal variance.

	Remote sensing method estimated AGB (Mg/plot)	Field-based estimated AGB (Mg/plot)
Mean	15.59640143	15.44066398
Variance	22.34621735	19.21471937
Observations	30	30
df	29	29
F-statistics	1.162973912	
P(F<=f) one-tail	0.343529655	
F Critical one-tail	1.860811435	

The result shows F-statistics is less than F-critical; thus, it has equal variance so, t-test equal variance was applied to test the significant difference.

### The t-test assuming equal variance

A t-test was conducted to find out if there is a significant difference or not between the remote sensing method, and field-based estimated AGB (Table 32).

Table 32: The t-test for a significant difference between field-based and remote sensing method estimated AGB.

	Remote sensing method estimated AGB (Mg/plot)	Field-based estimated AGB (Mg/plot)
Mean	15.59640143	15.44066398
Variance	22.34621735	19.21471937
Observations	30	30
df	58	
t Stat	0.132315593	
P(T<=t) one-tail	0.447596319	
t Critical one-tail	1.671552762	
P(T<=t) two-tail	0.895192637	
t Critical two-tail	2.001717484	

Thus, t-statistics < t-critical ( $P > 0.05$ ) then there is no significant difference between the estimated AGB.

#### 4.9. Above ground carbon estimation

Carbon was calculated based on the IPCC (2006), which is 0.47 of the estimated AGB from the field based and remote sensing method. The overall estimated carbon using the field-based and remote sensing method are described in Table 33 and Figure 28. The summery is indicated in Appendix 17.

Table 33: Descriptive statistics of carbon stock.

descriptive statistics	Field-based			Remote sense method		
	AGB (Kg)	AGBC (Kg)	AGBC (Mg)	AGB (Kg)	AGBC (Kg)	AGBC (Mg)
Minimum	8208.94	3858.20	3.86	7572.16	3558.91	3.56
Mean	15440.66	7257.11	7.26	15596.40	7330.31	7.33
Maximum	24728.76	11622.52	11.62	25960.53	12201.45	12.20
STDV	4383.46	2060.23	2.06	4727.18	2221.77	2.22
sum	463219.92	217713.36	217.71	467892.04	219909.26	219.91
Count	30	30	30	30	30	30

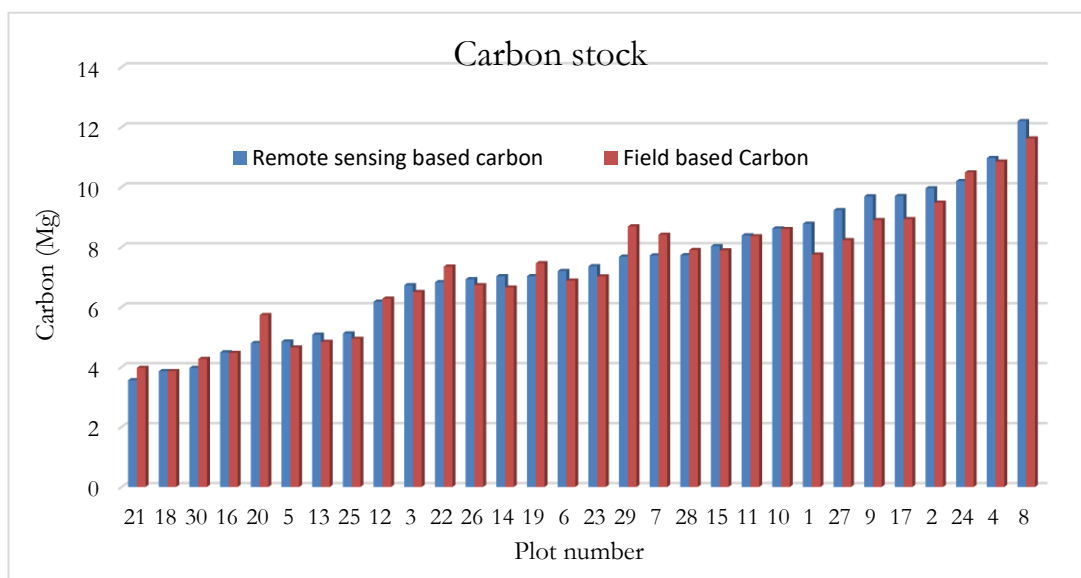


Figure 28: Remote sensing method and field-based estimated above-ground biomass carbon (Mg).

## 5. DISCUSSION

### 5.1. Field level upper crown tree identification

In this study, the upper canopy trees were identified using Avanza Map and Lucas Map in the field for the 30 sample plots. Maps like PDF, GeoPDF or GeoTIFF can be upload to the Avenza application (Avenza Maps). As it was explained in Section 1.2 and Figure 1, tropical rain forests have a multi-layered canopy structure. Thus, the identification of trees whether it is an upper canopy or lower canopy, and the process of tree matching using only hand-held GPS was difficult. So, the field based identified upper tree crowns was 89 % of the manually delineated tree crowns (polygons). Hence, the result of field-based identified upper canopy tree shows a little variation as compared to the manually delineated result. This difference is happened because the screen size of the Tablet and Mobile was slightly small. Thus, for some tree crowns especially for trees which have a narrow crown, identifying their crown using small screen Mobile inside the heterogeneous forest have created challenges. Another reason is the time difference between the two-image acquisitions could have a variation in tree crowns because few trees crowns were not visible in the 2017 orthomosaic image and their crowns become visible in 2018 orthomosaic image due to the nature of tree growth increment. Further, the field based identified tree crowns were used for the process of tree matching and the tree crowns which were not identified at field level was matched based on the position of the trees on the TLS point clouds, GPS coordinate, and tree parameter information (i.e., DBH, height).

There are no similar studies found that used Avenza Maps for upper canopy tree identification in the field. However, there are similar studies that used integration of two remote sensing methods for the upper and lower canopies in Ayer Hitam tropical forests, Malaysia. For instance, Wassihun, (2018) has used ALS for the upper canopy, and TLS for the lower canopy, Mtui (2017) has integrated UAV and TLS data for the upper canopy and lower canopy respectively, while Lawas (2016) did a complimentary use of ALS and TLS. In all mentioned studies they have used hand-held GPS coordinate, information of tree DBH & height, and position of the tree from the point cloud of TLS for the tree matching process. Thus, comparing with these studies, this research has additional input to reduce the error happened in the tree matching process by using the Avanza Map and Lucas Map data.

The possible errors observed and experienced in the field was a little shifting of the Avenza Map coordinate (navigation pointer) from the center of the sample plots during the data collection, but it is possible to correct the position by physically observing the actual setup of the plot location and the actual trees within the plot. Another challenging problem was examined for identifying of tree crowns which are grown up together because their crowns were interconnected and almost the crown of the trees was similar; consequently this could be a source of errors in making a placemark in the tree crown.

### 5.2. Descriptive analysis of the tree parameter data

Forest tree parameters recorded in the field and extracted from the remote sensing methods (TLS and UAV) are tested whether their distribution was normal or skewed. Skewness is the measure of a variable distribution for the level of symmetry. Therefore, the distribution can negatively skewed, normal, and a positively skewed distribution.

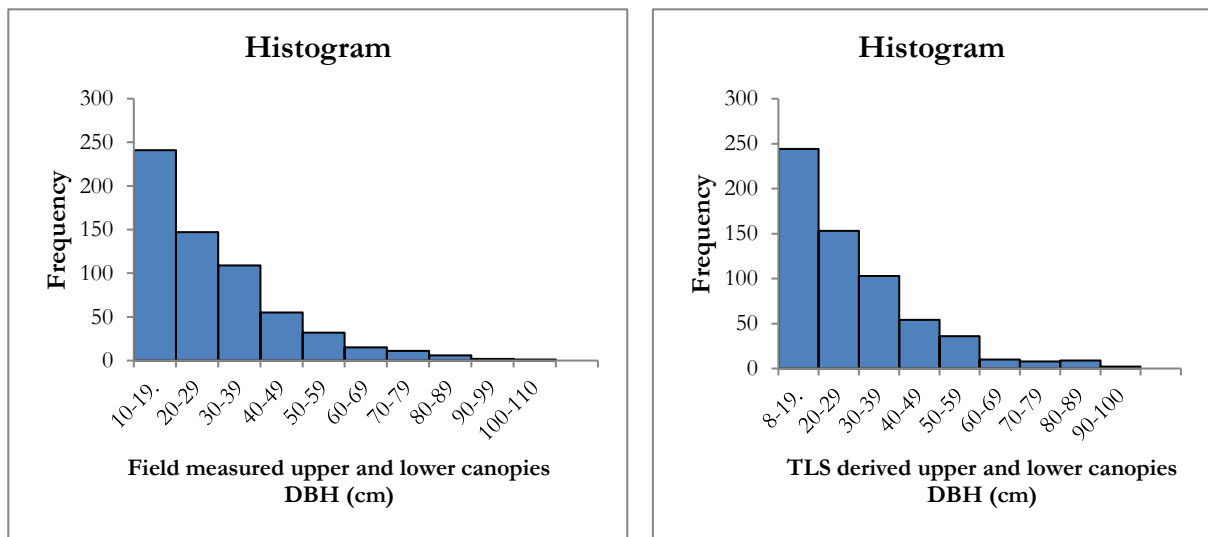


Figure 29: Distribution of field measured, and TLS derived DBH (cm) on a histogram.

The field measured, and TLS derived DBH (Figure 29) are positively skewed because the measurement was conducted for only trees which have  $\geq 10$  cm DBH. The upper and lower canopy tree heights were also not normally distributed as a result of the defined height threshold. Thus, the upper canopies were slightly skewed to the right while the lower canopies are skewed to the left (Appendix 4).

### 5.3. Tree extraction from TLS point cloud

In this study, 619 (89%) of the field-recorded trees were extracted from the TLS registered point cloud which were used to measure the tree parameter, i.e., height and DBH. Eighty (80) trees were missing because the tree tags mounted on the stem were not visible (readable). The reason is due to the blocking of the TLS point cloud by the existing foliage's, and other tree stems by creating a shadow behind on other standing trees. The other reason could be the far distance between the tree and the scanner position, because as the distance from the scanner increases the density of the point cloud also decreases as a result of the occlusions. Thus, mostly trees which are near to the scanner have more visible tree tags in the point cloud. The study by Antonarakis, (2011), reveals that trees which are far from the scanning position have less probability of detection. Moreover, the occlusions of foliage play a significant role for the trees missing.

Other similar works were conducted in Ayer Hitam tropical rain forest in Malaysia, such as a study by Mtui (2017) extracted 92%, and Bazezew (2017) obtained 93% of the total trees. Hence, compared with these results, this study achieves a little bit lower number of tree extraction. The reason can be due to the difference in the density of the undergrowth trees. Studies show that the extraction of a tree from the point cloud of TLS depends on the density of the forest and undergrowth trees. As pointed by Antonarakis, (2011) in riparian forests which have less undergrowth tree, all trees (100%) were detected. But in this study, the KRUS conservational forest has a high density of undergrowth tree (DBH < 10 cm). For this reason, the point cloud of TLS did not detect the tree tag of some of the missed trees. However, another similar study was conducted in Air Hitam tropical forest by Wassihun (2018) achieved 82%, Ghebremichael (2015) obtains 80%, and Madhibha (2016) achieves 80%. Hence, compared with these studies, this study obtains a higher result of tree extraction. Therefore, the result of this study has a comparable tree extraction with the studies carried out in the Air Hitam tropical forest tropical forests.



#### 5.4. Accuracy assessment of lower canopy tree height

The TLS derived lower canopy tree heights were used as a reference and to validate the tree height measured by Leica DISTO. Studies show that TLS height measurement for the lower canopy has higher accuracy than field height measurements. For instance, the TLS tree height measurements were compared with field height measurements by using a reference height (destructive method), and the TLS height had a high correlation with the reference height (Calders et al., 2015).

Of the total field recorded trees, 222 were categorized as lower canopies, and a comparison was conducted. The result has obtained a coefficient of determination ( $R^2$ ) of 0.8 and the RMSE was found 1.0 m (8%) (see Table 10). The result showed that the Leica DISTO D510 measurements were underestimated comparing with the TLS height in which the average height was 11.49m and 11.98m respectively. In addition, the t-test result shows that there is a significant difference between the height measurements of the lower canopy of Leica DISTO D510 and TLS at ( $P < 0.05$ ).

The obtained result of this study contradicts with the study performed by Mtui (2017) at Berklah tropical rain forest in Malaysia, where in his result the field measurement was overestimated by 0.17m. The reason could be the Leica DISTO D510 laser beam whether it blocked by near-by foliage which is not the actual peak of the tree or it was received by another crown or branches of the upper canopy trees that can lead to under and overestimation respectively. In this study, the Leica DISTO measurements were mostly affected by occlusions due to the difficulty to detect the exact peak of the actual tree and the subsequent height measurements. Thus, the probability of the error observed in the field was that tree heights are underestimated.

However, comparing with other similar studies in Ayer Hitam tropical rain forest this study has similar results in which the field measurement was underestimated comparing with the TLS height. For instance, A study by Sadadi (2016) achieved  $R^2$  of 0.62 with RMSE of 3.07m. While; Bazezew (2017) obtained  $R^2$  of 0.68 with RMSE 1.45m for the lower canopies. Even though the result was similar, their RMSE have some differences with this study. The reason could be due to the difference in the forest density and experience of the observer. Leica DISTO D510 laser beam needs open space to detect the exact peak of the tree. The observer has to try viewing the tree from different directions until the top of the tree will be online of view of the instrument. This was also stated by Hunter. (2013) who reveals that tree height measurement depends on the density of the forest and the experience of the spectator (observer). Also, the obtained RMSE of this study and the result achieved by Sadadi (2016) has a large difference. This is because this study was compared only for the lower canopy trees heights which means it has low occlusion comparing to the upper canopies while Sadadi (2016) was comparing all trees. Other studies show that in open forests the field height measurement can be performed with low RMSE (0.28m) and high  $R^2$  of 0.94 (Birdal et al., 2017). Therefore, the result of this study is within the range of Hunter et al. (2013) findings which reveals that the field-level measurement of tree height has errors ranging from 3-20 % in tropical forests.

In rare cases, TLS derived height could have hardly contributed errors. In some trees growing together, their branches are interconnected hence identifying, and separation of the actual peak of the tree from the point cloud of the TLS was challenging which was observed and recognized during the extraction of tree height. Thus, this was also stated by Jung et al. (2011) in trees which have interconnected crowns it can create errors in tree extraction and the subsequent tree height measurements.

### 5.5. Comparison of TLS derived DBH and field measured DBH

In this study, field measured DBH using diameter tap were used as a reference to assess the accuracy of TLS derived DBH. In KRUS tropical rainforest some of the tree stems have a very big trunk and covered by vegetation (Figure 30). Thus, measuring DBH without removing the shrubs, lianas or other climbers stacked on the stem is incorrect. These climbers on the stem were observed as a source of error in the DBH measurement in the field. Thus, the vegetations stacked on the stem were removed during the field data collection to reduce the possibility of errors.



Figure 30: Effect of vegetation stacked on tree stem for DBH measurement.

The accuracy assessment result between the DBH measured in the field and derived from TLS shows  $R^2$  of 0.99 and the RMSE was 1.59cm. In addition, the statistical t-test result shows there is no significant difference at ( $p < 0.05$ ) between the two measurements.

Comparing with other similar studies carried in Ayer Hitam tropical forests the obtained accuracy was comparable with the study carried by Wassihun (2018) who achieved  $R^2$  of 0.99 with RMSE 1.37, while Bazezew (2017) has achieved  $R^2$  of 0.98 with RMSE of 1.3 cm, whereas Mtui (2017) has achieved  $R^2$  of 0.98 with RMSE of 1.4 cm, and finally Ghebremichael (2015) has achieves  $R^2$  of 0.98 and RMSE of 1.7 cm. The reasons could be due to the adoption of the multi-scan position to scan all direction of the stem and the clearing of the forest ground in the plot before the TLS scanning starts. In other cases the achieved RMSE of this study was higher than the study conducted in southern Sweden, spruce dominated forest with RMSE of 0.38 cm (Lindberg et al., 2012). The reason for the RMSE difference could be due to the difference in the density of the forest and undergrowth trees because the KRUS secondary tropical forest has a dense multi-structured or multi-canopy tree. Also, this is mentioned by Stas (2011) in Moluccas, Indonesia, that the secondary forests have many stems which have  $< 10$  cm DBH. However, this study has higher accuracy compared with the study by Reddy et al. (2018) in central Indian forest which achieves  $R^2$  of 0.97 with RMSE 3.5 cm using only one scan position. The reason could be due to the number of the scan positions because in this study multiple scan positions (4) was applied. This was also stated by Maas et al. (2008) which obtains higher accuracy from multiple scans than single scan positions. Therefore, the obtained RMSE result of this study was acceptable. Because, having with 1-2 cm

range of RMSE errors from DBH measurement using TLS was considered as a good measurement based on the developed national allometric models (Liang et al., 2016).

In this study, the TLS DBH measurements show limited errors when it compared with the field measured DBH. The error is a result of mainly from the effect of the undergrowth trees density and tree trunks growing together (Figure 31) which blocks the point cloud of TLS partially. Also, in some trees, the stem shape was not a perfect circle, and this could become a source of uncertainties because in this study TLS-DBH was measured using the horizontal line (point to point) in the RiSCAN Pro software. As pointed by Saarinen et al. (2014) for trees stem which has not a perfect circular shape TLS-DBH measurement horizontally from a different position of the stem and averaging the result has a possibility to increase the accuracy. Another reason is same of the tree tags were pinned at 1.3m of the stem from the base of the tree (Figure 31) so, tree DBH which has less than the diameter (width) of the tree tag has an effect to get full shape of the stem DBH on the point cloud.

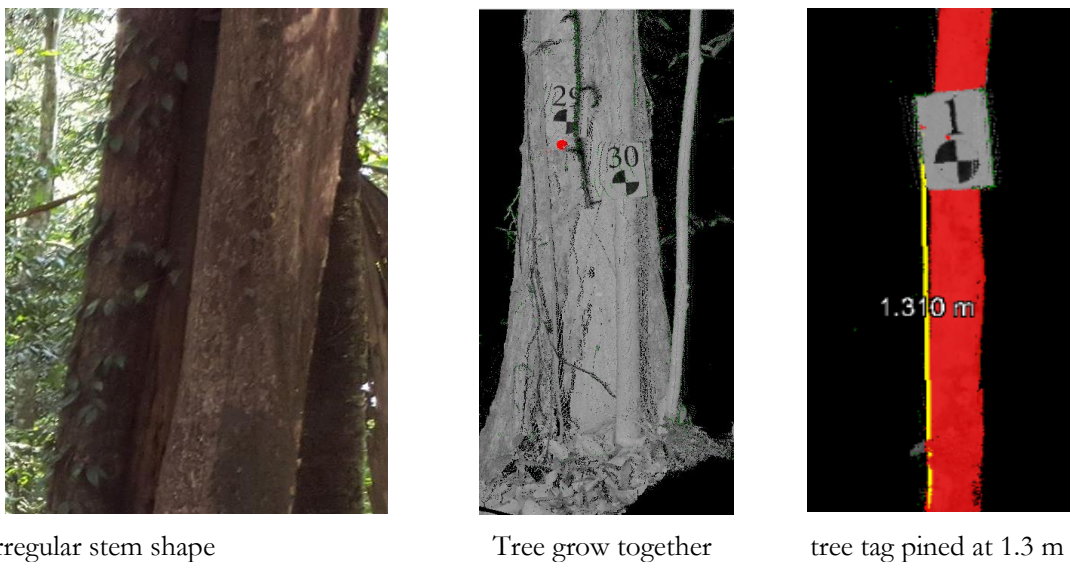


Figure 31: Illustration of stem condition and its effect in TLS- DBH measurements.

### 5.6. The accuracy of the upper canopy tree height measurements

The Leica DISTO D510 laser instrument was used as a reference to validate and to assess the accuracy of UAV-CHM derived upper canopies tree height measurement. In the tropical forest Air-borne LiDAR tree height measurement has higher accuracy, but it is expensive and not always available (Aicardi et al., 2017). Hence, the Leica DISTO D510 laser instrument can measure tree parameters better comparing with other hand-held instruments. A study by Williams et al. (1994) was tested five hand-held instruments to measure tree height unbiasedly and to determine which instrument can be more effective and accurate for tree height measurement comparatively. As a result, the laser height (Leica DISTO D510) was found the only one which has an unbiased result for tree height measurement in his work.

In this study, the obtained result shows a coefficient of determination  $R^2$  of 0.76 and the RMSE was 2.53 meter (13%). The result shows the UAV-CHM estimated height is overestimated by 1.19m of average height and it has a significant difference between the upper canopy tree height measurements (see Table 18). Other similar studies in Ayer Hitam tropical forests were made a comparison of tree heights derived from different remote sensing technologies. For instance, studies by Berhe (2018), and Begashaw (2018) were compared between Air-borne LiDAR measured and UAV derived tree height resulted in  $R^2$  of 0.83 with RMSE 3.9 m and  $R^2$  of 0.88 with RMSE 2.1m respectively. Compared with these results this study

obtains low accuracy. The reason for obtaining a low coefficient of determination can be due to the use of different reference height. Because, in their study they used ALS height measurement as a reference which has very high accuracy, while in this study Leica DISTO D510 was used as a reference which has less accuracy compared to ALS. Therefore, when the researchers use very accurate height reference, of course, their height assessment will much higher than using an instrument such as Leica DISTO D510 which already have a certain range of error. In other cases, a study by Bazezew (2017) was compared between the field measured height and Airborne LiDAR height, and he obtained  $R^2$  of 0.61 and RMSE of 3.24 m is achieved. Hence, the result obtained from this study is higher accuracy comparatively.

A study by Birdal et al. (2017) in an open forest, obtains a coefficient of determination  $R^2$  of 0.94 with RMSE of 28 cm among field measured and UAV derived tree heights. Thus, the result achieved in this study is lower comparing with (Birdal et al., 2017). The reason for obtained low accuracy could be due to the difference in the density of the forest. Indeed, the Leica DISTO have a limitation to detect the exact peak of the trees due to occlusions of foliage's and having limited free distance from the tree to the observer.

Therefore, the error obtained between the field measured and UAV-CHM derived height (RMSE 2.53) could be contributed from both the UAV-CHM derived height and the Leica DISTO height measurements. Because same part of the study area has an undulating landscape with open and closed canopies, thus, the DTM of the UAV could be more accurate at the forest which has flat terrain and less accurate at the undulating terrain forests depending on the openness of the forest. For instance, in plot 7, 20, 29 we have observed that the UAV derived height was slightly lower than the field measured height while in most of the other plots the UAV derived height was higher than the field measured heights. This has happened in some sample plots with a closed canopy which are found in the depression (valley) area. In this case, the interpolation of the DTM could be based on the flat terrain, and this can be influencing the CHM value. This was as a result of reducing the distance of ground interpolation of the DTM in the forests which have an open area and increases the interpolation distance in forests which have no open space (Lisein et al., 2013).

In this study, one of the most observed and experienced error in the field was the height measurement by Leica DISTO D510 which was mainly affected by the occlusion of foliages. Because the laser pulse sends by the Leica DISTO D510 could not see or detect the actual exact peak of the trees due to the blocking effect of the branches and the lower canopy trees (Figure 32). Hence, most of the laser pulses that hit the lowest branch which is not the actual peak of the trees, therefore this leads to underestimation. The previous study reveals that tree height measurement using Leica DISTO D510 needs open space to view the actual peak of the tree Williams et al. (1994).

### **5.7. Comparison of remote sensing method AGB integrated by separate height thresholds**

In this study, to integrate the tree parameters derived from TLS (i.e., height and DBH) and UAV (height) without missing or double counting of trees, a separate height threshold was applied for every plot. Further, the effect of defining a threshold on the estimation of AGB was analyzed. Of the total 658 extracted trees, 650 trees in which 274 (41%) upper and 376 (57%) were lower canopies using the TLS height thresholds. In other cases, 658 which is 436 (66%) upper and 222 (33%) were lower canopies using the UAV derived height thresholds (section 4.8.2). The integration result showed in the UAV derived thresholds there is no missing and double counting of individual trees. However, in the TLS defined height threshold eight (8) trees were miss-categorized (missed) which means these trees were categorized as upper canopies based on the TLS derived height threshold, but their canopies were not detected by UAV (Figure 32).

The comparison result of the estimated AGB integrated using the two techniques of height threshold shows  $R^2$  of 0.99, and the RMSE was 0.27 Mg which is 1.78% of the plot based AGB. Hence, integrating using the TLS derived height threshold is slightly underestimated by 0.059 (Mg). The reason for the small variation is created as a result of the missing trees. Another reason could be in some tree heights the TLS point cloud do not detect the actual top of the trees in the canopy layer in which trees recognized as part of the fully detected. Also, a t-test was conducted to find out if there is a significant difference among the estimated AGB integrated using the TLS and UAV defined thresholds. Hence, integrating the tree parameters using these two threshold techniques do not shows a significant difference in the estimated AGB at ( $P > 0.05$ ). Further, the AGB estimated using TLS derived threshold was compared with field-based AGB. The regression analysis result shows a coefficient of determination ( $R^2$ ) of 0.94 and the RMSE was 1.11 Mg. Comparatively the AGB obtained from UAV derived height threshold results shows lower RMSE than the AGB estimated by using TLS derived threshold.

Unfortunately, there are no more studies found for a comparison of AGB estimated by using two separate defined height thresholds. However, there are studies which used one of the height thresholds to integrate the upper and lower canopies tree parameters. For instance, the study conducted by (Bazew, 2017) in Ayer Hitam tropical forest was using ALS derived minimum height to integrate the lower and upper canopies. Similarly, the study by Mtui (2017) was using TLS derived fully detected tree height as a threshold to integrate the lower and upper canopies. In both studies, the height threshold was defined by categorizing all the sample plots to single and multiple canopies, and a generalized height threshold was determined. However, in this study, the threshold was defined for each sample plots (30) based on the height of the sample plot trees. Thus, determining the height threshold based on each sample plot for every plot could have advantageous for an accurate tree height measurement. Because in KRUS tropical forest of East Kalimantan, Indonesia, the tree height ranges of the plots have variation from one plot to another as a result of the sample plots are taken from different part of the forest.

In defining UAV minimum height, very short tree heights have occurred in rare cases. These trees are skipped as out layers during the digitization of crowns. Hence, this has occurred as a result of having a small open canopy space which made it possible for UAV to view the lower canopy trees. Also, this is stated by (Nurul-shida et al., 2014) work in which a big gab can be created by falling of big trees in the tropical forests. In applying the TLS defined thresholds, rare trees can be miss-categorized among the upper and lower canopies as mentioned above. In this study, in four plots are experienced, and this happened if the tree height is greater than the TLS derived height threshold and, also its crown is not visible to the UAV imaging (Figure 32). As mentioned in section 4.8.1 AGB of upper canopies trees are calculated using the input parameter DBH from TLS and height from UAV. Thus, these trees (8 trees) are categorized to upper canopy based on the threshold, but height cannot extract from UAV-CHM because their crown is not detected by UAV. The TLS derived height threshold was defined manually by observing the actual shape of the tree extracted from the point cloud of TLS. Thus, it is more subjective, and sometimes it is challenging to identify whether it is fully detected or not especially in trees which have interconnected crowns and growing together. As a result, this could be a source of errors that was observed and experienced in this study.

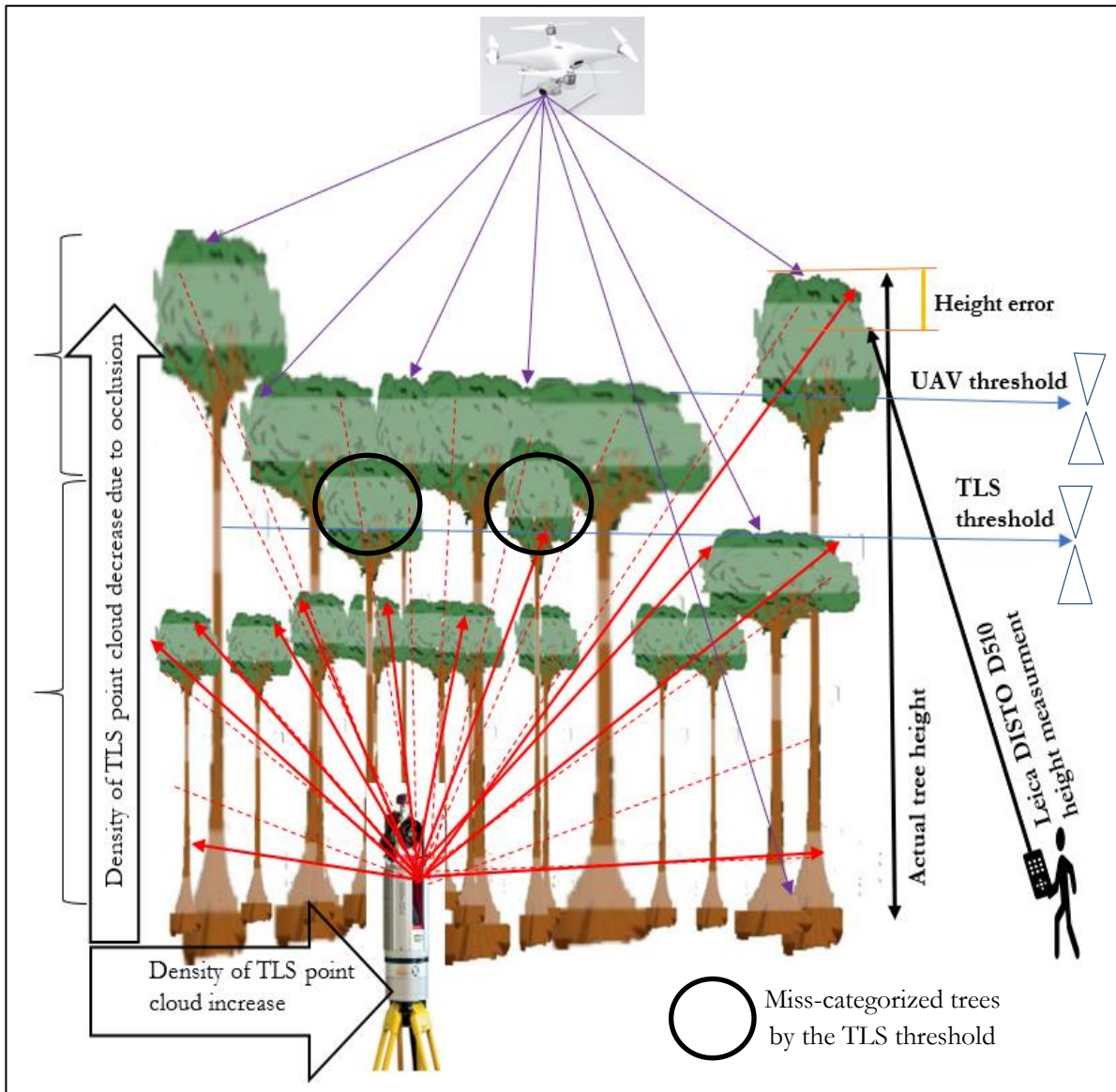


Figure 32: Illustration of tropical rain forest tree parameter acquisitions and its effects.

### 5.8. The accuracy of AGB estimated by remote sensing method

The field-based AGB was used to validate and assess the accuracy of remote sensing method AGB. Thus, the total estimated AGB is the summation of the lower and upper canopies integrated using the UAV derived height threshold. So, the result showed that a coefficient of determination  $R^2$  of 0.95 and the RMSE was 1.07Mg which is 6%. A t-test was conducted to check if there is a significant difference between the field-based and remote sensing method estimated AGB. The result of t-test indicates that there is no significant difference between the estimated AGB at higher than 95 % of confidence level ( $P > 0.05$ ).

The obtained result of this study is slightly lower than with the studies conducted in Ayer Hitam tropical forest Malaysia. For instance, the study by Lawas (2016), was a combination of TLS and ALS and has found  $R^2$  of 0.98. Also, a study by Mtui (2017) was integrated TLS for the lower canopy trees and CHM (From UAV and ALS) for the upper canopy trees, and he achieved  $R^2$  of 0.98. The reason could be due to

the type of remote sensing data used because in this study the integration of remote sensing was among UAV and TLS while in the studies mentioned above, the integration was between ALS and TLS to extract the upper and lower canopy tree parameters. Thus, the combination of ALS and TLS shows a slightly higher accuracy than the integration of UAV and TLS, because of the height measurement of ALS is more accurate compared with other remote sensing measurements in a dense forest. Moreover, CHM of UAV from which the height of the trees were derived is an inferential or an estimation method. While the ALS CHM is considering as a measured tree height, which is very accurate compared to the UAV SfM method. However, with the same study in tropical forest Malaysia, by Bazezew (2017) he has achieved  $R^2$  of 0.96 using integration of ALS and TLS. Thus, his results were closer with the result of this study.

The obtained result has a high correlation with ( $r$ ) of 0.97 because of the integration of the remote sensing technique to extract the tree parameter of the lower and upper canopies. The DBH of the upper canopy can be modeled from the Canopy Projection Area (CPA), but the TLS measurements of the DBH is more accurate. Besides, the remote sense method AGB shows a small difference with an average of 0.15 Mg overestimation. The reason could be from the error encountered in Leica DISTO D510 height measurement because the result of lower canopy accuracy assessment is an indicator that the Leica DISTO D510 was underestimated for the lower canopy trees when it compared with TLS height (see Table 10). Moreover, the mean of the plot based estimated AGB using field-based and remote sensing method was 15.44 and 15.59Mg plot<sup>-1</sup> which is equivalent to 308ton ha<sup>-1</sup> and 311ton ha<sup>-1</sup> respectively (see Table 29). Moreover, the plot based estimated AGB of this study was comparable with the studies conducted in the Indonesians tropical forests. For instance, it has an agreement with the study by (Toma et al., 2005) in Bukit Soeharto Educational Forest (BSEF), East Kalimantan, Indonesia which founds 280, 315 Mgha<sup>-1</sup> for the heavily and moderately disturbed secondary forests. Previously, the secondary forest of East Kalimantan was affected by illegal logging and fires. Thus the amount of AGB depends on the intensity of disturbance that has been occurred. Also, a study by Stas (2011) in the Moluccas, Indonesia which found 349.9 ton ha<sup>-1</sup> in primary forests using a destructive method and field-based.

### **5.9. Limitation of the study**

In this study area, there was no ALS data available. Thus, to validate the UAV-CHM derived tree height, the field measured tree height using Leica DISTO D510 was used. Hence, in the field, the Leica DISTO D510 height measurement has faced errors to view the exact actual peak of the tree in the multi-layered forests, especially for the emergent trees.

The first images acquired by UAV were facing a problem to generate good quality of orthomosaic images so, the images are collected again. As a result, data processing takes more time and effort.

The TLS weight was heavy (30kg) and to move from one sample plot to another sample plot by carrying the material it takes more time and efforts. Thus, the number of sample plots was only 30 plots.

## 6. CONCLUSIONS AND RECOMMENDATIONS

### 6.1. Conclusions

This study investigates the potential of integrating UAV, and TLS data to improve the accuracy of AGB estimation in the multi-strata tropical rain forests. From the SfM of UAV data, CHM was generated using image-based modeling process, and the tree heights are extracted from the CHM. TLS was used to extract the tree height of the lower canopies and DBH of the upper and lower canopies. Afterward, the tree parameters derived by the remote sensing were integrated using UAV derived, and TLS derived height thresholds for every plot. Then the accuracy of field measured lower canopy was compared with the TLS derived lower canopy tree height. Hence, the t-test result shows that there is a significant difference. While the TLS derived DBH of the upper and lower canopy trees, DBH were compared against field measured DBH. Hence, the t-test result reveals that there is no significant difference. Also, the UAV-CHM derived upper canopy height was compared against the field measured height. Thus, the t-test result indicates there is a significant difference.

The AGB was estimated using the same allometric equation for the field based and remote sensing method. The remote sensing method AGB was compared with the field-based AGB. Thus, the result shows it has a high correlation and statistically no significant difference. Therefore, the overall result shows that integration of UAV and TLS derived data can be used to extract the upper and lower canopy of the tropical forests and to estimate the subsequent AGB in a reasonable cost and accuracy. Based on the results the following answers are concluded to address the research questions.

#### 1. What is the accuracy of field measured height as compared to TLS derived height of the lower canopies?

The accuracy of field measured tree height using Leica DISTO D510 was compared with TLS derived lower canopy tree heights. The result shows  $R^2$  of 0.80 and the RMSE was 1m (8%). The statistical analysis reveals that there is a significant difference between the height measurement of the lower canopies ( $P < 0.05$ ). Hence, the null hypothesis ( $H_0$ ) which states there is no significant difference was rejected.

#### 2. How accurate is the TLS derived DBH, as compared to field measured DBH of the lower and upper canopy trees?

The accuracy of TLS derived tree DBH of the lower, and upper canopies were assessed with the corresponding field measured DBH. Hence, the result reveals that  $R^2$  of 0.99 and the RMSE was 1.59cm (5%). It has a high correlation with ( $r$ ) of 0.99, and the t-statistics reveals that there is no significant difference between the TLS derived and field measured DBH. Thus, the null hypothesis ( $H_0$ ) which states there is no significant difference was accepted.

#### 3. How accurate is the upper canopy tree height derived from UAV-CHM as compared to the field measured height?

The accuracy of upper canopy tree height derived from UAV-CHM was assessed using the field measured height using Leica DISTO D510. Hence, the result was found  $R^2$  of 0.76 and the RMSE was 2.53 m which is (13%). Thus, the statistical analysis reveals that there is a significant difference between the upper canopy tree height measurements. Therefore, the null hypothesis ( $H_0$ ) which states there is no significant difference was rejected.



**4. What is the amount of AGB estimated from the integration of UAV and TLS integrated using the UAV derived height and the TLS derived height as a threshold to integrate the upper and lower canopies?**

The tree parameters extracted using the two-remote sensing (UAV and TLS) was integrated using UAV derived, and TLS derived height threshold as upper and lower canopies, and the subsequent AGB was estimated based on the integration method. Thus, the AGB integrating using TLS threshold was compared with the AGB estimated using UAV derived height threshold in a plot based. Accordingly, the mean of AGB estimated using TLS threshold, and UAV derived threshold was 15.53 and 15.59 Mg plot<sup>-1</sup> respectively. Hence, the result reveals R<sup>2</sup> of 0.99 and the RMSE was 0.27 Mg. So, the obtained result shows that there is no significant difference between the estimated AGB using the two threshold techniques to integrate the upper and lower canopies. Hence, the null hypothesis (H<sub>0</sub>) which states there is no significant difference was accepted.

**5. How much is the AGB estimated using the integration of UAV and TLS data as compared to field-based AGB on a plot based?**

The accuracy of the remote sensing method estimated AGB was compared and validated using the field based estimated AGB on plot based. The remote sense method and the field based estimated AGB has a mean of 15.59 and 15.44 Mg plot<sup>-1</sup> which is equivalent to 311 and, 308ton ha<sup>-1</sup> respectively. And summation of the 30 plots was 468 Mg and 463 Mg respectively. The t-test analysis reveals that there is no significant difference between the remote sensing based and field-based estimated AGB. Hence the null hypothesis (H<sub>0</sub>) which states there is no significant difference was accepted.

## **6.2. Recommendation**

Tree height measurement using the Leica DISTO D510 for the emergent tree crowns was challenging in the field. So, selecting another more accurate technique of tree height measurement such as ALS tree height measurement is preferable to use as a reference height.

## LIST OF REFERENCES

---

- Abegg, M., Kukenbrink, D., Zell, J., Schaepman, M. E., & Morsdorf, F. (2017). Terrestrial laser scanning for forest inventories-tree diameter distribution and scanner location impact on occlusion. *Forests*, 8(6), 184. <https://doi.org/10.3390/f8060184>
- Aicardi, I., Dabove, P., Lingua, A. M., & Piras, M. (2017). Integration between TLS and UAV photogrammetry techniques for forestry applications. *IForest- Biogeosciences and Forestry*, 10(1), 41–47. <https://doi.org/10.3832/ifor1780-009>
- Antonarakis, A. S. (2011). Evaluating forest biometrics obtained from ground lidar in complex riparian forests. *Remote Sensing Letters*, 2(1), 61–70. <https://doi.org/10.1080/01431161.2010.493899>
- Asmare, M. F. (2013). *Air-borne LiDAR data and VHR worldview satellite imagery to support community based forest certification in Chitwan, Nepal*. MSc. Thesis. University of Twente, Faculty of Geo-information Science and Earth Observation (ITC). Enschede, The Netherlands. Retrieved from [https://library.itc.utwente.nl/papers\\_2013/msc/nrm/asmare.pdf](https://library.itc.utwente.nl/papers_2013/msc/nrm/asmare.pdf)
- Avenza Maps - How it works. (n.d.). Retrieved January 30, 2019, from <https://www.avenzamaps.com/maps/how-it-works.html>
- Basuki, T. M., van Laake, P. E., Skidmore, A. K., & Hussin, Y. A. (2009). Allometric equations for estimating the above-ground biomass in tropical lowland Dipterocarp forests. *Forest Ecology and Management*, 257(8), 1684–1694. <https://doi.org/10.1016/j.foreco.2009.01.027>
- Bazew, M. N. (2017). *Integrating Airborne LiDAR and Terrestrial laser scanner forest parameters for accurate estimation of above-ground biomass / carbon in Ayer hitam tropical forest reserve, Malaysia*. MSc. Thesis. University of Twente, Faculty of Geo-information Science and Earth Observation (ITC). Enschede, The Netherlands. Retrieved from [https://library.itc.utwente.nl/papers\\_2017/msc/nrm/bazew.pdf](https://library.itc.utwente.nl/papers_2017/msc/nrm/bazew.pdf)
- Beets, P. N., Kimberley, M. O., Oliver, G. R., Pearce, S. H., Graham, J. D., & Brandon, A. (2012). Allometric Equations for Estimating Carbon Stocks in Natural Forest in New Zealand. *Forests*, 3(3), 818–839. <https://doi.org/10.3390/f3030818>
- Begashaw, S. (2018). *Accuracy of DTM derived from UAV imagery and its effect on canopy height model compared to Airborne LiDAR in part of tropical rain forests of Berkelab, Malaysia*. MSc. Thesis. University of Twente, Faculty of Geo-information Science and Earth Observation (ITC). Enschede, The Netherlands. Retrieved from [https://library.itc.utwente.nl/papers\\_2018/msc/nrm/berhanu.pdf](https://library.itc.utwente.nl/papers_2018/msc/nrm/berhanu.pdf)
- Benz, U. C., Hofmann, P., Willhauck, G., Lingenfelder, I., & Heynen, M. (2004). Multi-resolution, object-oriented fuzzy analysis of remote sensing data for GIS-ready information. *ISPRS Journal of Photogrammetry and Remote Sensing*, 58(3–4), 239–258. <https://doi.org/10.1016/J.ISPRSJPRS.2003.10.002>
- Berhe, T. H. (2018). *Towards a UAV based standalone system for estimating and mapping above-ground biomass/carbon stock in Berkelab tropical rain forest, Malaysia*. MSc. Thesis. University of Twente, Faculty of Geo-information Science and Earth Observation (ITC). Enschede, The Netherlands Retrieved from <https://library.itc.utwente.nl/login/2018/msc/nrm/berhe.pdf>
- Bienert, A., Scheller, S., Keane, E., Mullooly, G., & Mohan, F. (2006). Application of Terrestrial Laser Scanners For The Determination Of Forest Inventory Parameters. *International Archives of Photogrammetry , Remote Sensing and Spatial Information Science*, 36, 5. <https://doi.org/10.1111/jam.12647>

- Birdal, A. C., Avdan, U., & Turk, T. (2017). Estimating tree heights with images from an unmanned aerial vehicle. *Geomatics, Natural Hazards, and Risk*, 8(2), 1144–1156. <https://doi.org/10.1080/19475705.2017.1300608>
- Brovkina, O., Novotny, J., Cienciala, E., Zemek, F., & Russ, R. (2017). Mapping forest aboveground biomass using airborne hyperspectral and LiDAR data in the mountainous conditions of Central Europe. *Ecological Engineering*, 100, 219–230. <https://doi.org/10.1016/j.ecoleng.2016.12.004>
- Brown, S. (2002). Measuring carbon in forests: Current status and future challenges. *Environmental Pollution*, 116(3), 363–372. [https://doi.org/10.1016/S0269-7491\(01\)00212-3](https://doi.org/10.1016/S0269-7491(01)00212-3)
- Calders, K., Newnham, G., Burt, A., Murphy, S., Raunonen, P., Herold, M., ... Kaasalainen, M. (2015). Nondestructive estimates of above-ground biomass using terrestrial laser scanning. *Methods in Ecology and Evolution*, 6(2), 198–208. <https://doi.org/10.1111/2041-210X.12301>
- Chave, J., Rejou-Mechain, M., Burquez, A., Chidumayo, E., Colgan, M. S., Delitti, W. B. C., ... Vieilledent, G. (2014). Improved allometric models to estimate the aboveground biomass of tropical trees. *Global Change Biology*, 20(10), 3177–3190. <https://doi.org/10.1111/gcb.12629>
- Dassot, M., Constant, T., & Fournier, M. (2011). The use of terrestrial LiDAR technology in forest science: application fields, benefits, and challenges. *Annals of Forest Science*, 68(5), 959–974. <https://doi.org/10.1007/s13595-011-0102-2>
- Diana, R., Hadriyanto, D., Hiratsuka, M., Toma, T., & Morikawa, Y. (2002). Carbon stocks of fast growing tree species and baselines after forest fire in East Kalimantan, Indonesia. *Forestry research Institute*, 153(1), 1-8. <https://doi.org/10.13140/2.1.4899.4247>
- Fan, J., Zeng, G., Body, M., & Hacid, M.-S. (2004). Seeded region growing: an extensive and comparative study. *Pattern recognition Letters*, 26(1), 1139–1156. <https://doi.org/10.1016/j.patrec.2004.10.010>
- FAO. (2010). *Global Forest Resources Assessment 2010. America* (Vol.163). Rome, Italy. Retrieved from <http://www.fao.org/docrep/013/i1757e/i1757e.pdf>
- FFPRI. (2012). REDD-plus cookbook: *how to measure and monitor forest carbon* | The REDD Desk. Retrieved January 25, 2019, from <http://theredddesk.org/resources/redd-plus-cookbook-how-measure-and-monitor-forest-carbon>
- Fritz, A., Weinacker, H., & Koch, B. (2011). A method for linking TLS- and ALS-derived trees. *SilviLaser*, 1–9. Retrieved from [http://www.locuscor.net/silvilaser2011/papers/009\\_Fritz.pdf](http://www.locuscor.net/silvilaser2011/papers/009_Fritz.pdf)
- Getzin, S., Wiegand, K., & Schoning, I. (2012). Assessing biodiversity in forests using very high-resolution images and unmanned aerial vehicles. *Methods in Ecology and Evolution*, 3(2), 397–404. <https://doi.org/10.1111/j.2041-210X.2011.00158.x>
- Ghebremichael, Z. M. (2015). *Airborne LiDAR and Terrestrial laser scanner in assessing above-ground biomass/carbon stock in tropical rain forest of Ayer hitam forest reserve, Maleaysia*. MSc Thesis. University of Twente, Faculty of Geo-information Science and Earth Observation (ITC). Enschede, The Netherlands. Retrieved from [https://library.itc.utwente.nl/papers\\_2016/msc/nrm/ghebremichael.pdf](https://library.itc.utwente.nl/papers_2016/msc/nrm/ghebremichael.pdf)
- Gibbs, H. K., Brown, S., Niles, J. O., & Foley, J. A. (2007). Monitoring and estimating tropical forest carbon stocks: Making REDD a reality. *Environmental Research Letters*, 2(4), 1–3. <https://doi.org/10.1088/1748-9326/2/4/045023>

- Gschwantner, T., Schadauer, K., Vidal, C., Lanz, A., Tomppo, E., di Cosmo, L., ... Lawrence, M. (2009). Common tree definitions for national forest inventories in Europe. *Silva Fennica*, 43(2), 303–321. <https://doi.org/10.14214/sf.463>
- Hirata, Y., Tsubota, Y., & Sakai, A. (2009). Allometric models of DBH and crown area derived from QuickBird panchromatic data in *Cryptomeria japonica* and *Chamaecyparis obtusa* stands. *International Journal of Remote Sensing*, 30(19), 5071–5088. <https://doi.org/10.1080/01431160903022977>
- Holopainen, M., Vastaranta, M., Hyypä, J., Holopainen, M., Vastaranta, M., & Hyypä, J. (2014). Outlook for the Next Generation's Precision Forestry in Finland. *Forests*, 5(7), 1682–1694. <https://doi.org/10.3390/f5071682>
- Hunter, M. O., Keller, M., Victoria, D., & Morton, D. C. (2013). Tree height and tropical forest biomass estimation. *Biogeosciences*, 10(12), 8385–8399. <https://doi.org/10.5194/bg-10-8385-2013>
- Hunter, M. O., Keller, M., Vitoria, D., & Morton, D. C. (2013). Tree height and tropical forest biomass estimation. *Biogeosciences Discussions*, 10(6), 10491–10529. <https://doi.org/10.5194/bgd-10-10491-2013>
- Hyde, P., Dubayah, R., Walker, W., Blair, J. B., Hofton, M., & Hunsaker, C. (2006). Mapping forest structure for wildlife habitat analysis using multi-sensor (LiDAR, SAR/InSAR, ETM+, Quickbird) synergy. *Remote Sensing of Environment*, 102(1–2), 63–73. <https://doi.org/10.1016/j.rse.2006.01.021>
- Indrarto, G. B., Murharjanti, P., Khatarina, J., Pulungan, I., Ivalerina, F., Rahman, J., ... Muharrom, E. (2012). The context of REDD+ in Indonesia: Drivers, agents and institutions. *CIFOR Occasional Paper*, 116. [http://www.cifor.org/publications/pdf\\_files/WPapers/WP92Resosudarmo.pdf](http://www.cifor.org/publications/pdf_files/WPapers/WP92Resosudarmo.pdf)
- IPCC. (2006). IPCC Guidelines for National Greenhouse Gas Inventories. Retrieved January 26, 2019, from <https://www.ipcc-nggip.iges.or.jp/public/2006gl/vol4.html>
- Jung, S.-E., Kwak, D.-A., Park, T., Lee, W.-K., & Yoo, S. (2011). Estimating Crown Variables of Individual Trees Using Airborne and Terrestrial Laser Scanners. *Remote Sensing*, 3(11), 2346–2363. <https://doi.org/10.3390/rs3112346>
- Kaasalainen, S., Krooks, A., Liski, J., Raunonen, P., Kaartinen, H., Kaasalainen, M., ... Makipaa, R. (2014). Change detection of tree biomass with terrestrial laser scanning and quantitative structure modelling. *Remote Sensing*, 6(5), 3906–3922. <https://doi.org/10.3390/rs6053906>
- Kachamba, D., Ørka, O. H., Gobakken, T., Eid, T., & Mwase, W. (2016). Biomass Estimation Using 3D Data from Unmanned Aerial Vehicle Imagery in a Tropical Woodland. *Remote Sensing*, 8(11), 1–18. <https://doi.org/10.3390/RS8110968>
- Larjavaara, M., & Muller-Landau, H. C. (2013). Measuring tree height: A quantitative comparison of two common field methods in a moist tropical forest. *Methods in Ecology and Evolution*, 4(9), 793–801. <https://doi.org/10.1111/2041-210X.12071>
- Lawas, cora J. C. (2016). *Complimentary use of Airborne LiDAR and Terrestrial laser scanner to assess above-ground biomass/ carbon in Ayer Hitam tropical rain forest reserve*. MSc. Thesis. University of Twente, Faculty of Geo-information Science and Earth Observation (ITC). Enschede, The Netherlands. Retrieved from [https://library.itc.utwente.nl/papers\\_2016/msc/nrm/lawas.pdf](https://library.itc.utwente.nl/papers_2016/msc/nrm/lawas.pdf)
- Layers of a Rainforest. (n.d.). Retrieved August 18, 2018, from <http://www.srl.caltech.edu/personnel/krubal/rainforest/Edit560s6/www/whlayers.html>
- Liang, X., Kankare, V., Hyypä, J., Wang, Y., Kukko, A., Haggren, H., ... Vastaranta, M. (2016).

- Terrestrial laser scanning in forest inventories. *ISPRS Journal of Photogrammetry and Remote Sensing*, 115, 63–77. <https://doi.org/10.1016/J.ISPRSJPRS.2016.01.006>
- Liang, X., Litkey, P., Hyyppa, J., Kaartinen, H., Vastaranta, M., & Holopainen, M. (2012). Automatic stem mapping using single-scan terrestrial laser scanning. *IEEE Transactions on Geoscience and Remote Sensing*, 50(2), 661–670. <https://doi.org/10.1109/TGRS.2011.2161613>
- Lindberg, E., Holmgren, J., Olofsson, K., & Olsson, H. (2012). Estimation of stem attributes using a combination of terrestrial and airborne laser scanning. *European Journal of Forest Research*, 131(6), 1917–1931. <https://doi.org/10.1007/s10342-012-0642-5>
- Lisein, J., Pierrot-Deseilligny, M., Bonnet, S., Lejeune, P., Lisein, J., Pierrot-Deseilligny, M., ... Lejeune, P. (2013). A Photogrammetric Workflow for the Creation of a Forest Canopy Height Model from Small Unmanned Aerial System Imagery. *Forests*, 4(4), 922–944. <https://doi.org/10.3390/f4040922>
- Maas, H. -G., Bienert, A., Scheller, S., & Keane, E. (2008). Automatic forest inventory parameter determination from terrestrial laser scanner data. *International Journal of Remote Sensing*, 29(5), 1579–1593. <https://doi.org/10.1080/01431160701736406>
- Madhibha, T. P. (2016). *Assessment of above-ground biomass with terrestrial LiDAR using 3D quantitative structure modelling in tropical rain forest of Ayer Hitam forest reserve, Malaysia*. MSc. Thesis. University of Twente, Faculty of Geo-information Science and Earth Observation (ITC). Enschede, The Netherlands. Retrieved from [https://library.itc.utwente.nl/papers\\_2016/msc/nrm/madhibha.pdf](https://library.itc.utwente.nl/papers_2016/msc/nrm/madhibha.pdf)
- Maniatis, D., & Mollicone, D. (2010). Options for sampling and stratification for national forest inventories to implement REDD+ under the UNFCCC. *Carbon Balance and Management*, 5(1), 1–14. <https://doi.org/10.1186/1750-0680-5-9>
- Micheletti, N., Chandler, J. H., & Lane, S. N. (2015). Structure from motion (SfM) photogrammetry. *British Society for Geomorphology Geomorphological Techniques*, 2(2), 1–12. Retrieved from <https://dSPACE.lboro.ac.uk/dSPACE-jspui/handle/2134/17493>
- Mohd Zaki, N. A., & Abd Latif, Z. (2017). Carbon sinks and tropical forest biomass estimation: a review on role of remote sensing in aboveground-biomass modelling. *Geocarto International*, 32(7), 701–716. <https://doi.org/10.1080/10106049.2016.1178814>
- Mohren, G. M. J., Hasenauer, H., Kohl, M., & Nabuurs, G. J. (2012). Forest inventories for carbon change assessments. *Current Opinion in Environmental Sustainability*, 4(6), 686–695. <https://doi.org/10.1016/j.cosust.2012.10.002>
- Mtui, Y. P. (2017). *Tropical rainforest above-ground biomass and carbon stock estimation for upper and lower canopies using Terrestrial laser scanner and canopy height model from Unmanned Aerial Vehicle (UAV) imagery in Ayer-Hitam, Malaysia*. MSc. Thesis. University of Twente, Faculty of Geo-information Science and Earth Observation (ITC). Enschede, The Netherlands. Retrieved from [https://library.itc.utwente.nl/papers\\_2017/msc/nrm/mtui.pdf](https://library.itc.utwente.nl/papers_2017/msc/nrm/mtui.pdf)
- Næsset, E., Gobakken, T., Holmgren, J., Hyyppa, H., Hyyppa, J., Maltamo, M., ... Soderman, U. (2004). Laser scanning of forest resources: The nordic experience. *Scandinavian Journal of Forest Research*, 19(6), 482–499. <https://doi.org/10.1080/02827580410019553>
- Newnham, G. J., Armston, J. D., Calders, K., Disney, M. I., Lovell, J. L., Schaaf, C. B., ... Danson, F. M. (2015). Terrestrial Laser Scanning for Plot-Scale Forest Measurement. *Current Forestry Reports*, 1(4), 239–251. <https://doi.org/10.1007/s40725-015-0025-5>
- Nex, F., & Remondino, F. (2014). UAV for 3D mapping applications: A review. *Applied Geomatics*, 6(1), 1–

15. <https://doi.org/10.1007/s12518-013-0120-x>
- Nonami, K. (2007). Prospect and Recent Research & Development for Civil Use Autonomous Unmanned Aircraft as UAV and MAV \*. *Journal of System Design and Dynamics*, 1(2), 120–128. <https://doi.org/10.1299/jsdd.1.120>
- Nurul-shida, S. faridah-hanum, I. Wanrazali, W>M. and Kamziah, K. (2014). (PDF) Community structure of trees in Ayer Hitam Forest Reserve, Puchong, Selangor, Malaysia. In *THE MALAYSIAN FORESTER 77 (1): 73-86 (2014)* (pp. 73–86). Retrieved from [https://www.researchgate.net/publication/270106458\\_Community\\_structure\\_of\\_trees\\_in\\_Ayer\\_Hitam\\_Forest\\_Reserve\\_Puchong\\_Selangor\\_Malaysia](https://www.researchgate.net/publication/270106458_Community_structure_of_trees_in_Ayer_Hitam_Forest_Reserve_Puchong_Selangor_Malaysia)
- Ohta, S., & Effendi, S. (1992). Ultisols of “lowland *Dipterocarp* forest” in East Kalimantan, Indonesia. *Soil Science and Plant Nutrition*, 38(2), 197–206. <https://doi.org/10.1080/00380768.1992.10416482>
- Ordonez, C., Martinez, J., Arias, P., & Armesto, J. (2010). Measuring building façades with a low-cost close-range photogrammetry system. *Automation in Construction*, 19(6), 742–749. <https://doi.org/10.1016/j.autcon.2010.03.002>
- Pan, Y., Birdsey, R. A., Fang, J., Houghton, R., Kauppi, P. E., Kurz, W. A., ... Hayes, D. (2011). A large and persistent carbon sink in the world’s forests. *Science*, 333(6045), 988–993. <https://doi.org/10.1126/science.1201609>
- Peltoniemi, M., Palosuo, T., Monni, S., & Makipaa, R. (2006). Factors affecting the uncertainty of sinks and stocks of carbon in Finnish forests soils and vegetation. *Forest Ecology and Management*, 232(1–3), 75–85. <https://doi.org/10.1016/j.foreco.2006.05.045>
- Pix4D. (2018). Menu Process & Processing Options... & 2. Point Cloud and Mesh & Point Cloud – Support. Retrieved December 3, 2018, from <https://support.pix4d.com/hc/en-us/articles/202557799>
- Ramirez, F. A., Armitage, R. P., & Danson, F. M. (2014). Testing the application of terrestrial laser scanning to measure forest canopy gap fraction. *Remote Sensing*, 5(6), 3037–3056. <https://doi.org/10.3390/rs5063037>
- Ravindranath, N.H., Ostwald, M. (2008). Introduction. In *Carbon Inventory Methods Handbook for Greenhouse Gas Inventory, Carbon Mitigation and Roundwood Production Projects* (pp. 1–11). Dordrecht: Springer Netherlands. [https://doi.org/10.1007/978-1-4020-6547-7\\_1](https://doi.org/10.1007/978-1-4020-6547-7_1)
- Reddy, R. S., Jha, C. S., & Rajan, K. S. (2018). Automatic Tree Identification and Diameter Estimation Using Single Scan Terrestrial Laser Scanner Data in Central Indian Forests. *Journal of the Indian Society of Remote Sensing*, 46(6), 937–943. <https://doi.org/10.1007/s12524-018-0753-7>
- RIEGL RIEGL VZ-400 VZ-400. (2017). Retrieved from [www.riegl.com](http://www.riegl.com)
- Ruiz, L. A., Hermosilla, T., Mauro, F., & Godino, M. (2014). Analysis of the influence of plot size and LiDAR density on forest structure attribute estimates. *Forests*, 5(5), 936–951. <https://doi.org/10.3390/f5050936>
- Saarinen, N., Vastaranta, M., Kankare, V., Tanhuanpaa, T., Holopainen, M., Hyypä, J., ... Hyypä, H. (2014). Urban-Tree-Attribute Update Using Multisource Single-Tree Inventory. *Forests*, 5(5), 1032–1052. <https://doi.org/10.3390/f5051032>
- Sadadi, O. (2016). *Accuracy of measuring tree height using Airborne LiDAR and Terrestrial laser scanner and its effect*

*on estimating forest biomass and carbon stock in Ayer Hitam tropical rain forest reserve, Malaysia*. MSc. Thesis. University of Twente, Faculty of Geo-information Science and Earth Observation (ITC). Enschede, The Netherlands. Retrieved from [https://library.itc.utwente.nl/papers\\_2016/msc/nrm/ojoatre.pdf](https://library.itc.utwente.nl/papers_2016/msc/nrm/ojoatre.pdf)

- Smith. (2015). Search | Britannica.com. Retrieved from [https://www.britannica.com/search?query=Smith%2C 2015 tropical rainforest](https://www.britannica.com/search?query=Smith%2C%202015%20tropical%20rainforest)
- Song, C., Dickinson, M. B., Su, L., Zhang, S., & Yaussey, D. (2010). Estimating average tree crown size using spatial information from Ikonos and Quick Bird images: Across-sensor and across-site comparisons. *Remote Sensing of Environment*, 114(5), 1099–1107. <https://doi.org/10.1016/j.rse.2009.12.022>
- Stas, S. (2011). *Aboveground Biomass and Carbon Stocks in A Secondary Forest in Comparison with Adjacent Primary Forest on Limestone in Seram, the Moluccas, Indonesia*. *Ecology & Natural Resources Management* (Vol. MSc Enviro). <https://doi.org/10.13140/RG.2.1.4473.8164>
- T. Vashum, K. (2012). Methods to Estimate Above-Ground Biomass and Carbon Stock in Natural Forests - A Review. *Journal of Ecosystem & Ecography*, 02(04), 1–7. <https://doi.org/10.4172/2157-7625.1000116>
- The World Bank. (2015). What is REDD+? | The Forest Carbon Partnership Facility. Retrieved June 5, 2018, from <https://www.forestcarbonpartnership.org/what-redd>
- Toma, T., Ishida, A., & Matius, P. (2005). Long-term monitoring of post-fire aboveground biomass recovery in a lowland dipterocarp forest in East Kalimantan, Indonesia. *Nutrient Cycling in Agroecosystems*, 71(1), 63–72. <https://doi.org/10.1007/s10705-004-0381-1>
- Trimurti, S. (2018). Differences Of Basidiomycotina Types In Natural Forest Arboretum Gardens Unmul Samarinda, *International Journal of Scientific and Technology Research*, ISSN 2277-86167, (1), 164-168.
- Turner, D., Lucieer, A., & Watson, C. (2012). An Automated Technique for Generating Georectified Mosaics from Ultra-High Resolution Unmanned Aerial Vehicle (UAV) Imagery, Based on Structure from Motion (SfM) Point Clouds. *Remote Sensing*, 4(5), 1392–1410. <https://doi.org/10.3390/rs4051392>
- UNAVOC. (n.d.) (2019). Cylindrical Target (White). Retrieved February 19, 2019, from <https://kb.unavco.org/kb/article/cylindrical-target-white-793.html>
- UNAVOC. (2013). Riegl TLS Field Operation Manual and Workflow, 400. Retrieved from <http://kb.unavco.org/kb/article/riegl-tls-field-operation-manual-and-workflow-786.html>
- UNFCCC. (2011). Report of the Conference of the Parties on its sixteenth session, held in Cancun from 29 November to 10 December 2010. *Decision 1/CP.16*, (March), 1–31. Retrieved from <https://unfccc.int/resource/docs/2010/cop16/eng/07a01.pdf>
- United Nations. (2018). UNFCCC Process - KP Introduction. Retrieved June 5, 2018, from <https://unfccc.int/process/the-kyoto-protocol>
- Wang, C. (2006). Biomass allometric equations for 10 co-occurring tree species in Chinese temperate forests. *Forest Ecology and Management*, 222(1–3), 9–16. <https://doi.org/10.1016/J.FORECO.2005.10.074>
- Wassihun, A. N. (2018). *Effect of forest stand density on the estimation above-ground biomass/ carbon stock using Airborne and Terrestrial LiDAR parameters in Berkelab tropical rain forest, Malaysia*. MSc. Thesis. University of Twente, Faculty of Geo-information Science and Earth Observation (ITC). Enschede, The

Netherlands. Retrieved from <https://library.itc.utwente.nl/login/2018/msc/nrm/wassihun.pdf>

Westoby, M. J., Brasington, J., Glasser, N. F., Hambrey, M. J., & Reynolds, J. M. (2012). "Structure-from-Motion" photogrammetry: A low-cost, effective tool for geoscience applications. *Geomorphology*, 179, 300–314. <https://doi.org/10.1016/j.geomorph.2012.08.021>

Williams, M. S., Techniques, M. I., Forest, R. M., Station, R. E., Service, U. F., St, W. P., ... Sciences, F. (1994). Five Instruments for Measuring Tree Height : An Evaluation. *Southern Journal of Applied Forestry*, 18(2), 76–82(7). Retrieved from <http://www.ingentaconnect.com/content/saf/sjaf/1994/00000018/00000002/art00008>

Yuen, J. Q., Fung, T., & Ziegler, A. D. (2016). Review of allometric equations for major land covers in SE Asia: Uncertainty and implications for above- and below-ground carbon estimates. *Forest Ecology and Management*, 360, 323–340. <https://doi.org/10.1016/j.foreco.2015.09.016>

Zhang, J., Hu, J., Lian, J., Fan, Z., Ouyang, X., & Ye, W. (2016). Seeing the forest from drones: Testing the potential of lightweight drones as a tool for long-term forest monitoring. *Biological Conservation*, 198, 60–69. <https://doi.org/10.1016/J.BIOCON.2016.03.027>



## LIST OF APPENDIX

---

Appendix 1: Slope correction table.

Slop (percent)	Radius (meter)	Slop (percent)	Radius (meter)	Slop (percent)	Radius (meter)	Slop (percent)	Radius (meter)
0	12.62	27	12.84	54	13.45	81	14.31
1	12.62	28	12.86	55	13.48	82	14.35
2	12.62	29	12.87	56	13.51	83	14.38
3	12.62	30	12.89	57	13.53	84	14.42
4	12.62	31	12.91	58	13.56	85	14.45
5	12.62	32	12.93	59	13.59	86	14.49
6	12.63	33	12.95	60	13.62	87	14.52
7	12.63	34	12.97	61	13.65	88	14.56
8	12.64	35	12.99	62	13.68	89	14.6
9	12.64	36	13.01	63	13.72	90	14.63
10	12.65	37	13.03	64	13.75	91	14.67
11	12.65	38	13.05	65	13.78	92	14.71
12	12.66	39	13.07	66	13.81	93	14.74
13	12.67	40	13.09	67	13.84	94	14.78
14	12.68	41	13.12	68	13.87	95	14.82
15	12.69	42	13.14	69	13.91	96	14.85
16	12.7	43	13.16	70	13.94	97	14.89
17	12.71	44	13.19	71	13.97	98	14.93
18	12.72	45	13.21	72	14	99	14.97
19	12.73	46	13.24	73	14.04	100	15
20	12.74	47	13.26	74	14.07	101	15.04
21	12.75	48	13.29	75	14.1	102	15.08
22	12.77	49	13.31	76	14.14	103	15.12
23	12.78	50	13.34	77	14.17	104	15.15
24	12.79	51	13.37	78	14.21	105	15.19
25	12.81	52	13.39	79	14.24		
26	12.82	53	13.42	80	14.28		

Appendix 2: Field data collection sheet.

Data collection sheet (KRUS educational Forest Indonesia 2018)							
Recorder:		Plot centre		Plot			Date: --
Forest type:				Plot No:	Radius:	Slop:	Photo No:
S/N	Tree No.	Lat.	Long.	DBH (cm)	Height (m)	species	Remark
1							
2							
3							
.							
.							
.							
.							
.							
.							
.							
.							
.							
.							
.							
40							

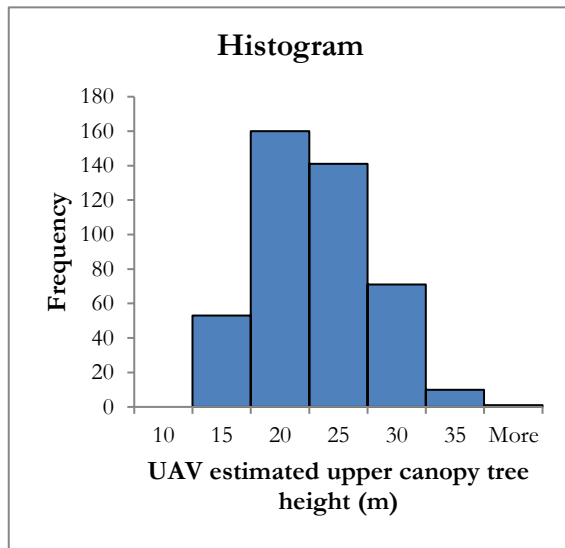
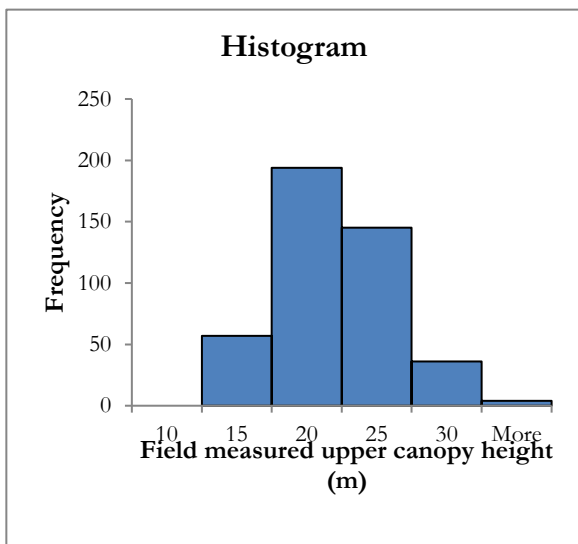
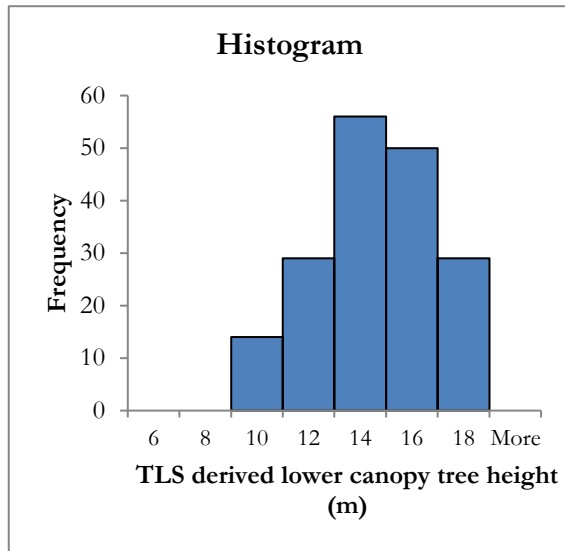
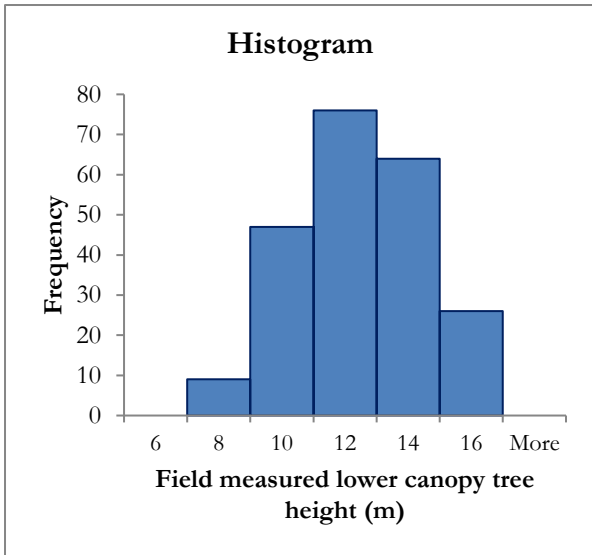
Appendix 3: Illustration of the UAV flight plan.

A) Flight mission

S/N	parameters	setting
1	Front overlap	80%
2	Side overlap	60%
3	View angle	Nadir
4	speed	Moderate

B) Technical parameters of UAV flight mission

Appendix 4: Distribution of tree parameters.



Appendix 5: Summary of field recorded biometric data.

Plot No	Latitude	Longitude	No. of trees	Mean DBH (cm)	Mean Tree Height	Average ABG/tree (kg)/plot	Total AGB /plot (ton/ha)
1	117.21778	-0.45046	27	27.84	16.13	626.89	338.52
2	117.21738	-0.45094	22	29.70	16.90	925.27	407.12
3	117.21687	-0.45070	18	30.03	17.18	781.01	281.16
4	117.21700	-0.45015	20	39.70	18.44	1153.98	461.59
5	117.21826	-0.45061	27	23.25	15.28	368.89	199.20
6	117.21839	-0.45108	29	24.61	14.24	504.79	292.78
7	117.21751	-0.45273	17	34.17	15.34	1052.33	357.79
8	117.21764	-0.45357	24	29.40	18.24	1039.52	498.97
9	117.21436	-0.44894	17	35.51	18.91	1147.32	390.09
10	117.21152	-0.44517	24	28.05	19.61	778.77	373.81
11	117.21269	-0.44692	25	27.17	17.90	713.02	356.51
12	117.21337	-0.44701	33	22.72	15.25	416.25	274.72
13	117.21363	-0.44802	23	23.99	16.50	447.40	205.81
14	117.21310	-0.44811	26	25.73	16.12	554.90	288.55
15	117.21258	-0.44819	29	25.80	15.28	582.13	337.63
16	117.21074	-0.44855	37	21.78	15.07	280.43	207.52
17	117.21117	-0.44863	21	32.12	17.06	909.71	382.08
18	117.21143	-0.44810	26	22.48	14.68	315.73	164.18
19	117.20992	-0.44867	31	26.52	16.25	516.43	320.18
20	117.20975	-0.44815	27	25.30	15.28	451.62	243.87
21	117.21044	-0.44798	19	25.90	15.86	444.12	168.77
22	117.21413	-0.44345	17	36.47	18.23	959.59	326.26
23	117.21405	-0.44309	21	30.30	15.50	710.77	298.52
24	117.21313	-0.44437	20	38.39	19.59	1116.44	446.58
25	117.21317	-0.44415	17	29.35	16.32	618.89	210.42
26	117.20744	-0.45115	23	30.32	17.63	624.39	287.22
27	117.20853	-0.45143	21	32.96	16.88	837.58	351.78
28	117.20961	-0.45252	19	32.55	17.02	891.87	338.91
29	117.21058	-0.45282	20	33.86	16.79	931.87	372.75
30	117.21220	-0.45215	19	28.27	14.38	485.77	184.59

Descriptive statistics	No. of trees	Mean DBH (cm)	Mean Tree Height	Average ABG/tree (kg)/plot	Total AGB plot (Mg)	Total AGB plot (ton/ha)
Mean	23.3	28.39	16.46	706.3	15.61	312.4
STDV	5.1	16.32	5.12	261.1	4.390009	87.8
Variance	26.1	22.8	26.2	68194.2	19.27218	7708.9
Minimum	17.0	10	6.69	280.4	8.21	164.2
Maximum	37.0	101.5	34	1154.0	24.95	499.0
Sum	699.0			21187.7	468.39	9367.9
Count	699	699	699	30.0	30	30.0

Appendix 6: Relationship between field measured, and TLS derived height of the lower canopy trees.

Regression Statistics	
Multiple R	0.89652
R Square	0.803748
Adjusted R Square	0.802856
Standard Error	0.859015
Observations	222

ANOVA					
	df	SS	MS	F	Significance F
Regression	1	664.8587	664.8587	901.0055	9.7E-80
Residual	220	162.3396	0.737907		
Total	221	827.1984			

	Coefficients	Standard Error	t Stat	P-value	Lower 95%	Upper 95%	Lower 95.0%	Upper 95.0%
Intercept	0.8392	0.3597	2.3331	0.0205	0.1303	1.5482	0.1303	1.5482
TLS derived tree height (m)	0.8900	0.0297	30.0168	0.0000	0.8316	0.9485	0.8316	0.9485

Appendix 7: Relationship between field measured and TLS derived DBH of the lower and upper canopies.

Regression Statistics	
Multiple R	0.996166796
R Square	0.992348285
Adjusted R Square	0.992335883
Standard Error	1.432035003
Observations	619

ANOVA					
	df	SS	MS	F	Significance F
Regression	1	164095.9	164095.9	80018.51	0
Residual	617	1265.297	2.050724		
Total	618	165361.2			

	Coefficients	Standard Error	t Stat	P-value	Lower 95%	Upper 95%	Lower 95.0%	Upper 95.0%
Intercept	0.086605479	0.114953	0.753397	0.451499	-0.13914	0.312353	-0.13914	0.312353
Field DBH (cm)	0.976409901	0.003452	282.8754	0	0.969631	0.983188	0.969631	0.983188

Appendix 8: Relationship between field measured and UAV derived upper canopy tree heights.

Regression Statistics	
Multiple R	0.876554038
R Square	0.768346982
Adjusted R Square	0.767813219
Standard Error	2.24146702
Observations	436

ANOVA					
	df	SS	MS	F	Significance F
Regression	1	7232.257	7232.257	1439.492	6.5E-140
Residual	434	2180.492	5.024174		
Total	435	9412.749			

	Coefficient	Standard Error	t Stat	P-value	Lower 95%	Upper 95%	Lower 95.0%	Upper 95.0%
Intercept	1.133696826	0.52403	2.163421	0.031054	0.103745	2.163648	0.103745	2.163648
Field measured height (m)	1.003201955	0.026441	37.94063	6.5E-140	0.951233	1.055171	0.951233	1.055171

Appendix 9: Relationship between the AGB estimated using UAV derived, and TLS derived height threshold to integrate the upper and lower canopy trees.

Regression Statistics	
Multiple R	0.99834861
R Square	0.996699946
Adjusted R Square	0.996582087
Standard Error	0.278061496
Observations	30

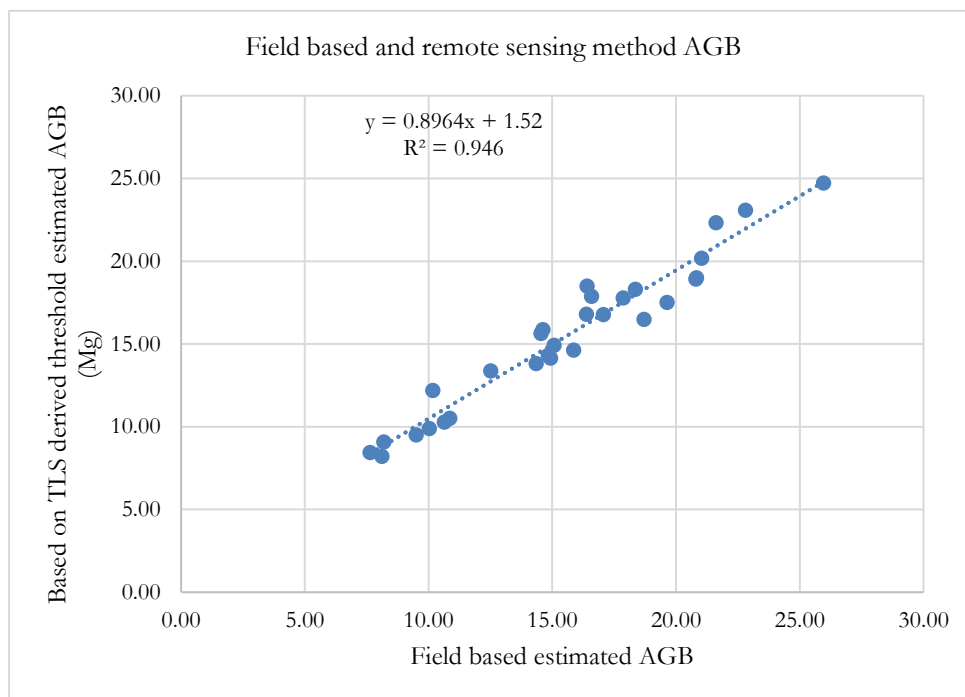
ANOVA					
	df	SS	MS	F	Significance F
Regression	1	653.8576	653.8576	8456.71	2.72E-36
Residual	28	2.164909	0.077318		
Total	29	656.0225			

	Coefficients	Standard Error	t Stat	P-value	Lower 95%	Upper 95%	Lower 95.0%	Upper 95.0%
Intercept	-0.190699991	0.178322	-1.06942	0.294015	-0.55598	0.174575	-0.55598	0.174575
X Variable 1	1.00841687	0.010966	91.96037	2.72E-36	0.985954	1.030879	0.985954	1.030879

Appendix 10: Descriptive statistics of field-based and remote sensing estimated AGB.

descriptive statistics	RS method (TLS height threshold)		Field-based	
	No. of trees	AGB (Mg/plot)	No. of trees	AGB (Mg/plot)
Minimum	13.00	7.63	13.00	8.21
mean	21.67	15.53	21.93	15.4407
Maximum	32.00	25.96	32.00	24.73
Standard Deviation	4.54353146	4.7562	4.69727	4.38
sum	650.00	465.87	658.00	463.22
Count	30	30	30	30

Appendix 11: Scatter plot between field-based and remote sensing method estimated AGB.



Appendix 12: The t-test for field-based and remote sensing method estimated AGB.

	Remote sense method (TLS height threshold)	Field-based estimated AGB
Mean	15.52741816	15.44066398
Variance	22.63288514	19.21471937
Observations	30	30
df	58	
t Stat	0.073454044	
P(T<=t) one-tail	0.470848776	
t Critical one-tail	1.671552762	
P(T<=t) two-tail	0.941697552	
t Critical two-tail	2.001717484	

Appendix 13: Relationship between field-based and remote sensing method estimated AGB.

Regression Statistics	
Multiple R	0.97265
R Square	0.94604
Adjusted R Square	0.94411
Standard Error	1.12439
Observations	30

ANOVA					
	df	SS	MS	F	Significance F
Regression	1	620.6233	620.6233	490.899499	2.72116E-19
Residual	28	35.3992	1.264257		
Total	29	656.0225			

	Coefficients	Standard Error	t Stat	P-value	Lower 95%	Upper 95%	Lower 95.0%	Upper 95.0%
Intercept	-0.7661	0.763587	-1.00333	0.324295522	-2.33026403	0.79800929	-2.33026	0.798009
X Variable 1	1.05535	0.047632	22.15625	2.72116E-19	0.957783245	1.152924	0.957783	1.152924

Appendix 14: Relationship between field-based and remote sensing method estimated AGB.

Regression Statistics	
Multiple R	0.974706365
R Square	0.950052497
Adjusted R Square	0.948268658
Standard Error	1.075174318
Observations	30

ANOVA					
	df	SS	MS	F	Significance F
Regression	1	615.6723	615.6723	532.5886	9.21E-20
Residual	28	32.36799	1.156		
Total	29	648.0403			

	Coefficients	Standard Error	t Stat	P-value	Lower 95%	Upper 95%	Lower 95.0%	Upper 95.0%
Intercept	-0.633831778	0.730163	-0.86807	0.392736	-2.1295	0.861838	-2.1295	0.861838
Field based AGB (Mg)	1.051135704	0.045547	23.07788	9.21E-20	0.957836	1.144435	0.957836	1.144435



Appendix 15: Summary of field-based and remote sensing method upper canopies tree parameters.

Plot No.	Tree No.	Field based						RS method					
		DBH (cm)			Height (m)			DBH (cm)			Height (m)		
		Mean	Min	Max	Mean	Min	Max	Mean	Min	Max	Mean	Min	Max
1	18	32.43	10.50	73.00	13.20	12.30	27.00	31.73	9.50	73.00	22.02	12.10	31.97
2	12	43.77	15.50	89.10	20.55	15.60	26.80	43.26	14.90	88.50	23.30	17.20	26.33
3	7	45.47	23.10	64.80	23.27	18.60	27.50	44.24	21.40	63.20	25.59	18.12	30.85
4	14	47.68	19.00	65.70	20.69	16.70	24.50	46.03	20.10	64.50	22.63	16.80	25.00
5	17	29.27	15.20	49.20	18.01	11.20	23.50	28.32	14.60	47.68	19.65	11.54	27.30
6	20	29.65	17.40	101.50	16.31	10.10	25.60	28.84	17.00	99.90	17.03	10.50	29.20
7	11	45.45	24.30	86.10	18.70	12.30	24.20	44.79	23.40	85.40	17.13	11.64	24.43
8	16	36.87	11.00	92.30	21.92	15.50	34.00	36.78	10.00	90.60	23.52	14.56	36.12
9	10	48.19	29.50	79.40	23.25	18.20	29.90	47.08	28.90	80.20	26.32	17.20	31.13
10	15	35.43	16.00	83.50	23.48	15.20	30.80	34.64	16.00	81.60	24.08	15.20	32.21
11	16	35.91	15.30	80.00	21.78	14.50	30.50	35.11	14.30	79.60	22.56	14.50	30.35
12	16	30.89	20.50	78.90	19.79	16.40	28.20	28.61	18.70	77.80	22.15	16.10	28.66
13	12	30.50	17.60	66.10	19.76	15.80	27.70	30.74	18.30	67.20	21.18	17.20	27.60
14	13	36.99	16.10	59.90	20.49	16.50	26.40	36.31	14.50	58.10	22.52	14.50	27.24
15	11	39.09	13.70	84.10	19.41	12.20	26.50	38.96	15.20	84.20	21.51	16.00	27.60
16	15	29.35	21.30	35.00	18.53	15.40	22.20	28.95	20.90	34.20	19.27	15.97	22.29
17	12	43.51	24.60	77.50	21.13	14.20	27.00	43.69	25.30	76.00	23.06	13.77	31.21
18	17	27.26	11.90	43.20	17.09	12.00	21.30	26.99	11.20	42.30	17.15	12.91	21.33
19	22	31.37	10.70	59.70	18.49	12.00	24.20	30.27	9.80	56.80	19.04	15.86	28.65
20	24	26.75	14.10	73.50	15.97	11.40	26.50	24.55	11.72	72.30	15.56	10.23	25.24
21	12	32.15	26.50	49.70	18.28	13.20	26.00	31.19	24.50	48.60	17.30	14.20	23.16
22	13	41.62	23.20	59.50	19.95	14.50	26.30	40.33	24.10	58.90	19.88	15.19	25.78
23	14	38.51	15.00	68.50	17.99	14.10	23.20	36.66	14.50	67.50	20.56	13.86	28.64
24	16	43.78	29.00	76.20	21.27	17.20	26.20	42.71	28.60	74.90	22.02	16.12	25.96
25	14	33.13	11.00	55.10	17.84	11.50	23.10	31.81	9.50	49.54	19.59	11.30	27.32
26	14	37.55	26.30	54.50	20.45	18.60	24.60	36.53	25.60	53.20	22.18	16.21	28.60
27	15	39.96	15.50	68.30	19.52	12.60	25.30	38.45	13.40	66.30	23.14	13.62	29.60
28	12	39.53	10.40	70.40	20.68	14.50	30.40	38.07	13.00	68.70	22.54	15.32	27.01
29	14	39.56	18.20	91.30	19.41	14.10	24.80	38.98	17.50	89.60	18.09	12.29	21.06
30	14	33.43	13.80	60.90	15.81	12.00	20.10	31.68	14.30	58.00	16.67	13.31	18.82

Appendix 16. Summary of field-based and remote sensing method lower canopies tree parameters.

Plot No.	No. of trees	Field based						Remote sensing method					
		DBH (cm)			Height (m)			DBH (cm)			Height (m)		
		Mean	Min	Max	Mean	Min	Max	Mean	Min	Max	Mean	Min	Max
1	5	19.26	10.00	44.60	9.02	7.30	11.40	17.38	8.50	43.20	9.37	7.10	11.50
2	8	12.51	10.00	16.50	12.54	9.30	14.30	12.69	8.50	16.50	12.76	9.58	15.00
3	10	19.63	11.90	29.90	13.55	10.30	15.90	19.05	10.20	31.20	13.36	10.30	16.50
4	6	21.10	14.60	43.60	13.20	12.30	14.10	19.93	12.60	44.10	14.05	13.20	15.20
5	9	13.10	10.00	18.30	10.52	9.10	12.30	14.06	9.80	17.50	10.41	9.00	11.00
6	9	13.43	10.50	16.80	9.64	8.70	10.90	13.52	10.20	17.50	10.39	9.80	10.90
7	6	13.48	10.80	19.90	9.17	6.70	10.60	14.13	10.50	21.20	9.45	6.08	10.90
8	6	13.80	10.00	17.20	10.68	8.30	12.40	13.70	10.50	15.60	11.61	8.90	12.50
9	4	17.47	11.00	13.80	12.23	10.30	14.20	17.70	9.60	32.10	12.73	11.12	14.50
10	7	16.20	10.50	24.60	12.27	10.30	13.90	15.56	10.20	22.30	12.48	10.30	13.50
11	8	11.81	10.00	15.00	11.13	9.80	12.60	11.85	9.80	14.50	11.92	10.50	12.49
12	12	15.34	10.00	32.50	11.19	7.80	13.50	16.03	9.70	33.20	11.73	8.30	14.60
13	11	16.88	10.00	33.80	12.95	9.80	14.50	17.04	10.20	33.00	13.54	9.40	15.60
14	10	14.48	10.00	21.90	11.72	7.40	13.90	14.41	10.20	19.90	11.83	9.00	12.30
15	17	17.81	10.00	52.40	12.79	9.50	15.90	16.99	9.10	50.40	13.50	11.10	15.74
16	17	15.86	10.40	31.60	12.59	9.40	14.50	15.65	10.20	30.90	13.29	9.20	15.00
17	8	17.00	11.80	27.00	11.51	8.50	12.90	17.27	10.90	25.10	11.93	9.90	12.90
18	9	13.44	10.00	19.80	10.12	8.50	11.80	14.59	11.40	21.20	10.81	8.90	12.40
19	8	14.15	10.40	23.20	10.49	9.00	11.40	14.15	10.90	22.30	11.09	9.00	12.20
20	3	13.63	11.30	15.50	9.73	9.60	9.80	13.20	11.80	14.60	9.70	9.60	9.80
21	7	15.19	12.20	18.50	11.70	10.20	13.20	15.13	10.80	17.90	12.93	11.44	13.90
22	0	0.00	0.00	0.00	0.00	0.00	0.00	0.00	0.00	0.00	0.00	0.00	0.00
23	7	13.89	10.80	15.70	10.53	8.30	12.10	13.44	10.20	16.50	10.42	9.80	10.90
24	4	16.82	13.00	19.90	12.85	10.20	14.90	17.20	14.50	21.30	12.22	10.42	14.00
25	3	11.73	10.00	14.50	9.20	8.60	10.00	13.03	9.10	16.50	9.81	9.03	10.61
26	8	20.20	14.60	25.40	13.69	10.90	15.60	19.06	12.50	26.00	14.09	12.00	14.90
27	5	15.32	13.00	18.50	10.36	8.90	11.90	16.36	13.80	19.00	10.62	10.35	10.80
28	6	20.98	11.30	52.00	10.33	7.80	13.20	21.08	12.00	51.20	10.93	7.72	14.50
29	5	21.16	14.30	33.80	9.92	9.40	10.30	20.40	15.30	32.10	10.70	9.38	11.70
30	4	12.62	11.40	14.70	9.68	7.10	10.60	12.68	10.50	15.20	10.97	8.05	12.50

Appendix 17: Summary of remote sensing method estimated AGB/carbon of the lower and upper canopies.

Plot No.	Latitude	Longitude	No. of trees	AGB (kg)	AGB (Mg)	AGB (ton/ha)	AGBC (Mg)
1	117.21778	-0.45046	23	18683.04	18.683036	373.66	8.78
2	117.21738	-0.45094	20	21192.64	21.192642	423.85	9.96
3	117.21687	-0.45070	17	14313.44	14.313445	286.27	6.73
4	117.21700	-0.45015	20	23336.42	23.336425	466.73	10.97
5	117.21826	-0.45061	26	10317.25	10.317247	206.34	4.85
6	117.21839	-0.45108	29	15321.38	15.321383	306.43	7.20
7	117.21751	-0.45273	17	16434.48	16.434482	328.69	7.72
8	117.21764	-0.45357	22	25960.53	25.960529	519.21	12.20
9	117.21436	-0.44894	14	20609.21	20.609212	412.18	9.69
10	117.21152	-0.44517	22	18342.62	18.342621	366.85	8.62
11	117.21269	-0.44692	24	17857.48	17.857478	357.15	8.39
12	117.21337	-0.44701	28	13141.81	13.141805	262.84	6.18
13	117.21363	-0.44802	23	10813.12	10.813123	216.26	5.08
14	117.21310	-0.44811	23	14956.45	14.956450	299.13	7.03
15	117.21258	-0.44819	28	17076.63	17.076635	341.53	8.03
16	117.21074	-0.44855	32	9543.16	9.543155	190.86	4.49
17	117.21117	-0.44863	20	20639.08	20.639080	412.78	9.70
18	117.21143	-0.44810	26	8211.49	8.211486	164.23	3.86
19	117.20992	-0.44867	30	14947.68	14.947679	298.95	7.03
20	117.20975	-0.44815	27	10218.39	10.218390	204.37	4.80
21	117.21044	-0.44798	19	7572.16	7.572157	151.44	3.56
22	117.21413	-0.44345	13	14539.96	14.539962	290.80	6.83
23	117.21405	-0.44309	21	15656.57	15.656575	313.13	7.36
24	117.21313	-0.44437	20	21707.87	21.707874	434.16	10.20
25	117.21317	-0.44415	17	10885.64	10.885636	217.71	5.12
26	117.20744	-0.45115	22	14753.48	14.753479	295.07	6.93
27	117.20853	-0.45143	20	19627.81	19.627808	392.56	9.23
28	117.20961	-0.45252	18	16441.52	16.441525	328.83	7.73
29	117.21058	-0.45282	19	16339.95	16.339948	326.80	7.68
30	117.21220	-0.45215	18	8450.78	8.450776	169.02	3.97
Descriptive statistics			No. of trees	AGB (kg)	AGB (Mg)	AGB (ton/ha)	
Minimum			13.00	7572.1568	7.5722	151.4431	
Mean			21.93	15596.4014	15.5964	311.9280	
Maximum			32.00	25960.5295	25.9605	519.2106	
STDV			4.70	4727.1786	4.7272	94.5436	
SUM			658.00	467892.0430	467.8920	9357.8409	
Count			30.00	30.0000	30.0000	30.0000	

Appendix 18: Orthomosaic image of 2017 and 2018 KRUS tropical rain forest.

